UPPSALA
UNIVERSITET

Digital Comprehensive Summaries of Uppsala Dissertations from the Faculty of Science and Technology 711

Ocean Wave Energy

Underwater Substation System for Wave Energy Converters

MAGNUS RAHM

ACTA
UNIVERSITATIS
UPSALIENSIS
UPPSALA
2010

ISSN 1651-6214
ISBN 978-91-554-7713-4
urn:nbn:se:uu:diva-112915

Dissertation presented at Uppsala University to be publicly examined in Ångströmlaboratoriet, Polhemsalen, Lägerhyddsvägen 1, Uppsala, Friday, March 5, 2010 at 13:00 for the degree of Doctor of Philosophy. The examination will be conducted in English.

Abstract
Rahm, M. 2010. Ocean Wave Energy. Underwater Substation System for Wave Energy Converters. Acta Universitatis Upsaliensis. *Digital Comprehensive Summaries of Uppsala Dissertations from the Faculty of Science and Technology* 711. 114 pp. Uppsala.
ISBN 978-91-554-7713-4.

This thesis deals with a system for operation of directly driven offshore wave energy converters. The work that has been carried out includes laboratory testing of a permanent magnet linear generator, wave energy converter mechanical design and offshore testing, and finally design, implementation, and offshore testing of an underwater collector substation. Long-term testing of a single point absorber, which was installed in March 2006, has been performed in real ocean waves in linear and in non-linear damping mode. The two different damping modes were realized by, first, a resistive load, and second, a rectifier with voltage smoothing capacitors and a resistive load in the DC-link. The loads are placed on land about 2 km east of the Lysekil wave energy research site, where the offshore experiments have been conducted. In the spring of 2009, another two wave energy converter prototypes were installed. Records of array operation were taken with two and three devices in the array. With two units, non-linear damping was used, and with three units, linear damping was employed. The point absorbers in the array are connected to the underwater substation, which is based on a 3 m^3 pressure vessel standing on the seabed. In the substation, rectification of the frequency and amplitude modulated voltages from the linear generators is made. The DC voltage is smoothened by capacitors and inverted to 50 Hz electrical frequency, transformed and finally transmitted to the on-shore measuring station. Results show that the absorption is heavily dependent on the damping. It has also been shown that by increasing the damping, the standard deviation of electrical power can be reduced. The standard deviation of electrical power is reduced by array operation compared to single unit operation. Ongoing and future work include the construction and installation of a second underwater substation, which will connect the first substation and seven new WECs.

Keywords: wave energy, wave power, wave energy converter, direct-drive, permanent magnet linear generator, point absorber, array, farm, park, offshore, marine, substation, electrical transmission system

Magnus Rahm, Department of Engineering Sciences, Electricity, Box 534, Uppsala University, SE-75121 Uppsala, Sweden

ISSN 1651-6214
ISBN 978-91-554-7713-4
urn:nbn:se:uu:diva-112915 (http://urn.kb.se/resolve?urn=urn:nbn:se:uu:diva-112915)

Till min älskade son, Emil.

List of Papers

This thesis is based on the following papers, which are referred to in the text by their Roman numerals.

I **Stålberg, M.**, Waters, R., Eriksson, M., Danielsson, O., Thorburn, K., Bernhoff, H., and Leijon, M. "Full-Scale Testing of PM Linear Generator for Point Absorber WEC". *Proceedings of the* 6^{th} *European Wave and Tidal Energy Conference, EWTEC*, Glasgow, UK, September, 2005.

II Waters, R., **Stålberg, M.**, Danielsson, O., Svensson, O., Gustafsson, S., Strömstedt, E., Eriksson, M., Sundberg, J., and Leijon, M. "Experimental results from sea trials of an offshore wave energy system". *Applied Physics Letters*, 90:034105, 2007.

III **Stålberg, M.**, Waters, R., Danielsson, O., and Leijon, M. "Influence of Generator Damping on Peak Power and Variance of Power for a Direct Drive Wave Energy Converter". *Journal of Offshore Mechanics and Arctic Engineering*, 130(3), 2008.

IV Waters, R., **Rahm, M.**, Svensson, O., Strömstedt, E., Boström, C., Sundberg, J., and Leijon, M. "Energy absorption in response to wave frequency and amplitude - offshore experiments on a wave energy converter". *Submitted to AIP Journal of Renewable and Sustainable Energy*, January 20, 2010.

V Engström, J., Waters, R., **Stålberg, M**., Strömstedt, E., Eriksson, M., Isberg, J., Henfridsson, U., Bergman, K., Asmussen, J., and Leijon, M. "Offshore experiments on a direct-driven Wave Energy Converter". *Proceedings of the* 7^{th} *European Wave and Tidal Energy Conference, EWTEC*, Porto, Portugal, September, 2007.

VI Boström, C., Lejerskog, E., **Stålberg, M.**, Thorburn, K., and Leijon, M. "Experimental results of rectification and filtration from an offshore wave energy system". *Renewable Energy*, 34(5):1381-1387, 2009.

VII Boström, C., Waters, R., Lejerskog, E., Svensson, O., **Stålberg, M.**, Strömstedt, E., and Leijon, M. "Study of a Wave Energy Converter Connected to a Nonlinear Load". *IEEE Journal of Oceanic Engineering*, 34(2), 2009.

VIII Leijon, M., Boström, C., Danielsson, O., Gustafsson, S., Haikonen, K., Langhamer, O., Strömstedt, E., **Stålberg, M.**, Sundberg, J., Svensson, O., Tyrberg, S., and Waters, R. "Wave Energy from the North Sea: Experiences from the Lysekil Research Site". *Surveys in Geophysics*, 29(3), 2008.

IX Leijon, M., Waters, R., **Rahm, M.**, Svensson, O., Boström, C., Strömstedt, E., Engström, J., Tyrberg, S., Savin, A., Gravråkmo, H., Bernhoff, H., Sundberg, J., Isberg, J., Ågren, O., Danielsson, O., Eriksson, M., Lejerskog, E., Bolund, B., Gustafsson, S., and Thorburn, K."Catch the wave to electricity". *IEEE Power and Energy Magazine*, 7(1):50-54, 2009.

X Boström, C., **Rahm, M.**, Svensson, O., Strömstedt, E., Savin, A., Waters, R., and Leijon, M. "Temperature measurements in a linear generator and marine substation for wave power". *Submitted to the* 29^{th} *International Conference on Ocean, Offshore and Arctic Engineering, OMAE2010*, Shanghai, China, June 6-11, 2010.

XI **Rahm, M.**, Boström, C., Svensson, O., Grabbe, M., Bülow, F., and Leijon, M. "Laboratory experimental verification of a marine substation". *Proceedings of the* 8^{th} *European Wave and Tidal Energy Conference, EWTEC*, Uppsala, Sweden, September, 2009.

XII Svensson, O., Boström, C., **Rahm, M.**, and Leijon, M. "Description of the control and measurement system used in the Low Voltage Marine Substation at the Lysekil research site". *Proceedings of the* 8^{th} *European Wave and Tidal Energy Conference, EWTEC*, Uppsala, Sweden, September, 2009.

XIII **Rahm, M.**, Boström, C., Svensson, O., Grabbe, M., Bülow, F. and Leijon, M. "Offshore underwater substation for wave energy converter arrays". *Submitted to IET Renewable Power Generation*, November 20, 2009.

XIV **Rahm, M.**, Svensson, O., Boström, C., Waters, R. and Leijon, M. "Power smoothing in an offshore wave energy converter array". *Submitted to AIP Journal of Renewable and Sustainable Energy*, November 3, 2009.

XV Boström, C., Svensson, O., **Rahm, M.**, Lejerskog, E., Savin, A., Strömstedt, E., Engström, J., Gravråkmo, H., Haikonen, K., Waters, R., Björklöf, D., Johansson, T., Sundberg, J., and Leijon, M. "Design proposal of electrical system for linear generator wave power plants". *Proceedings of the* 35^{th} *Annual Conference of the IEEE Industrial Electronics Society, IECON*, Porto, Portugal, November, 2009.

The author has contributed to the following papers which are not included in the thesis.

XVI **Stålberg, M.**, Waters, R., Danielsson, O., Leijon, M. "Influence of Generator Damping on Peak Power and Variance of Power for a Direct Drive Wave Energy Converter". *Proceedings of the* 26^{th} *International Conference on Ocean, Offshore and Arctic Engineering, OMAE2007*, San Diego, California, USA, 2007.

XVII Tyrberg, S., **Stålberg, M.**, Boström, C., Waters, R., Svensson, O., Strömstedt, E., Savin, A., Engström, J., Langhamer, O., Gravråkmo, H., Haikonen, K., Tedelid, J., Sundberg, J., and Leijon, M. "The Lysekil Wave Power Project: Status Update". *Proceedings of the* 10^{th} *World Renewable Energy Conference, WREC*, Glasgow, UK, 2008.

XVIII Solum, A., Deglaire, P., Eriksson, S., **Stålberg, M.**, Leijon, M., and Bernhoff, H. "Design of a 12kW vertical axis wind turbine equipped with a direct driven PM synchronous generator". *Proceedings of the European Wind Energy Conference & Exhibition, EWEC*, Athens, Greece, 2006.

Contents

Nomenclature and abbreviations

A	m^2	Area
$\mathbf{B}$	T	Magnetic induction
B_{max}	T	Magnetic induction amplitude
B_r	T	Remanent magnetic induction
c_p	m/s	Phase speed
c_g	m/s	Group speed
d	m	Sheet thickness in lamination
E	V	No-load voltage
F	N	Force
f	Hz	Wave frequency
f_e	Hz	Electrical frequency
g	m/s^2	Acceleration of gravity
$\mathbf{H}$	A/m	Magnetic field strength
H_c	A/m	Coercive field strength
H_{m0}	m	Significant wave height
H_s	m	Significant wave height
I	A	Current
i	A	Current
k	m^{-1}	Wave number
k_a	$W/V^{3/2}$	Anomalous loss material constant
k_e	Wm/V^2	Eddy-current loss material constant
k_h	$J/(m^3T^2)$	Hysteresis loss material constant
$\mathbf{l}$	m	Magnetic dipole separation distance
l_s	m	Length of linear generator stator
l_t	m	Length of linear generator translator
$\hat{l}$	-	Unity vector
$\mathbf{l}$	m	Magnetic dipole separation distance
$\mathbf{M}$	A/m	Magnetization
m	kg	Mass
m_0	m^2	Zeroth spectral moment
m_{core}	kg	Mass of stator core

N	–	Number of coil turns
P	W	Electrical power
P_{cable}	W	Resistive power loss in WEC cable
P_{mech}	W	Mechanical power
P_{Cu}	W	Copper loss in generator
P_{tot}	W	Total electromagnetic and electric generator loss
p	Am	Polar strength
R	Ω	Resistance
$S(f)$	m^2/Hz	Spectral density function
T	s	Wave period
$T_{m_{0-1}}$	s	Energy period
U	V	Voltage
V	m^3	Volume
W_a	W/kg	Anomalous loss density
W_{ec}	W/m^3	Eddy current loss density
W_h	W/m^3	Hysteresis loss density
$\dot{x}$	m/s	Speed
Φ	Wb	Magnetic flux
γ	Ns/m	Damping factor
λ	m	Wavelength
λ_m	m	Magnetic wavelength
μ_0	Vs/Am	Permeability of free space
μ_r	–	Relative permeability
ω	rad/s	Wave frequency
ρ	kg/m^3	Density of water

AC	Alternating Current
AGM	Absorbed Glass Mat
AW	Absorption Width
AWS	Archimedes Wave Swing
CFE	Centrum för Förnybar Elenergiomvandling
CSI	Current Source Inverter
DAQ	Data Acquisition
DC	Direct Current
DFIG	Doubly Fed Induction Generator
EMEC	European Marine Energy Centre
FEM	Finite Element Method
FPGA	Field Point Gate Array
HVDC	High Voltage Direct Current

IGBT	Insulated Gate Bipolar Transistor
L#	Lysekil, refers to WECs 1, 2, 3, ... ,10.
LG	Linear Generator
MLI	Multilevel Inverter
MOSFET	Metal-Oxide-Semiconductor Field-Effect Transistor
MPPT	Maximum Power Point Tracking
Nd-Fe-B	Neodymium-Iron-Boron
OSU	Oregon State University
OWC	Oscillating Water Column
PA	Point Absorber
PAC	Programmable Automation Controller
PM	Permanent Magnet
PMLG	Permanent Magnet Linear Generator
PMSG	Permanent Magnet Synchronous Generator
PTO	Power Take-Off
PTP	Point-To-Point
PVC	Poly Vinyl Chloride
PWM	Pulse Width Modulation
ROV	Remotely Operated Vehicle
THD	Total Harmonic Distortion
VSI	Voltage Source Inverter
WEC	Wave Energy Converter

1. Introduction

1.1 Renewable energy resource base

"Wind, water and solar technologies can provide 100 *percent of the world's energy, eliminating all fossil fuels."* This statement was recently made by Jacobson and Delucchi in the 2009 November issue of the Scientific American [1]. True or not, there are huge amounts of renewable energy available on Earth. Jacobson and Delucchi estimated that even if unavailable areas, and the areas that from an energy density point of view are the least favourable, are subtracted, still about $40-85$ TW of wind power and about 580 TW of solar power is available [1]. Today, virtually no power is harnessed from ocean waves, the potential of which has been estimated to be in the range of $1-10$ TW [2]. The global electricity generation in 2010 is projected[1] to be about 20600 TWh, corresponding to a mean power of 2.35 TW. So even if the available wave power is 1 TW rather than 10 TW, a little more than 40% of the world's current electricity demand could be covered by wave energy in the future. In addition to wind, solar and wave energy, other renewable flowing (i.e. not biomass) sources that can be utlilized are conventional hydro, tidal streams, other ocean currents, osmotic power (salt gradients) and ocean thermal gradients. Replacing the world's use of the fossil fuels coal, oil and natural gas is thus not an energy resource base problem. However, even though the necessary amount of energy is available, it might not be available when we need it. The intermittency of renewable energy sources might therefore call for the need for huge energy storage units.

1.2 Wave energy conversion principles

This thesis deals with conversion of wave energy to electricity. Wave energy can certainly be converted and used more or less directly to perform mechanical work, e.g. for seawater desalination purposes. However, electricity is a high-value energy carrier which, with high efficiency and without any pollution, can be converted into many other useful energy forms such as mechanical energy or heat. Electricity is also efficiently transmitted over long distances.

[1] The U.S. Energy Information Administration, http://www.eia.doe.gov 2009-12-08

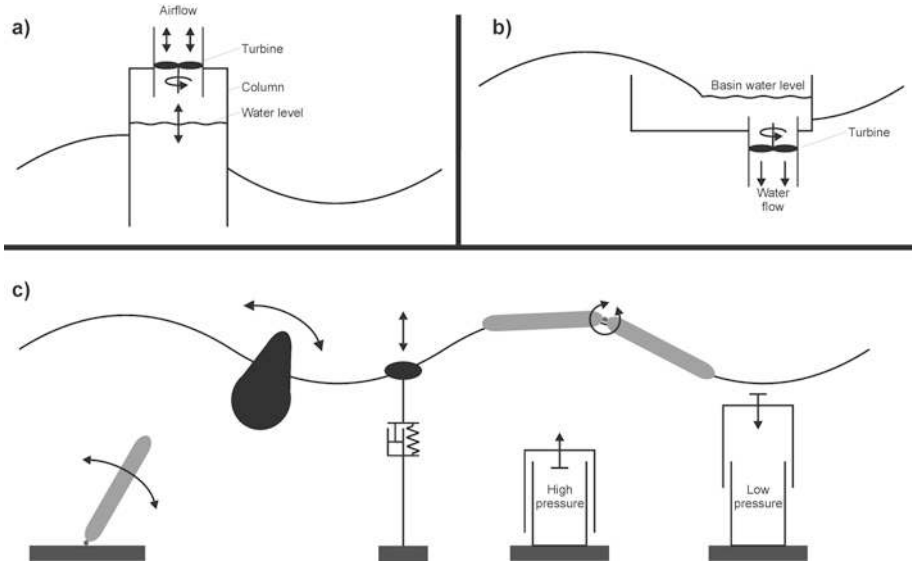

Figure 1.1: Wave energy converter characterization according to operational principle. (a) Oscillating water column device. (b) Overtopping device, (c) Oscillating (wave activated) bodies.

Wave energy converter (WEC) devices can be classified in numerous ways. Below, a classification according to operational principle is listed. a), b), and c) refer to Figure 1.1.

a) Oscillating water column devices (OWC)
b) Overtopping devices
c) Oscillating bodies, or wave activated devices

The above principles are utilized by different developers of wave energy conversion technology. 63 wave energy concepts are currently listed on the website of the Portuguese non-profit organization the *Wave Energy Centre*[2], which claims that these are the major concepts being developed. Many of the concepts are found in the recent wave energy technology reviews made by B. Drew [3] and A.F.O. Falcão [4].

1.2.1 Oscillating water column devices

The oscillating water column was the concern of the first patent in wave energy. It was filed already in 1799 and the inventors were two Frenchmen, father and son *Girard* [5]. As a result of the surface elevation, the waves incident on an oscillating water column device pressurize air inside a shaft (column). The shaft is open in both ends. One end faces the atmosphere and the other faces the waves and somewhere in the shaft, an air turbine is fitted for power take-

[2]The Wave Energy Centre, http://www.wavec.org 2009-12-08

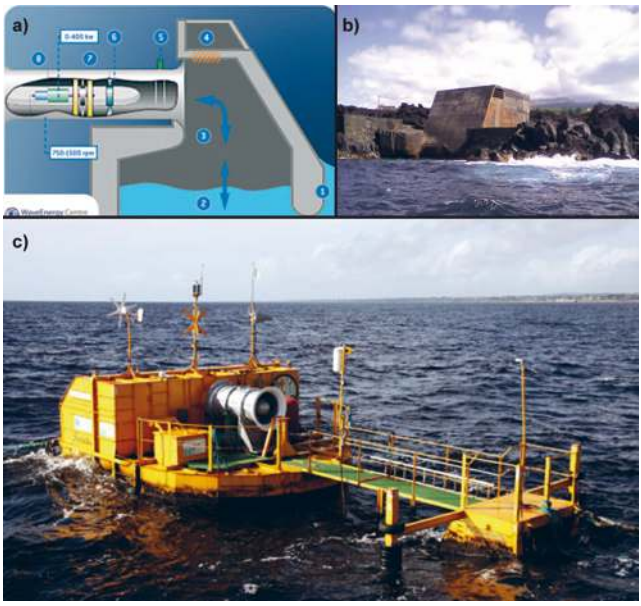

Figure 1.2: Oscillating water column devices. (a) The *Pico OWC Power Plant* operational principle. (b) Pico Plant on the Azores. (c) Ocean Energy Ltds *OE Buoy* OWC.

off (PTO). By controlled valves, or by the use of an omni-directional turbine type (Wells turbine), the air pressure is transformed into a high-speed rotational motion. OWCs can be floating or fixed in either offshore or shoreline locations. The *Pico plant*[3] (see [6]) is a well-known shoreline OWC on the Azores and the *OE Buoy*[4] from Ocean Energy Ltd. is an example of a floating OWC, see Figure 1.2.

1.2.2 Overtopping devices

In an overtopping device, the waves are allowed to spill into a reservoir, which is slightly elevated from the mean water level. The water runs back from the basin via low-head hydro turbines. A very well-known overtopping device is the Danish *Wave Dragon*[5], which is a floating wave energy converter [7]. An early shoreline overtopping device, the *Tapchan* (*tapered channel*), developed by the Norwegian University of Science and Technology (NTNU) in Trondheim, Norway, was built by company *Norwave A/S* at Toftestallen and tested for several years starting in 1985. Tapchan was a 350 kW plant with an 8500 m^2 basin having its water level about 3 m above the mean ocean surface.

[3] http://www.pico-owc.net 2009-12-07
[4] http://www.oceanenergy.ie 2009-12-07
[5] The Wave Dragon WEC, http://www.wavedragon.net/ 2009-12-07

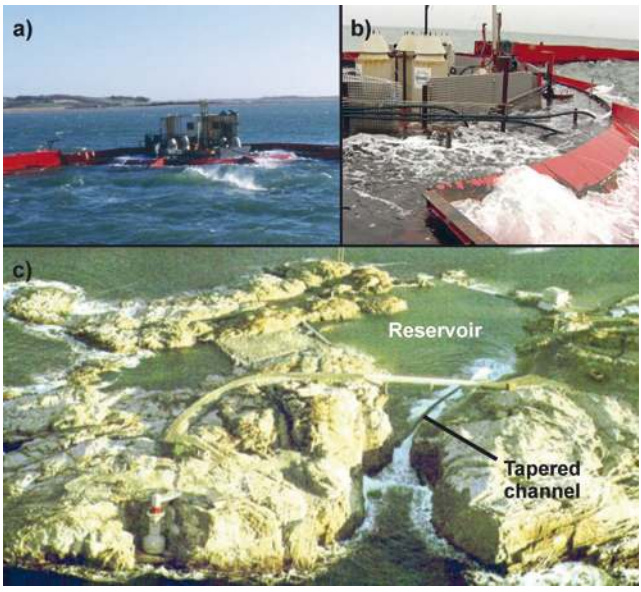

Figure 1.3: Overtopping devices. (a) The *Wave Dragon* prototype, front view. (b) The reservoir platform with hydro turbines. (c) The Norwegian *Tapchan* by Norwave A/S.

It is claimed that about $42-43\%$ of the wave energy hitting the 55 m wide opening was converted to electricity [8]. The Wave Dragon[6] and the Tapchan[7] WECs are shown in Figure 1.3.

1.2.3 Oscillating body devices

The group oscillating, or wave activated, bodies includes most other devices that are not included in the previous two classes of devices. The possible translational modes of oscillation are surge, sway and heave which are back-and-forth, from side-to-side and up-and-down respectively. Oscillation can also take place in the three rotational modes roll, pitch and yaw. These correspond to rotation about the x-axis, y-axis and z-axis respectively with waves traveling in the negative x-direction. Some devices utilize the relative motion between two, or several, bodies moving in one of the mentioned modes of oscillation. Below, a few examples of oscillating body devices are given.

If a device is narrow and extended primarily in the direction of the waves (in another classification such a device is referred to as an *attenuator*), the device is often sectioned and the relative motion between these sections of the full-length device is utilized. Hydraulic rams in combination with high-pressure gas accumulators for smoothing of absorbed power and accommodation to

[6]Athena Web, Science films online, http://www.athenaweb.org/ 2009-12-07
[7]Leipzig University, http://www.uni-leipzig.de 2009-12-07

Figure 1.4: An oscillating body device, the *Pelamis* wave energy converter.

rotating high-speed (induction) generators are primarily adopted in these devices [9]. The *Pelamis*[8] device is one example which is shown in Figure 1.4.

The so-called *oscillating wave surge devices* swing back and forth similarly to seaweed. The Finish wave energy device the *Wave Roller*[9] and the *Oyster*[10] wave energy converter, developed by Scottish company Aquamarine Power, are two such devices, which are shown in Figure 1.5.

Point absorbers (PA), being much smaller than the incident wavelength, have the benefit of being capable of converting more power than is incident on their width. The ratio of converted useful power to body volume (which requires material use etc.) may therefore be high. The class point absorbers is the concern of the present thesis, see further Sections 1.3 and 2.1.

One of the first point absorber devices was developed in Norway, see Figure 2.1 in Section 2.1, Chapter 2. An example of a modern device is the *CETO* wave energy device developed by Carnegie Wave Energy Ltd.[11] in Australia. This is based on submerged heaving point absorbers. Like in the Oyster wave energy device (see Section 1.2.3), water is pumped to shore where pelton hydro turbines and electric generators are placed. The concept is said also to be very well adapted for desalination purposes.

Below a traveling wave, the water pressure fluctuates as a result of the surface elevation. This effect is utilized by *submerged pressure differential de-*

[8]http://www.pelamiswave.com 2009-12-07

[9]The WaveRoller, AW-Energy Oy, http://www.aw-energy.com 2009-12-08

[10]Aquamarine Power, http://www.aquamarinepower.com 2009-12-07

[11]Carnegie Group, http://www.carnegiecorp.com.au/ 2009-12-09

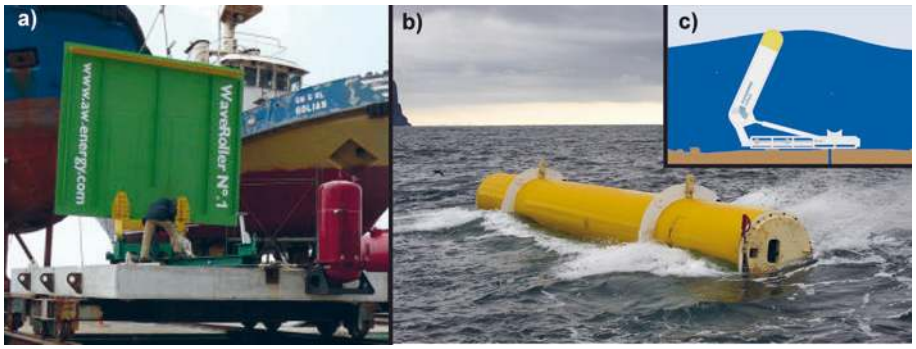

Figure 1.5: Oscillating body devices. (a) The *Wave Roller* from AW-Energy. (b) The *Oyster* WEC, by Aquamarine Power, in sea trials at the European Marine Energy Centre, Orkney, Scotland. Image courtesy of Aquamarine Power. (c) The principle of operation of the Oyster.

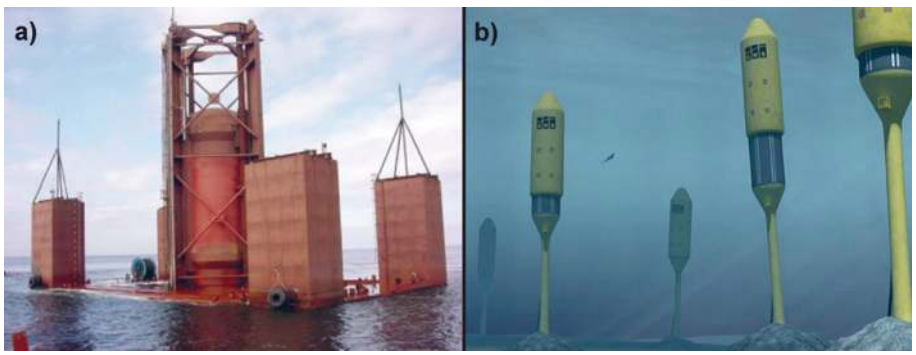

Figure 1.6: An oscillating body device. (a) The Archimedes Wave Swing 2 MW prototype. (b) Computer rendering of an AWS park.

vices. A volume of gas is compressed resulting in the relative motion between two bodies of which one is fixed to the seabed or e.g. by some reaction plate. The 2 MW PA *Archimedes Wave Swing*[12] (AWS) prototype and a computer rendering of a park of AWS devices are shown in Figure 1.6. The concept of the AWS is described and an estimation of its annual energy yield is made in [10].

1.3 The Uppsala University wave energy concept

At Uppsala University in Sweden, a wave energy converter concept is being researched. The WEC is a heaving point absorber with a directly driven permanent magnet linear generator (LG) placed on the seabed, see Figure 1.7.

[12] AWS Ocean Energy, http://www.awsocean.com 2009-12-07

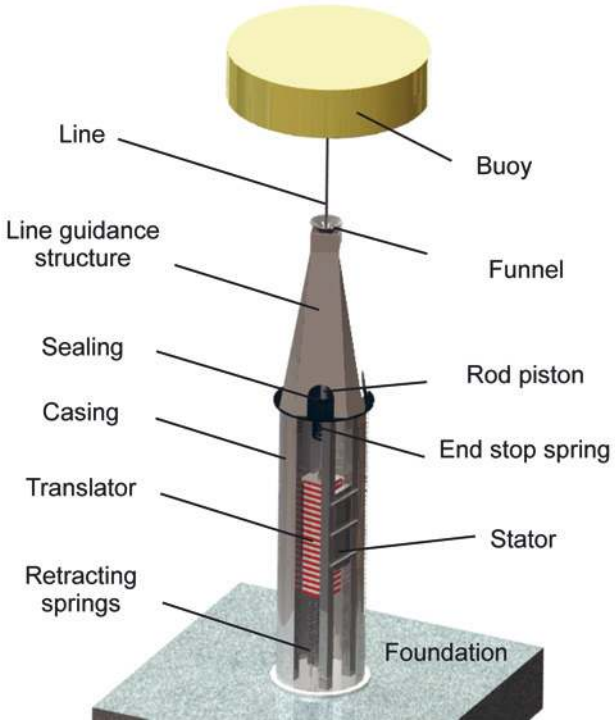

Figure 1.7: The Uppsala University wave energy converter.

The axisymmetric buoy is connected to the moving part of the linear generator, the translator, via a line and a piston. The sealed piston leads through the hull of the WEC and thus prevents seawater from entering. A bearing system maintains the air-gap between the LG translator and stator. Wave energy is converted to electricity in bursts of varying electrical frequency and voltage amplitude, see Section 3.5. Thus, the LG can not be directly coupled to the electric grid. In large waves, a steel compression spring, shown in the top of the linear generator casing in Figure 1.7, and a rubber cushion act as end stop. A set of retracting springs are attached beneath the translator pulling it downwards as it descends in wave troughs.

To date, four WECs have been built and deployed at *the Lysekil research site*, see Figure 1.8 and further Section 1.4. Ten WECs in total will be deployed at the site. They are referred to as L1-L10. L1 was deployed on March 13, 2006, L2 was deployed on February 7, 2009, L3 was deployed on February 10, 2009 and L9 was deployed on October 30, 2009. The wave power company Seabased AB builds WECs L4-L8. The construction of wave energy converter L10 commenced in the spring of 2009. It is designed and built by Uppsala University.

WECs L2-L3 are electrically identical to L1. However, some mechanical changes were made, e.g. changing the way the inner mechanical structure was

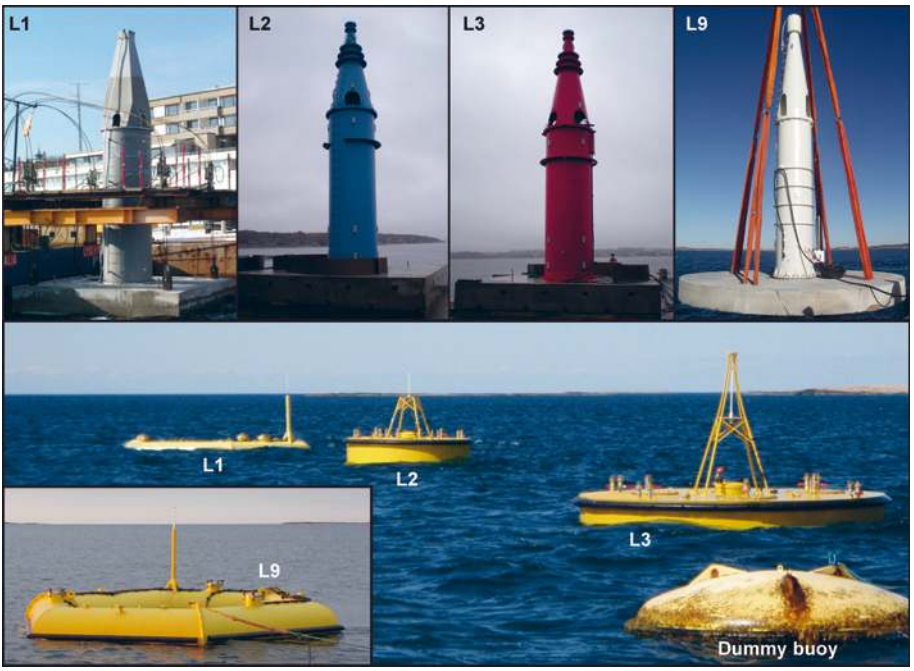

Figure 1.8: The WEC prototypes L1, L2 and L3 in the harbour of Lysekil prior to their respective deployments. The WEC buoys at the Lysekil wave energy research site as of June 2009. L9 being was deployed on October 27, 2009, and the buoy of L9 was put in place on October 30.

fastened to the casing in the lower end. Some beams of the inner structure have been moved and some parts are mounted in a slightly different manner in order to facilitate a smoother mounting procedure. The line guidance structure was redesigned. Instead of having four sides it is cone-shaped as seen in Figure 1.8. The funnel is mounted differently to facilitate maintenance. Some alterations were also made to the piston and piston sealing in the upper capsule lid.

In the offshore experiments of WEC array operation reported on in this thesis, the buoys of L1, L2 and L3, which are shown in Figure 1.8, were used. The buoy of L1 is a ring-shaped buoy made from six pipe sections of diameter 0.71 m. The buoy of L2 is cylindrical with diameter 3 m and height 1.2 m. The buoy of L3 is also cylindrical with diameter 4.2 m and height 0.62 m and thus has the same volume, 8.5 m^3, as the buoy of L2.

WEC L9 is quite different from L1-L3. L9 has a larger generator with eight sides instead of four (as in [11–14]) to reduce the required diameter, and thus volume, of the capsule. The mechanical structure and casing has been re-designed from scratch and from an analysis of buoy line force measurements from the Lysekil research site, the foundation weight could be reduced compared to the 50 tonne foundations of L1-L3. At the time of writing, L9 operates with a ring-shaped buoy made from six pipe sections of diameter 1.02 m.

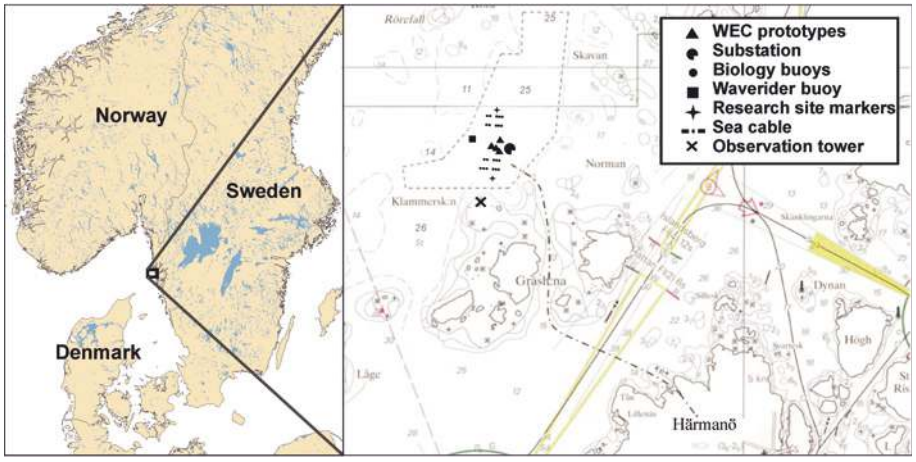

Figure 1.9: The Lysekil wave energy research site (N 58 11.700', E 011 22.450').

The fluctuating power from each WEC in the array is fed to an underwater collector substation. The voltage is rectified and the WECs are connected in parallel on the DC-side. The DC-voltage is smoothened by means of capacitors and inverted to 50 Hz before transformation to a more suitable transmission voltage. The electrical power is converted to heat in a resistive load in a measuring station on land.

1.4 The Lysekil wave energy research site

Uppsala University has developed a wave energy research site some 100 km northwest of Gothenburg on the Swedish west coast, see Figure 1.9. The site is called the *Lysekil wave energy research site* and is being built up within the *Lysekil project* at Uppsala University. The University has permission to conduct technical and biological research here until 2014. This is partly done within the Swedish Centre for Renewable Electric Energy Conversion (CFE).

On the research site, covering about 40000 m^2, 10 WECs will be deployed along with two underwater collector substations. A sea cable connects the WECs, via a substation, to the measuring station on the nearby island Härmanö. The depth at the site is 25 m and the seabed is even, consisting of sandy silt, the thickness of which is about 1 m [15]. The site environmental consents also cover the installation of up to 30 *dummy buoys*, see Figure 1.8. These are available for biological research. Most of the buoys have already been installed (21 dummy buoys all together in March and May, 2007) and some even decommissioned. The site has a wave measuring buoy, a *Waverider*, to measure the sea state. This was installed in 2004. South of the area, a lattice tower for observation and buoy motion studies was erected in 2007. It is equipped with a camera with panning and high zooming capability, communication and

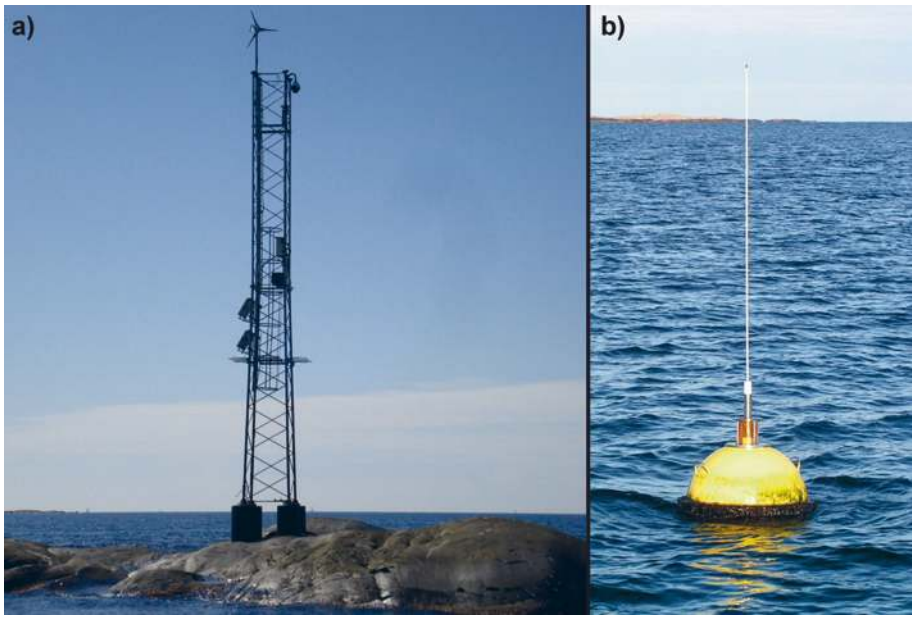

Figure 1.10: (a) The observation tower south of the buoy area and (b) the Waverider wave measuring buoy.

the necessary energy supply equipment: batteries, a small wind turbine and photo voltaic solar panels. The observation tower and Waverider are seen in Figure 1.10.

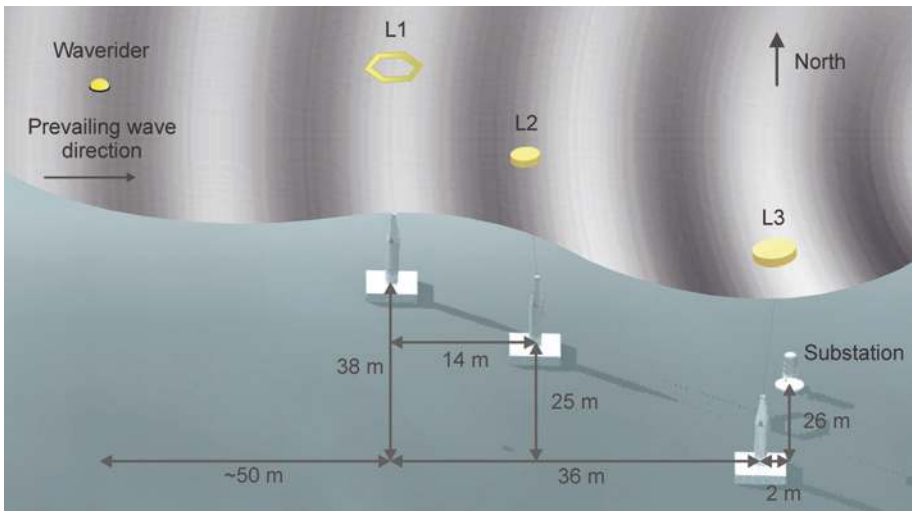

Figure 1.11: The Lysekil research site with the relative positions of the WECs L1, L2 and L3, the underwater collector substation and the Waverider wave measuring buoy. L1 has a ring-shaped buoy and L2 and L3 have cylindrically shaped buoys.

The average wave climate at the Lysekil research site, based on a study of eight years of satellite data, is 2.6 ± 0.3 kW/m [16]. The wave energy (in terms of number of kilowatt hours per year per meter wave front) is primarily available in combinations of significant wave heights of about $1 - 2.5$ m and wave periods of about $4 - 7.5$ s.

The relative positions of the first three WECs, the underwater collector substation and the Waverider wave measuring buoy are seen in Figure 1.11.

2. Background

2.1 Historic overview of point absorbers

The early scientific work on point absorbers was carried out by several people in the mid- and late nineteen seventies. K. Budal and J. Falnes, D.V. Evans, J.N. Newman and C.C. Mei were a few of these pioneers [17–20]. In 1975-1976 they independently published on the fundamental theory of power extraction from ocean waves and deduced expressions for maximum absorbed power. They showed theoretically that point absorbers may absorb much more power than is incident on its width, i.e. equivalently they may have an *absorption width* (AW) higher than 100 percent. The simile with the antenna of a frequency-tuned radio receiver was made by Budal and Falnes in [17].

Below, a few of the vast amount of further studies made on point absorbers and PA arrays are briefly reviewed to give a view of the development to date.

A single heaving cylindrical PA and an array of PAs for which the spacing was equal or smaller than the wavelength of the incident waves, were studied by Budal and Falnes in [21]. If the buoys were to be operated with optimal phase and amplitude control, it could be concluded that the array would absorb 50% and 100% of the incident wave power in one and two degrees of freedom respectively. This was later validated by Budal and Falnes through physical modelling of resonating buoys in a wave flume [22]. First they used a static wave reflector behind the row of PAs and then they used a second row of PAs as a dynamic wave reflector. They also introduced the concept of *virtual resonance*, a type of phase control which is usually referred to as *latching*. Latching is implemented by locking the position of the body twice per half wave cycle allowing for the excitation force on the buoy and the maximum buoy speed to coincide, a condition which must be fulfilled to achieve maximum power capture [23]. Further Budal and Falnes were working on the implementation of a real device for large-scale implementation in farms together with a group at the University of Trondheim [24], see Figure 2.1. Their work began in 1973.

An analysis of the effect of motion constraints on spherical PAs in an infinite array was made in addition to previous results on power capture [25]. If the PA heaving amplitude is constrained to move not more than twice the amplitude of the waves, the AW can exceed the sphere diameter by 8%. If the sphere oscillation amplitude was limited to the same amplitude as the waves, the AW was limited to 70% and for half the wave amplitude, the AW was at most 40%.

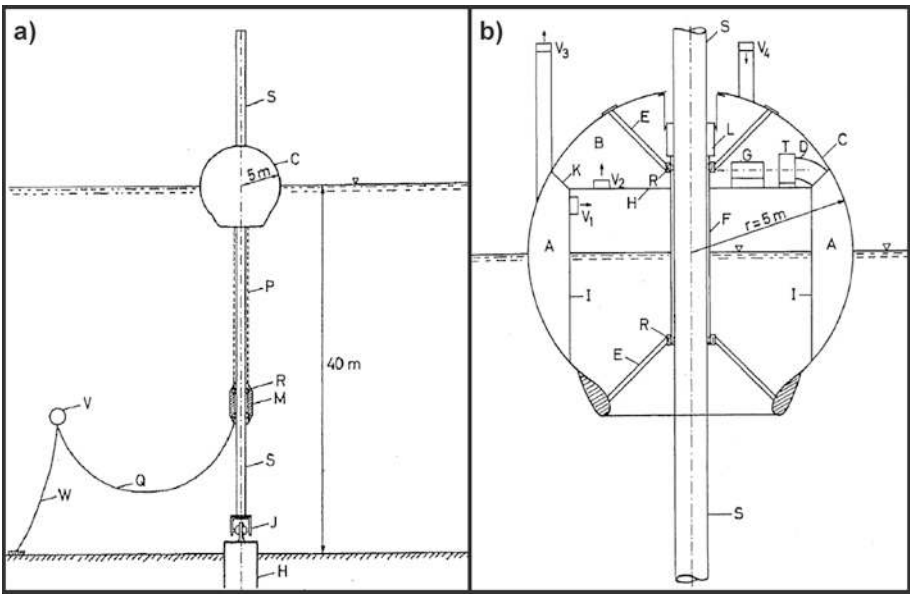

Figure 2.1: A sketch of the Norwegian wave energy converter with full-scale measures. (a) The mooring of the device with heaving point absorber body C, strut S, moving mass M with rollers R, universal joint J, anchor H, flexible cable Q, buoyant body V and mooring cable W. (b) The point absorber hull and its interior components. The hull is opened at its lower end allowing for pressure variations inside the hull resulting from the wave and body motions. Figures from [24].

In [26] a numerical model is used to study the amplitude-constrained phase control of oscillating bodies, a cylindrical buoy with a hemispherical bottom and a submersed sphere, in irregular waves. Assuming sinusoidal body motion, the effect of the phase difference between the oscillation velocity and the excitation force on the absorbed power was shown. It was concluded that the natural period of the body has relatively little influence on the absorbed power if the wave period is less than approximately 3 s. The effect of motion constraints on spherical point absorbers in heave and surge was studied in [27] where it was concluded that higher AWs could be obtained with motion both in heave and surge than if the body moved in heave only. The frequency response of the body was also broader when two degrees of freedom were allowed.

A case study of energy extraction from waves typical for the Belgian part of the North Sea was made in [28]. A few different cylindrical buoy shapes with different bottom shapes and supplementary masses were simulated and the simulations validated by physical model testing in a wave flume. In the study, resonance tuning was made to maximize the power capture. A 90 degree cone with cylindrical extension was found to have the best hydrodynamical

performance and simulations indicated a possible AW of nearly 60% as an average over a range of wave heights.

Hydrodynamical array interaction effects were studied in [29]. Methods for calculating these effects were later studied and evaluated in [30,31]. For a five member array, the wave interaction effects were investigated and an attempt was made to find an optimal formation of the oscillating bodies in the array in [32]. Damping optimization of array members was studied in [33]. In this study it was concluded that it is more efficient in terms of increasing the absorbed power to apply individual damping optimization to the array members rather than to use the optimal control parameters for one buoy on all the array members. A 14% increase in power absorption was found as a result of choosing the best optimization method investigated.

In [34] a single body and two different array configurations of axisymmetric (cylindrical) heaving PAs are investigated by using the point absorber approximation and a boundary element method code respectively. No amplitude constraint to the body excursions is applied, nor phase control. The effect of the ratio of buoy draft to radius is simulated for the single PA. The array configurations were varied with respect to distance between PA bodies and body radius for a draft of 3 m in different angles of incident irregular waves. Results show that the use of arrays of small PAs may be a good solution for deployment. When ignoring hydrodynamical interference between devices, it was also shown that restricting the available ocean area for deployment, clearly it is better in terms of attaining an as high annual energy capture as possible to deploy many small devices compared to fewer ones with larger rated power.

The benefits of latching control on a generic one-degree of freedom WEC and to a specific four-degree of freedom device was investigated by A. Babarit [35]. Two methods are derived and applied in the two cases mentioned.

The influence of the distance between array members on the power captured by the array is investigated in [36]. Two point absorbers are placed in-line in the wave direction and the performance of the two-body array is studied in regular and irregular waves. The study shows that an increase in array power capture can be made, but only due to a significant increase in the AW of the front system whereas the AW of the rear system is always reduced as a result of its location in the array instead of in isolation. In general, the aim to increase the array power by optimization of wave interaction effects is relatively unrealistic for systems implemented in practice.

The possible increase in power production from wave interaction effects is sensitive to e.g. wave directionality. Therefore, in the design and implementation of real devices it is suggested e.g. by P. McIver [29] that one rather try to reduce the negative effects of destructive wave interference.

2.2 Hydrodynamical properties of the Uppsala PA

In the concept considered in this thesis, an axisymmetric buoy is used. The buoy is allowed to move in all six degrees of freedom, or rather, since the buoy is connected to the generator by means of a wire (line), there are no mechanical means to restrict the buoy motion. However, the heave motion seem to be a very dominating contributer to the power capture. Simulations considering only the heave motion correspond very well to prototype measurements taken in real ocean waves [37]. The correspondence is best when the buoy motion is heavily damped. In a coupled hydrodynamical potential theory and electromagnetic generator model, the simulation deviations from experiments are $5-11\%$, some of which may depend on the neglectance of mechanical losses in the WEC prototype [38].

Simulations based on a potential theory model has shown that in harmonic waves, the response of the device is better in wave frequencies close to the resonance frequency of the system. In a wave spectrum (real ocean waves), which can be rather broad-band, the device response due to resonance is not as pronounced [39]. Changing the system's resonance frequency during operation is difficult since it is primarily dependent on the added mass and the buoy radius. In addition, operating the WEC in resonance may produce very large amplitude motions, which can be difficult to handle in the WEC system at hand. The pitch length of the translator is limited since it would otherwise produce a very tall machine. The added construction material might then be poorly utilized. For these reasons the approach taken in this project is to use a broad-band frequency response of the device to make reasonably good use of waves in a large range of wave frequencies, which are present in broad-band spectra. However, the results of a recent study indicate that by adding a fixed spherical submerged zero-buoyancy body on the buoy line, the resonance frequency of the system can be altered in such a way that the AW at optimum load can be increased by 100% [40].

The variation in damping of the buoy motion can be realized by connecting different loads to the generator or by controlling the power extraction by some algorithm. As explained in Section 3.2, an alteration of the buoy speed and phase in relation to the wave elevation is then introduced, which affects the radiation of waves from the PA. This in turn affects the AW of the device.

2.3 Power smoothing by energy storage

An even power output from a wave energy plant makes grid integration easier since voltage fluctuations to some extent are mitigated. Steven H. Salter, a pioneer in experimental testing of wave energy device and the inventor of the *Edinburgh Duck* (Salter's Duck), proposed that about 100 seconds of energy storage would produce a completely steady output from a single device in

any typical sea state [41]. The benefit of overtopping devices with reservoirs thereby becomes clear.

Another means of reducing the output power fluctuations is adding energy storage units of several different kinds to a system generating power from ocean waves. This was studied in [42] for a combined wind and wave energy conversion system. Here, a flywheel energy storage system, a compressed air energy storage system, an aqua electrolyzer and fuel cell system are combined with a diesel engine generator to smooth the power output and provide security of supply for different time-varying loads from the combined offshore wind and wave energy conversion system. It was concluded from the study that the production system could meet the load demand.

In [43] the use of supercapacitors was studied for electrical energy storage. However, it was concluded that the lifetime of supercapacitors yet is too poor to be useful in commercial WEC installations.

Hydraulic energy storage for smoothened grid power using a doubly fed induction generator (DFIG) was examined in a wave-to-wire dynamic model in [44]. The resulting grid voltage fluctuations in the 33 kV grid connection point were calculated from a 0.6 MW wave farm of 30 WECs.

To grid connect direct driven point absorbers utilizing the linear generator topology, power conditioning of some sort has to be made. One type of linear generator, called a vernier hybrid machine, can reach very high force density but is rather difficult to regulate due to high inductance. To address this issue, and the fluctuating output power from such machines, a prototype generator and an AC/AC converter were built and investigated in [45]. DC-link capacitors were used to smoothen the output power, but it is reported that a large number of capacitors would be necessary to absorb the power fluctuations from a direct driven linear generator.

2.4 Power smoothing by spatial distribution

An early study of the use of power electronics for power smoothing in wave energy can be found in [46]. A thyristor-based speed controller is used as grid interface of an induction machine which is run by a variable speed prime mover. Firing pulses and closed-loop control are accommodated by a microprocessor controller. A great reduction in the ratio of maximum to mean power was achieved.

In [47], grid interfacing is discussed, especially with regard to active control of the power take-off unit. Power electronics is used as interface components and the issue of power smoothing is especially stressed.

The combined power from several WECs in park operation is anticipated to give a smoother output power than the output of single devices. This will facilitate grid connection. Reductions in the variation in power output from a

linear generator wave farm with an HVDC offshore grid layout were the result of the study in [48].

In [49] several platforms with closely spaced point absorbers were placed in a farm layout. An analysis of the total power from the farm shows a reduction of the variation in the predicted output power compared to individual devices. The smoothing effect was larger in regular sine waves than in the irregular sea studied.

The variation in output power from a farm of SEAREV wave energy converters was quantified in [50].

Several researchers have studied how the combined power from several difference sources, distributed over a larger geographical area, could facilitate grid connection. One such study analyzes the electrical network layout in Scotland by introducing a number of scenarios for utilization of wave and tidal energy plants to identify important restrictions for further analysis and more detailed research [51].

2.5 Linear generators

There are many types of linear electrical machines and many different designs have been simulated and tested. This section focuses on linear generators and does not concern the design of linear motors nor actuators.

Extensive theoretical and experimental work in this area has been made at the University of Durham and the University of Edinburgh in the UK [45, 52–58]. Different types of permanent magnet linear generators (PMLGs) have been investigated, such as *variable reluctance*, *vernier hybrid* and *air-cored tubular* LGs. The generators are intended for directly driven wave energy converters. A review of LG systems for the wave energy application was made in [59].

The first LG deployed at sea for testing in ocean waves was the AWS device [10,60,61]. The second was the Uppsala wave energy converter described in Section 1.3. More recently, Oregon State University (OSU) in cooperation with Columbia Power Technologies deployed a 10 kW WEC[1,2]. The Oregon state University PMLG is based on a circular stator which is fixed in a floating large-draft spar buoy. On this spar buoy, a saucer-shaped buoy reciprocates in the heave mode. The translator magnets are fixed on the inner periphery of the saucer-shaped buoy. The buoyancy of the spar provides the necessary reaction force to the reciprocating buoy. The WEC buoy design is mainly carried out in composite materials. Some simulation results and first experimental results from the wave-flume testing of a small-scale (50 W) unit similar to this device can be found in [62]. The construction of a succeeding PMLG prototype of

[1]The Oregon State University OSU, Wallace Renewable Energy Systems Facility, http://eecs.oregonstate.edu/wesrf/ 2009-12-08

[2]Columbia Power Technologies, http://www.columbiapwr.com/ 2009-12-08

1 kW is described in [63]. Results from ocean testing of the 10 kW device are reported on in [64, 65] and the general wave energy OSU research activities including the 1 kW and 10 kW units are presented in [66].

Some PMLG types are compared in [60] and a design of a transverse flux PM machine is investigated. The suitability for direct driven WECs of the respective machines are evaluated. Another PMLG design and WEC concept is presented in [67–69] where optimization procedures were used to design an LG machine. A prototype was built and tested in a laboratory environment and the experiments showed agreement with the simulations within $\pm 10\%$. Optimum load control and power conditioning of a PMLG was investigated in [70]. A four-sided 16 kW PMLG was designed in [71]. The modeling methodology was presented and an optimization of the geometry of the PMLG was made.

In [72] a number of small-scale machines and drives were first tested in reciprocating motion (sinusoidal speed variation), and then compared and evaluated. It is suggested that significant de-rating of nameplate efficiency does not have to be made since the speed variation does not have large influence on the efficiency.

Some advantages and disadvantages of air-cored tubular PMLGs over iron-cored PMLGs can be identified, see e.g. [73]. They lack the large attraction forces between stator and translator that iron-cored machines have to handle. End-windings can be virtually excluded and the no-load cogging forces vanish. In addition, the generator can easily be made circular (in the horizontal plane for a vertically oriented LG), which in some cases can be beneficial to increase the compactness of the machine. An obvious disadvantage is the amount of magnetic material required to compensate for the increased reluctance of the magnetic circuit in order to produce the same magnetic flux as in the corresponding iron-cored machine. The hard magnetic material is by-far the most expensive material used in both these machine topologies. To provide mechanical support for the stator winding, casting the stator winding in some plastic-based material (such as epoxy resin) might be a feasible solution. However, this requires detailed analyses of the cooling of the stator winding. This could otherwise cause large problems due to excessive heating of the winding from resistive losses.

To achieve more time-efficient calculations of the produced magnetic induction in air-cored tubular PMLGs, intended for directly driven WECs, a polynomial fit method was evaluated and compared with finite element analysis in [74]. An optimization of material use of PM material, copper, and steel from a capital cost perspective with regard to average produced power was also conducted.

2.6 Grid connection schemes for offshore renewables

The chosen electrical transmission system for a wave farm has to be able to handle the total power to be transmitted without considerable transmission losses. It has to be as robust and cost-effective as possible and it should influence the local environment as little as possible. The most suitable design will depend on the number of WECs in the wave farm, the power of each unit, the transmission distance from each individual WEC to some offshore substation or electrical socket and the transmission distance to shore etc. Legal issues might also influence the design, e.g. whether or not transmission cables will have to be buried in the seabed or not.

A preliminary over-all design of an electrical system for a wave energy plant can be made rather crude. Approximate voltage levels and cable dimensions are chosen to achieve reasonable transmission losses. Within reasonable cable transmission distances, a regular three-phase AC transmission can be chosen. A common approach is to elevate the voltage in several steps, reaching the maximum voltage at the longest transmission distance in the offshore grid. The WEC unit size will also influence this. The larger the individual nominal power of the WEC, the higher the transmission voltage from each WEC to some central offshore substation needs be to in order to achieve reasonable transmission losses. At higher power levels and at longer transmission distances, the voltage should be higher. General electrical engineering issues like these are discussed in [75, 76].

Some general issues regarding electrical grid interfacing with some emphasis on variable speed PM synchronous generators are discussed in [77]. A number of areas from other sectors of the renewable energy industry are highlighted where technology transfer could be made.

Polinder investigates an alternative choice of power electronic converter for grid connection of a single AWS device [61]. The current source inverter (CSI) utilized for grid connection of the first AWS prototype has higher losses than would a voltage source inverter (VSI). The study concludes that grid connection of a single device might result in heavy grid voltage fluctuation, but it is mentioned that multiple units placed in a "sensible way" probably would produce a more constant output. In [78], farm connection alternatives for the AWS device are evaluated. The study investigates solutions previously suggested for offshore wind farms.

In [79], a suggestion for a 200 MW grid layout for 50 units of the *Wave Dragon* WEC device was made, the planned distance to shore being 25 – 100 km, see Figure 2.2. A DC transmission was suggested for all ranges of distance to shore, from transmission voltage $\pm$ 50 kV to $\pm$ 150 kV, the latter being high enough for transmitting the total farm power of 200 MW at the largest distance (100 km). The umbilical cable for transmission of power from the floating structure to the seabed cable is also briefly discussed and is said

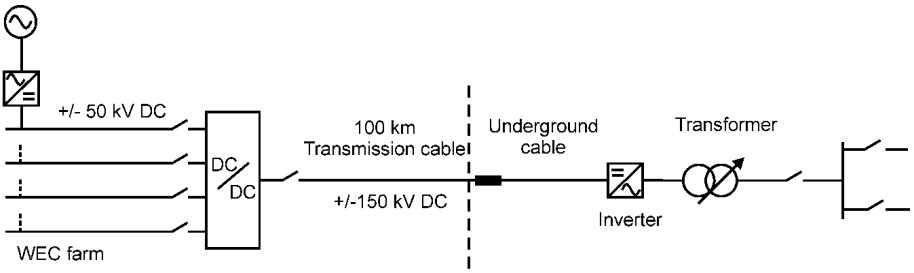

Figure 2.2: A proposed 200 MW HVDC transmission system for a farm of 50 Wave Dragon devices. Figure made in accordance with [79].

to be commercially available as long no rotations larger than 45 degrees are present.

An interconnection layout with transmission cables for farms of hinged attenuator devices is described in [80].

A solution for a point absorber farm layout with a self-reacting submersed platform is presented in [81]. The output of individual linear generators are rectified and the power added together. The intention is to use some kind of platform-based offshore substation solution to gather the power from individual attenuators prior to transmission to the on-shore grid in a single transmission cable.

The solution to use an underwater substation in the electrical system of the wave energy converter concept considered in this thesis, was patented in [82]. The solution is patented for generating electrical energy from marine sources including offshore wind farms. It also includes the use of an energy storage unit, e.g. a flywheel, to smooth the absorbed power.

A *maximum power point tracking* (MPPT) algorithm may be implemented to maximize power output from an electricity production device. MPPT algorithms have been used with success e.g. in solar photo voltaic applications[3]. The use of an MPPT algorithm makes optimized power output possible without knowing beforehand the power curve of the device (e.g. the coefficient of power to tip-speed ratio curve for a wind power plant).

A WEC array layout using two AWS devices was studied in [83]. An MPPT algorithm was incorporated in the voltage control system to facilitate the feeding of power to the grid from a DC-bus with a capacitive filter. A DC-DC converter was employed to maintain a fixed DC-voltage on the DC-link and the DC-DC converter was found to be able to maintain the voltage even under cyclically varying output DC voltage from the two linear generator AWS machines. In [84], another MPPT algorithm for wave energy devices is presented. In laboratory tests, the feasibility of the control algorithm was shown

[3]Steca, http://www.stecasolar.com 2009-12-19

in terms of optimizing the energy yield. A time constant in the vicinity of an order of magnitude larger than the average wave period proved most efficient.

In [85] four different interconnection options for direct driven linear permanent magnet point absorber devices are presented. The reduced (resistive) transmission losses are valued against an increasing level of complexity in the system. A high voltage direct current (HVDC) transmission is recommended for the combined case of power levels above 10 MW, transmission distance of more than 10 km and a required transmission voltage above 10 kV.

A very similar approach to such a farm interconnection scheme of directly driven LG WECs is investigated in [69]. A decentralized system with one rectifier, DC-link, inverter and transformer for each LG WEC is compared with a slightly more centralized approach with ten LG WECs interconnected on the same DC-link having only one inverter and transformer. The DC-voltage ripple, the utilization time of the inverters and the variation in combined output power were compared between the two different solutions where the centralized approach was found to be significantly more efficient.

Two different sites in the Baltic and North Sea, one on the Swedish west coast and one on the Danish west coast, are investigated in terms of annual energy yield in [86]. Different grid layouts are discussed. The sites host parks of different sizes and hence some different options for the electrical system are chosen for each site. Some other offshore transmission options are studied and discussed in [87].

In [88] three different grid interface solutions are compared for closely spaced platform-based point absorbers. One of the solutions studied was a direct driven linear generator and the other two were geared rotating generators. A down-scaled hydraulic PTO and a PTO based on a geared induction generator with a full converter was built and tested in real seas. PTO efficiency values in excess of 85% are claimed.

2.7 European wave energy test sites and pilot zones

There are a number of wave energy test sites and pilot zones in Europe, which are listed below. The list, however, is not claimed to be complete. The vast majority of the sites is not yet operational but are in the planning phase or have started to be built. The initiative to several of the sites and pilot zones is taken by national governments or local authorities to promote the development of marine renewable energy technologies (some of the test sites are intended for tidal energy in addition to wave energy), but wave energy in particular. From a local or regional perspective, the aim of most sites is also to increase the production of renewable electricity meeting the increasing demand for energy in general and electric energy in particular.

- The Nissum Broads (Nissum Bredning), about 300 km northwest of Copenhagen, Denmark, 2003 [89, 90].

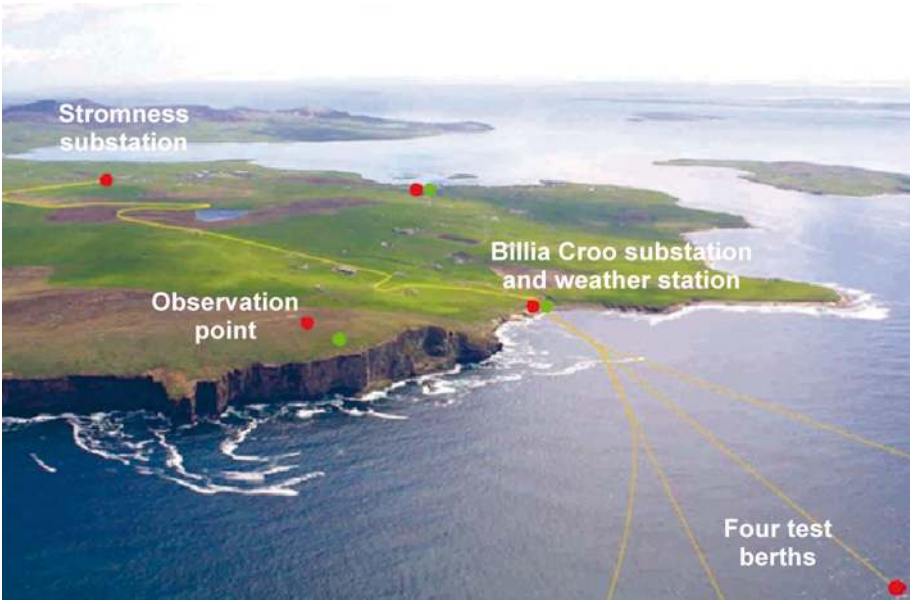

Figure 2.3: The wave energy test site of the European Marine Energy Center, EMEC.

- Galway Bay Test Site[4], 1/4 scale, Ireland, 2004.
- EMEC[5], Orkney, Scotland, completed in 2006.
- Wave Energy Pilot Zone, Near Nazare in the northern part of Portugal, 2008 [91].
- Wave Hub[6], England, under construction.
- SEM-REV, near Nantes in Pays de la Loire, France. To be operational for 2010 [92].
- Belmullet Wave Energy Test Site[7], Annagh Head in Co. Mayo, west coast of Ireland. To be completed in 2011/2012.
- Biscay Marine Energy Platform[8] (BIMEP), on the northern coast of Spain. To be operational for 4^{th} quarter of 2011.

The Lysekil wave energy research site is primarily intended for research of the concept developed at Uppsala University and not for electricity production. It is not open to external developers as most of the sites listed above.

Only four of the above test sites have yet been taken into operation. Nissum Broads being the first one upon the sea trials of the WEC prototype *Wave Dragon* in 2003 [89]. The electrical infrastructure of the test sites/pilot zones

[4]The Marine Institute in Ireland, http://www.marine.ie 2009-12-08
[5]The European Marine Energy Centre, http://www.emec.org.uk/ 2009-12-07
[6]Halcrow, Wave Hub Development and Design Phase: Final Design Report, http://www.southwestrda.org.uk, 2009-12-07
[7]Sustainable Energy Ireland, The Irish Energy Agency, http://www.sei.ie 2009-12-08
[8]EVE, Ente Vasco de la Energia, The Biscay Marine Energy Platform, http://www.eve.es/ 2009-12-07

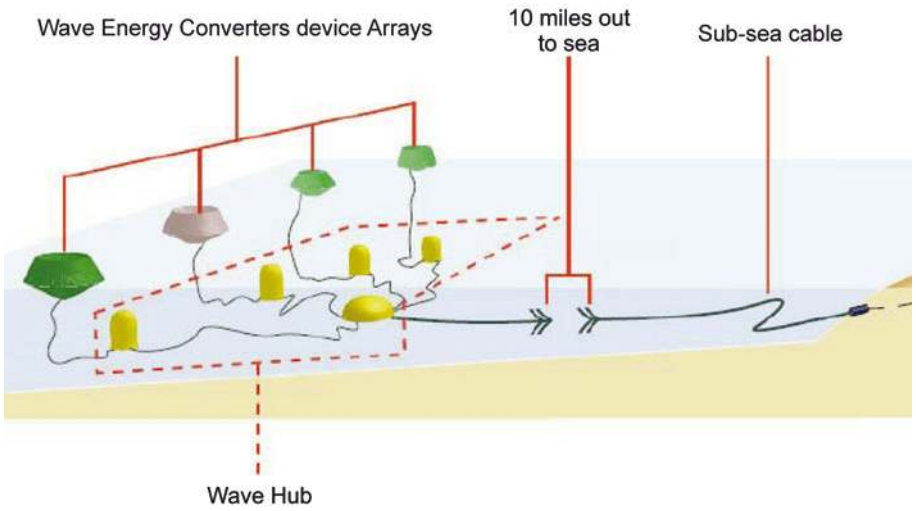

Figure 2.4: The Wave Hub design concept.

will include a switching station (an underwater socket) to which device developers can connect their devices. An exception is Wave Hub, which will have an underwater collector substation. Often the costs for the extension of the on-land grid are covered by the national governments, the test site project owners or alike and the costs for device cables will have to be covered by developers.

The European Marine Energy Center, EMEC, is perhaps the most well-known test site operational today, see Figure 2.3. The electrical infrastructure at EMEC has the possibility of connecting devices to its on-shore substation at Billia Croo, Mainland Orkney via four underwater sockets. An update on the activities at EMEC as of 2007 was made in [93].

The Wave Hub is one of very few underwater collector substation projects in the world [94–97]. See Figure 2.4 for a view of the concept. The Wave Hub project will have four collector substation at the seabed to which the WECs or WEC arrays will be connected at 11 kV. The collector substations will contain step-up $11/24$ kV transformers and switchgear. Individual 24 kV cables connect to a *termination and distribution unit*. From this, a single 24 kV cable will transmit the combined power approximately 25 km to shore where additional voltage step-up to 33 kV will take place. The collector substations are 5 MW each. The total maximum connection power of Wave Hub will thus be 20 MW. The depth at the 8 km^2 site is about $50 - 60$ m.

2.8 Grid connection

2.8.1 Regulations

Grid connection of electricity producing units imposes the application of certain regulations and bylaws. The standard *IEEE 1547-2003* specifies requirements for design of distributed resources and their interconnection with area electric power systems [98]. The main rule is to minimize the impact of the distributed resource on the area electric power system. More specifically, for Swedish generating plants of nominal power 1.5 MW or larger, the regulations in [99] are applicable. However, these basically follow the requirements of the standard IEEE 1547-2003. The regulations to be applied depend on the size of the plant and on the voltage level on which the plant is connected. As a general rule, the smaller the plant power, the fewer the regulations to be applied and the less strict they are. This is somewhat in accordance with the impact the operation of the plant may have on the receiving grid.

With the aim to deliver high-grade electricity to the grid, a number of parameters are used to quantify the level of disturbance. In particular e.g. the parameters listed below are used to characterize voltage disturbances.

- Voltage unbalance
- Flicker emissions
- Harmonics
- Voltage variations
- Transients

Voltage unbalance refers to the phases of a three-phase system where the voltage of one phase is only allowed to deviate to a certain extent compared to the other two phases.

Flicker is a visible light variation in domestic lighting which has its origin in voltage fluctuations. Flicker can be annoying and the maximum flicker emission from a production unit is therefore limited. Voltage variations include flicker, but refers to a broader spectrum of disturbances.

Harmonics is all the frequency content but the fundamental frequency component. Harmonic components might give rise to unwanted mechanical loads (vibrations) in electrical machinery. Harmonics can also give rise to an increased eddy-current loss, which in turn results in increased heating of components. The harmonics disturbance is measured by the total harmonic distortion (THD) and appears as a distorted shape of the voltage (or current) wave form.

Voltage variations can appear over various time periods and can be due e.g. to fluctuations in the primary energy source. Plants of $1.5-25$ MW should be able to maintain its active power production within $90-105\%$ of the nominal voltage on the high-voltage side of the grid-interfacing transformer withing a frequency range of $49-51$ Hz. They should also be able to maintain power production during voltage dips of 75% during 250 ms on one or several phases

followed by a remaining voltage sag of 10%. This facilitates maintained production upon disconnected faults in the receiving grid [99].

Transients are fast voltage fluctuations which are created e.g. from connections or disconnections of generators in the vicinity of the plant or from lightning. Transients on the grid are also generated from switching withing the plant, e.g. disconnection of WECs in a farm.

2.8.2 Power quality in WEC electrical systems

Good power quality, in the broad sense, can be facilitated by a sensible choice of system solution. Below, a few studies that discuss grid connection and control to increase power quality are briefly reviewed.

Single devices and device types with no individual energy buffer are likely to face the largest power quality problems in grid connection operation. Heavily fluctuating output power may have large influence on the power quality and different PTO systems have different challenges. The use of a full-bridge frequency converter (see Section 3.8) based on the VSI technology could facilitate voltage control to some extent but the active power fluctuations are believed to be more difficult to handle since it disturbs the frequency control. Frequency control is carried out by the regulation of active power and voltage control by reactive power regulation. However, the benefits of a full-bridge converter facilitates grid fault ride-through capability to a large extent [100].

Simulations of the grid connection of a floating wave energy converter with a sea cable connection under distorted grid voltage conditions was studied in [101]. An active harmonic compensator was implemented in the inverter control. It was concluded by the authors that the compensator could reduce the 5^{th} and 7^{th} harmonic in the grid so that the THD could be reduced from 10.6% to 6%.

A portable data acquisition (DAQ) system with a 30 kW variable electrical loading system intended for testing of WECs in real seas is described in [102]. An active (controlled) three-phase insulated gate bipolar transistor (IGBT) rectifier is used to emulate a linear and non-linear load respectively. At the output of the rectifier, which has DC-link capacitors, a DC-DC buck converter is placed and at the output there is a resistive load.

A way to reduce the THD in the output voltage and current and at the same time achieve more flexible voltage regulation is to use a *multilevel inverter* (MLI). Such an inverter is also especially suitable for high voltage applications since the voltage applied to the individual power electronic switches ideally is much lower than that in a two-level inverter [103], see further Section 3.8.

3. Theory

The waves considered in this thesis are wind generated waves only. Other types of water waves are *tsunamis* and *tidal waves*. Tsunamis are created by seismic effects, such as e.g. earthquakes. Tidal waves result from the rotation of the Earth combined with the gravitational forces exerted on it mainly by the Moon and the Sun.

The fundamental theory of electromagnetism, except that of Section 3.5, is generic and can be applied to all generators no matter the type. Section 3.5 considers only linear generators. Unless stated otherwise, the theory of Section 3.1 is based on [104], that of Section 3.3 is based on [105] and the theory of Section 3.7 to Section 3.8.3 is based on [106].

3.1 Real ocean waves

Swells are progressive waves that have traveled outside the region in which they were created. A *wind sea*, on the other hand, is made up of waves that have been and are being created by the local winds. While the spectra of swells can be very narrow-banded, a wind sea is highly irregular meaning that they, at best, can be approximated by a linear combination, a *Fourier series*, of harmonic components. What is here referred to as *real ocean waves* can be swells, wind sea, or a mixture of both.

3.1.1 The dispersion relation

As harmonic waves progress towards the shoreline, the waves transform. They get steeper and suddenly, when the depth further decreases, they might break. Breaking waves are highly non-linear. As such, they have to be explained by rather complex mathematical descriptions, see e.g. [107]. For linear waves, that is real ocean waves which can be described by a linear combination of harmonic waves of different frequencies, the *deep-water approximation* simplifies theoretical analyses. It can be used in situations where the surface waves, in reality, are not noticeably influenced by the presence of the seabed.

Water waves are *frequency dispersive*. This means that the phase speed, c_p, of an individual wave in a group of harmonic waves traveling at the group

speed, c_g, is dependent on the frequency of that individual wave. This is expressed in the *dispersion relation*

$$\omega^2 = gk\tanh(kh) \quad \left[1/\mathrm{s}^2\right], \tag{3.1}$$

where ω is the angular frequency of a harmonic wave, g is the acceleration of gravity, h is the water depth and k is the angular wave number

$$k = \frac{2\pi}{\lambda} \quad \left[\mathrm{m}^{-1}\right], \tag{3.2}$$

where λ is the wavelength. If in Eq. 3.1 $kh \gg 1$, then $\tanh(kh) \to 1$ and the dispersion relation simplifies to the deep-water approximation

$$\omega^2 = gk \quad \left[1/\mathrm{s}^2\right]. \tag{3.3}$$

3.1.2 Wavelength, speed and period

It is widely accepted that the deep-water approximation can be used if the depth is equal to or larger than half the wavelength. The wavelength of a harmonic component is

$$\lambda = \frac{2\pi}{k} = \frac{2\pi g}{\omega^2} = \left(\frac{g}{2\pi}\right) T^2 \approx 1.56T^2 \quad [\mathrm{m}], \tag{3.4}$$

where T is the time period of the wave. The phase speed of a harmonic wave is defined as

$$c_p \equiv \frac{\omega}{k} = \frac{g}{\omega} \quad [\mathrm{m/s}]. \tag{3.5}$$

The corresponding group speed, c_g, in deep water is

$$c_g \equiv \frac{\partial \omega}{\partial k} = \frac{g}{2\omega} = \frac{c_p}{2} \quad [\mathrm{m/s}]. \tag{3.6}$$

3.1.3 Wave spectrum

The spectral density function, or simply the spectrum, of a sea state is denoted

$$S(f) \quad \left[\mathrm{m}^2/\mathrm{Hz}\right]. \tag{3.7}$$

From the spectrum, so-called *spectral moments*, which give statistical information about the waves, are defined as

$$m_n = \int_0^\infty f^n S(f) df \quad \left[\mathrm{m}^2\mathrm{Hz}^\mathrm{n}\right]. \tag{3.8}$$

The significant wave height, H_s or equivalently H_{m_0}, can then be calculated as

$$H_{m_0} \equiv 4\sqrt{\int_0^\infty f^0 S(f) df} = 4\sqrt{m_0} \quad [\mathrm{m}], \tag{3.9}$$

where m_0 is the zeroth spectral moment. The energy period, T_E, or equivalently $T_{m_{0-1}}$, of the spectrum is calculated as

$$T_{m_{0-1}} \equiv \frac{m_{-1}}{m_0} \quad [\mathrm{s}]. \tag{3.10}$$

Using Eq. 3.9 and Eq. 3.10, the wave energy transport can be written as

$$J = \frac{\rho g^2}{64\pi} T_{m_{0-1}} H_{m_0}^2 \quad [\mathrm{W/m}]. \tag{3.11}$$

3.2 Point absorbers

A point absorber is a damped oscillator with its body immersed or submerged in the ocean responding to the motion of the waves. To be characterized as a point absorber, the body dimensions (e.g. diameter of buoy) has to be significantly smaller than the incident wavelength.

3.2.1 Single point absorbers

A single axisymmetric point absorber moving only in heave, radiates circular (symmetrical) waves as a result of its oscillation, see Figure 3.1. For the PA to absorb energy, these circular waves have to interfere destructively with the incident waves. To achieve maximum AW, the natural frequency and phase of the PA has to match those of the incident waves, i.e. the radiated waves should have the same wavelength and phase as the incident waves [104]. If this is the case and no restrictions are applied to the oscillator's amplitude, an AW of

$$AW_{max} = \frac{1}{k} = \frac{\lambda}{2\pi} \quad [\mathrm{m}] \tag{3.12}$$

can be achieved [17–19]. If a single axisymmetric point absorber is allowed to move in the three translational modes, surge, heave and sway, then the maximum AW that can be achieved is three times as large,

$$AW_{max} = \frac{3}{k} = \frac{3\lambda}{2\pi} \quad [\mathrm{m}], \tag{3.13}$$

as compared to motion only in heave [19].

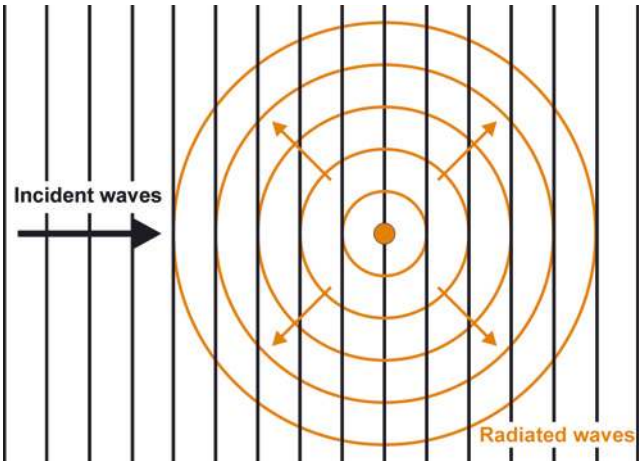

Figure 3.1: A heaving point absorber radiating circular waves as a result of its oscillation.

Budal and Falnes considered an absorption limit for single oscillating bodies moving only in heave. If the buoy is assumed to have a maximum oscillation amplitude of half its draft, i.e. that the buoy is never fully submerged (or that it never leaves the water surface), and if the maximum excitation force is assumed to be equal to the hydrostatic lifting force, then the ratio of absorbed power to the buoy volume, V, is limited by

$$\frac{P}{V} < \frac{\pi \rho g H}{4T} \quad \left[\mathrm{W/m^3}\right] \tag{3.14}$$

where ρ is the density of water, and H is the height (twice the amplitude) of a sinusoidal wave.

The *Froude-Krylov Approximation* can be utilized if the ratio of PA diameter to the wavelength is less than about 0.2, then the excitation (scattering) force on the body can be calculated solely from integrating the pressure from the waves on the wetted body surface without considering the impact from diffracted waves, a quantity that is more complicated to attain. However, with considerably smaller body diameter, viscosity effects might become more important [108].

For oscillating PA bodies that are non-symmetric, the maximum AW is not the same as for axisymmetric bodies. Newman showed theoretically that the maximum AW that could be reached for these types of body in horizontal body motion (surge) is

$$AW_{max} = \frac{\lambda}{\pi} cos^2\theta \quad [\mathrm{m}], \tag{3.15}$$

which thus for $\theta = 0, \pi$ becomes λ/π, which evidently is twice that of an axisymmetric body in heave [109]. θ is the angle of the incident waves on the non-symmetric body.

The above limits for single bodies may be difficult or very difficult to reach in practice. This is due to the constrained body amplitudes which is often necessary in real systems. The smaller the diameter of an axisymmetric body, the larger the oscillation amplitude required to reach the maximum AW.

3.2.2 Point absorber arrays

If an infinite row of equally spaced point absorbers oscillate in an optimum manner in monochromatic harmonic waves, provided that the spacing is less than one wavelength, all of the incident power can be absorbed by the array. This requires that the bodies are either oscillating in at least two degrees of freedom (e.g. heave and surge) or that the bodies are significantly asymmetric. If the motion is restricted to one degree of freedom only, and the bodies in the straight infinite row instead are axisymmetrical, the maximum absorbed power is half the incident wave power.

3.3 Magnetism

3.3.1 The origin of magnetic flux density

In the center of a 1 m-diameter circular coil with one single turn, a magnetic field strength, **H** of 1 A/m, is produced if a steady current of 1 A runs through the coil [105]. Naturally, in a real magnetic circuit the current path is arbitrary. *Ampere's law*

$$Ni = \oint \mathbf{H} d\mathbf{l} \quad [\mathrm{A}], \tag{3.16}$$

relates the number of turns, N, in a circuit carrying the current, i, to the magnetic field, **H**. **l** is a line vector. Ni equals the integral of $\mathbf{H}d\mathbf{l}$ around a closed path enveloping the current-carrying conductor.

In the presence of a magnetic field, a magnetic flux, Φ, is always present. The unit of magnetic flux is 1 Wb or 1 Vs. If a magnetic flux of this magnitude is uniformly reduced to zero in 1 s, a voltage, E, of 1 V is induced in the conductor enclosing the flux. This is utilized in the design of electrical machines e.g. to calculate the no-load voltage and is called *Faraday's law* which states

$$E = -N\frac{d\Phi}{dt} \quad [\mathrm{V}], \tag{3.17}$$

where $d\Phi/dt$ is the rate of change of magnetic flux. The minus sign in front of N is a result of *Lenz's law* which states *"induced voltage is in a direction which opposes the flux change producing it"*.

If a magnetic field, $\mathbf{H}$, is applied to a medium, a magnetic flux density, or magnetic induction, $\mathbf{B}$ measured in T or $\mathrm{Vs/m^2}$, is produced in that medium. Different media respond differently to an applied magnetic field. In free space, magnetic induction is related to the applied magnetic field by the permeability of free space, μ_0, according to

$$\mathbf{B} = \mu_0 \mathbf{H} \quad [\mathrm{T}], \tag{3.18}$$

where $\mu_0 = 4\pi \times 10^{-7}$ H/m. As will be seen in Section 3.3.3, in many materials there is a non-linear relationship between the magnetic induction and the externally applied magnetic field, i.e. μ is a function and not a constant. Ferromagnetic materials, e.g. steel, is one such class of materials where this holds true. In these materials, if the magnitude of the applied positive (or negative) field is limited the relationship can, as an approximation, be assumed linear in that region. The resulting constant value of dB/dH is denoted relative permeability, μ_r, and is a material-specific parameter. In the general case,

$$\mathbf{B} = \mu \mathbf{H} = \mu_r \mu_0 \mathbf{H} \quad [\mathrm{T}]. \tag{3.19}$$

Eq. 3.19 can be used e.g. to calculate the magnetic induction in air ($\mu_{r,air} \approx 1$) and in soft magnetic materials such as steel or iron.

Even though the external magnetic field, $\mathbf{H}$, is zero, a material can still have magnetic induction, $\mathbf{B}$. We introduce the magnetization, $\mathbf{M}$, which, as $\mathbf{H}$, is measured in A/m.

According to Gauss's law (here given in integral form)

$$\oint \mathbf{B} d\mathbf{A} = 0, \tag{3.20}$$

all flux entering a closed surface will also leave it. This can also be phrased as that "there are no magnetic monopoles" or "all flux lines of $\mathbf{B}$ must be closed". However, in the study of magnetic materials, two convenient mathematical models, which are artefacts rather than real physical entities, that are commonly used to explain magnetic materials are the *current loop* and the *magnetic pole*. Choosing the latter for further explanation, a magnetic dipole moment, $\mathbf{m}$, can be defined as

$$\mathbf{m} = p\mathbf{l} \quad \left[\mathrm{Am^2}\right], \tag{3.21}$$

where p is the pole strength, i.e. two opposite magnetic monopoles of pole strength p, separated by a distance $\mathbf{l}$, forms a magnetic dipole, which can be

considered as the most elementary entity in magnetism. A strong permanent magnet, which is a magnetic dipole, produces a strong magnetic flux, Φ. The pole strength might therefore be written in terms of the magnetic flux as

$$p = \frac{\Phi}{\mu_0} \quad [\mathrm{Am}], \tag{3.22}$$

and using this and Eq. 3.21, the magnetization, or the magnetic moment per unit volume, can be written as

$$\mathbf{M} = \frac{\mathbf{m}}{V} = \frac{p\mathbf{l}}{A\,|\mathbf{l}|} = \frac{\Phi}{\mu_0 A}\hat{l} = \frac{BA}{\mu_0 A}\hat{l} = \frac{\mathbf{B}}{\mu_0} \quad [\mathrm{A/m}], \tag{3.23}$$

where $\hat{l}$ is a unity vector. The magnetic induction, $\mathbf{B}$, can now be written in terms of the magnetization and magnetic field as

$$\mathbf{B} = \mu_0(\mathbf{H} + \mathbf{M}) \quad [\mathrm{T}]. \tag{3.24}$$

This expression is always valid since, as opposed to in Eq. 3.19, a value of the magnetic induction can be found even when there is no external magnetic field.

3.3.2 Hard magnetic materials

Electric machines such as generators and motors can be constructed with permanent magnets. Permanent magnets are made from hard magnetic materials. The specific property of hard magnetic material, which make them highly suitable for permanent magnets, is the high energy required to change their magnetization. They have a wide hysteresis-loop, meaning they have a large coercive field in combination with a high remanent induction. Hence, PMs have a high energy product, $(\mathbf{BH})_{\max}$. The energy product is defined in the second quadrant of the hysteresis curve and is a measure of the amount of useful work the permanent magnet can perform outside the magnet. The higher the energy product of the hard magnetic material, the stronger the magnetic field the magnet can produce in a magnetic circuit of e.g. an electric machine per unit volume.

Permanent magnets can be demagnetized primarily in two ways:

- by heating the magnet above the Curie temperature.
- by applying an opposing magnetic field equal to or larger than the coercive field, H_c.

Quite commonly mechanical impact is also listed as a reason for demagnetization. However today the coercive fields of good PM materials are too high for this to occur [110]. The risk upon mechanical impact is rather to physically

break the magnet since the PM materials, e.g. sintered Nd-Fe-B, are brittle and thus easily can be scattered.

The coercivity of commercial Nd-Fe-B magnets is around 1.12 MA/m and the remanent induction is about 1.3 T. The energy product is approximately 320 kJ/m^3.

3.3.3 Soft magnetic materials

The most important feature of soft magnetic materials is their extremely high relative permeability. This facilitates leading magnetic flux in predestined paths, which is very useful in the design of magnetic circuits. The use of soft magnetic material also facilitates sources of magnetic field (PMs or a current-carrying coil of conductor) to perform much better than would they in a magnetic circuit with only air as conductor of the field.

Soft magnetic materials, and in the area of general electric machinery this is exclusively various steel qualities, are alloyed with other elements to give them certain qualities. As an example, a few percent of Si is added to reduce the conductivity of the material. This is important to lower the *eddy-current losses*, see Section 3.4.2.

3.4 Electromagnetic losses in electrical machines

Considering the almost exclusively used materials, steel and Cu, as the core material and conductor material respectively in electrical machines, the electromagnetic losses can be classified as iron losses and Cu-losses. (In this thesis, insulation polarization losses are excluded.) Depending on the design of the machine, there might also be eddy-current losses in other materials in, or close to, the actual magnetic circuit. All together, the following electromagnetic losses are generally considered and will be explained in Sections 3.4.1 - 3.4.4:

- hysteresis losses, W_h
- eddy-current losses, W_{ec}
- anomalous losses, W_a
- resistive losses, P_{Cu}.

The total loss, provided that the same loss occur in all parts of the core, is simply calculated as

$$P_{tot} = (W_h + W_{ec} + W_a)V_{core} + P_{Cu} \quad [\mathrm{W}], \tag{3.25}$$

where V_{core} is the total volume of the core to attain the loss in W from the loss densities.

In the following sections, it should be noted that when applying the theory to linear generators, the electrical frequency, f_e, is a time-dependent function rather than a constant.

3.4.1 Hysteresis losses

The hysteresis loss is dependent on the appearance of the hysteresis curve of the material. The larger the enclosed area of the hysteresis curve, the larger the hysteresis loss. The hysteresis curve can be altered e.g. by heat treatment and the way the steel is rolled during the manufacturing process. Several of the properties can be changed independently of the other, e.g. the coercivity and the remanence. The hysteresis loss density can be calculated using the expression

$$W_h = k_h f_e B_{max}^n \quad \left[\mathrm{W/m^3}\right], \tag{3.26}$$

where k_h is a material-specific constant which is also dependent on the stacking pressure in the stator (or e.g. in the core of a transformer). f_e is the electrical frequency and B_{max} is the peak of the magnetic induction. In most cases when generators are considered $n = 2$ but in a more general case the value could be $1.5 < n < 2.5$ [111].

3.4.2 Eddy-current losses

Eddy-current losses result from induced voltages (which drive currents). In a conducting material subjected to a varying magnetic field, a voltage will be induced. This voltage will drive a (short-circuit) current in the conducting material, be it a conductor or some part of the magnetic circuit, in such a direction that the field created by this current opposes the direction of the source field. Using a readily available steel alloy with low conductivity, as already mentioned in Section 3.3.3, for the stator core, the eddy-current loss can be reduced. Further reductions can be made by reducing the size of the induced loss current loops. This is made by laminating the core. Lower losses are achieved the thinner the sheet thickness in the lamination. However, reducing the sheet thickness adds cost in the manufacturing process since more plates will have to be produced.

In generators, non grain-oriented steel is used and the eddy-current loss is usually calculated by

$$W_{ec} = k_e f_e^2 B_{max}^2 \quad \left[\mathrm{W/m^3}\right], \tag{3.27}$$

where k_e is dependent on the sheet thickness in the lamination and is inversely proportional to the material resistivity.

Eddy-currents also appear in the windings of electrical machines and in the PM magnets and back-iron, and other parts, of a rotating or linear PM generator taken that a flux change is present. However, from an engineering perspective, these losses can in some cases be neglected, primarily in the very low-frequency application considered in this thesis. In a PMLG, the translator is likely to partly slip out the stator due to the difference in length between the two and the motion pattern of the translator. The reluctance of the magnetic circuit in which the magnets on the translator is located will change greatly. This flux change will induce eddy-current losses in the PMs and in the translator back iron.

3.4.3 Anomalous losses

On a microscopic level, a ferromagnetic material consists of magnetic domains. The walls between, or boundaries of, these domains are characterized more or less by the transition from one direction to another of the magnetic moment. The magnetic moment of the domains will be affected by an applied external field and the domain walls will then move slightly. This requires some energy and hence a loss arises. The loss associated with domain structure changes is referred to as anomalous losses and can be calculated as

$$W_a = k_a \left(\frac{dB}{dt} \right)^{3/2} \quad \left[\mathrm{W/m^3} \right], \tag{3.28}$$

where k_a is a material-specific constant which can be determined from experiments. The anomalous losses are sometimes referred to as *excess losses*.

3.4.4 Resistive losses

Resistive losses occur as a result of the resistivity of the stator winding conductor material. The resistance is slightly temperature-dependent, but if the cooling of the stator winding is sufficient, only a limited temperature increase will occur and hence the resistance can be considered constant. In a linear generator, due to the unbalanced, asymmetric, nature of the output from the point of view of damping the generator in a non-linear fashion and the fluctuating amplitude and frequency of the voltage, the phase currents will differ greatly in amplitude and also in frequency at a specific time instant. The resistive losses are therefore calculated from the *momentary* line currents as

$$P_{Cu} = R_g (I_A^2 + I_B^2 + I_C^2) \quad [\mathrm{W}] \tag{3.29}$$

in place of $P_{Cu} = 3R_g I^2$ which can be used in balanced three-phase systems. R_g is the phase resistance of the linear generator and $I_{A,B,C}$ are the three line currents respectively.

3.5 No-load voltage of an LG in sinusoidal oscillation

Considering a purely sinusoidal motion of the LG translator, the induced three-phase no-load voltages can, by using Faraday's law (Eq. 3.17), be described by

$$E_n(t) = -N\frac{d\Phi}{dt} = -\hat{V}_p cos(\omega t) cos\left(\frac{\pi d}{\lambda_m} sin(\omega t) + n\frac{2\pi}{3}\right) \quad [\mathrm{V}] \tag{3.30}$$

for $n = -1, 0, 1$, and where $\hat{V}_p$ is

$$\hat{V}_p = N\hat{\phi}\omega\pi\frac{d}{\lambda} \quad [\mathrm{V}]\,. \tag{3.31}$$

N is the number of coil windings, Φ is the time-varying magnetic flux with amplitude $\hat{\phi}$, d is twice the amplitude of the translator oscillation and λ_m is the distance between two magnets with the same polarity, i.e. the magnetic wavelength [45].

3.6 Damping

The damping applied to the buoy can, as a simplification, be calculated from the electric power and Cu-losses in the LG and WEC cable by setting

$$P_{mech} \approx P + P_{Cu} + P_{cable} \quad [\mathrm{W}]\,, \tag{3.32}$$

where P_{mech} is the mechanical power, which is equal to the absorbed wave power, P is the electrical power delivered to the load. P_{Cu} is the copper loss in the generator, and P_{cable} is the resistive power loss in the cable between the WEC and the substation and dump load respectively (same), see Section 4.5.2. All the mechanical losses in the WEC and iron losses in the LG will then be neglected. Second, the speed, $\dot{x}$, of the translator can be calculated from e.g. the zero-crossings of the phase voltages. In addition, a factor compensating for the varying overlap between stator and translator is given in [37] and is

$$A_{fac} = \begin{cases} 0, & \text{if } |x| \geqslant \frac{1}{2}(l_t + l_s) \\ 1, & \text{if } |x| \leqslant \frac{1}{2}(l_t - l_s) \\ \frac{1}{l_s}\left[\frac{1}{2}(l_t + l_s) - |x|\right], & \text{else,} \end{cases} \tag{3.33}$$

where x is the translator position, and l_t and l_s are the length of the translator and stator respectively. The damping factor, γ, is then

$$\gamma = \frac{P_{mech}}{A_{fac}\dot{x}^2} \quad [\mathrm{Ns/m}]\,. \tag{3.34}$$

Due to the unsymmetrical nature of the three-phase voltage, the electrical power, P, (and the corresponding resistive losses) has to be calculated from the *momentary* values of phase voltages and currents according to

$$P = U_{LN_A} I_A + U_{LN_B} I_B + U_{LN_C} I_C \quad [\mathrm{W}]\,. \tag{3.35}$$

3.7 Three-phase diode rectifiers

In a balanced three-phase system, the line-to-neutral voltage vectors have constant length and rotates with the electrical frequency f_e. When connecting this to a six-pulse diode rectifier, the diodes in the rectifier conduct in the sequence shown in Figure 3.2. The line-to-line voltage applied to the bridge rectifier during each time interval is indicated below the curves.

3.8 Three-phase inverters

A *three-phase full-bridge inverter* is used to convert DC to three-phase AC, see Figure 3.3. Terms that are also commonly used are *frequency converter*, *DC-to-AC converter* or just *three-phase inverter*. It requires a minimum of six semiconductors. A three-phase inverter also requires a driver circuit and a unit providing digital level control signals. The insulated gate bipolar transistors (IGBTs) 1, 3 and 5 in Figure 3.3 are called the *high side* and the IGBTs 2, 4 and 6 are called the *low side*. The timing of the switching of the high and low side semiconductors thus have to be controlled carefully to avoid closing a low-side and a high-side switch in the same "leg" simultaneously which would result in a short-circuit of the DC-voltage source.

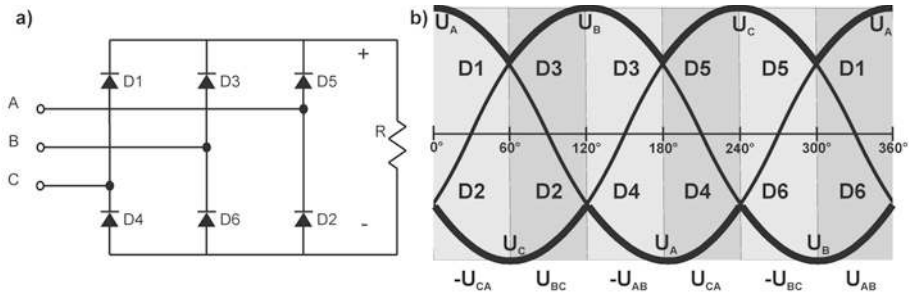

Figure 3.2: (a) A three-phase diode rectifier. (b) Sinusoidal line-to-neutral voltages of a balanced three-phase system connected to a six-pulse diode rectifier. The D's indicate which diodes conduct during each interval. The line-to-line voltage applied to the rectifier during each time interval is indicated below the curves.

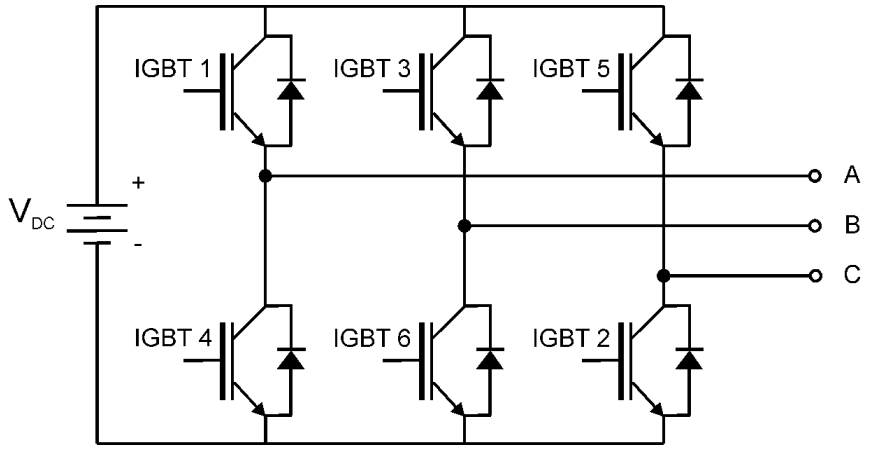

Figure 3.3: A three-phase IGBT-inverter with DC source.

As mentioned in Section 2.8.2, the multilevel inverter topology has potential to reduce THD and increase the flexibility in voltage control. Such an inverter would also be quite suitable for the underwater substation system researched in this thesis. The most common layouts of multilevel inverters are three or five levels. As an example, a single-phase five-level MLI intended for solar photo voltaics was simulated and tested in [112]. Improvements in THD were shown compared to a three-level inverter. A comparison of state of the art MLIs is made in [113]. Three categories of MLIs are listed:

1. Neutral Point (or Diode) Clamped MLI
2. Flying Capacitor MLI
3. Cascade Cell MLI.

A control method for balancing the DC-link voltage in a three-level Neutral Point clamped MLI is presented in [103]. A snubber circuit for a Flying Capacitor MLI is suggested and explained in [114]. In [115], another DC-link voltage control method is proposed for a Cascade Cell MLI which is designed for use in a static synchronous compensator.

3.8.1 The insulated gate bipolar transistor

The insulated gate bipolar transistor, see Figure 3.4, being first demonstrated in 1982, is the most widely used power semiconductor in the range of a few kilowatt to a few megawatt. It dominates applications from about 600 V to 3 kV and above 600 V, the IGBT has lower on-state losses than MOSFETs. Single-chip IGBTs can handle at least 100 A and block voltages of about 3 kV. Several IGBT-chips paralleled in one package is called an IGBT *module* and can thus handle currents of several hundred amperes.

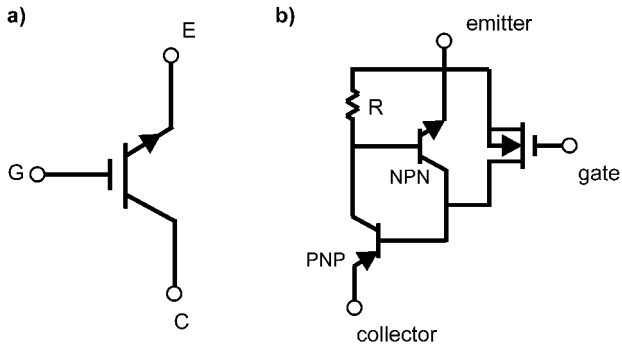

Figure 3.4: (a) The IGBT circuit symbol and (b) the IGBT equivalent circuit.

For switching, the IGBT requires a driver circuit and a control signal. The driver has to be capable of supplying a sufficient charge to the gate of the IGBT in sufficiently short time.

3.8.2 Pulse width modulation

The *pulse width modulation* (PWM) method is very common for the switching of power electronic components. The method is based on the creation of a carrier wave and a modulation signal. The carrier wave is often a triangular or saw-tooth wave of constant (high) frequency, which is compared with the modulation signal. The output voltage wave form will have the same frequency as the modulation signal. The desired appearance of the output voltage hence determines the choice of modulation waveform. For sinusoidal output, a sinusoidal wave form is chosen as modulation signal and for simple DC step-down of a DC-voltage, a DC-signal is chosen. When the modulation signal is greater in amplitude than the carrier wave, the signal to the driver circuit, which is to amplify this control signal to switch the power semiconductor device, is high (one), otherwise low (zero). The load will only appreciate the average value of the output voltage. The switching frequency will instead show as harmonic content in the output voltage. The higher the switching frequency, the smaller the size of passive components required to filter the high-frequency harmonic components in the output.

3.8.3 Losses in switched semiconductor devices

Theoretically, the on and off-state of an IGBT are both loss-free. Either the current is zero (off-state) or the voltage is zero (on-state). Unfortunately, in reality there are losses in both cases.

On-state losses (conduction losses) are due to the inherent voltage-drop of the semiconductor device, which during current conduction will produce a power loss equal to the voltage drop times the current. The on-state voltage

drop is reduced with higher gate-to-emitter voltage applied. For an IGBT, the voltage drop is usually in the range of 1 - 2 V.

Switching losses are due to that during a switching event, primarily at the turn-off of the device, a voltage is present at the same time as some current is still flowing. To reduce the switching losses, the turn-on and turn-off events have to be made as quickly as possible. The careful design of driver circuits thus is very important to achieve high efficiencies in inverters. Choosing a very high switching frequency will also strongly influence the switching losses. However, to lower electromagnetic noise emissions in electrical machines, inverters and motor drives can have switching frequencies of about $10-20$ kHz.

4. Experimental work

The author has made different contributions to the equipment installed at the Lysekil wave energy research site and to laboratory experimental set-ups. In this chapter, these contributions are described in detail. The main areas are linear generator prototype testing, WEC prototype mechanical structure design, WEC electrical connections and finally collector substation design, construction, implementation and testing. The author's contributions to each respective paper are specified in Chapter 9.

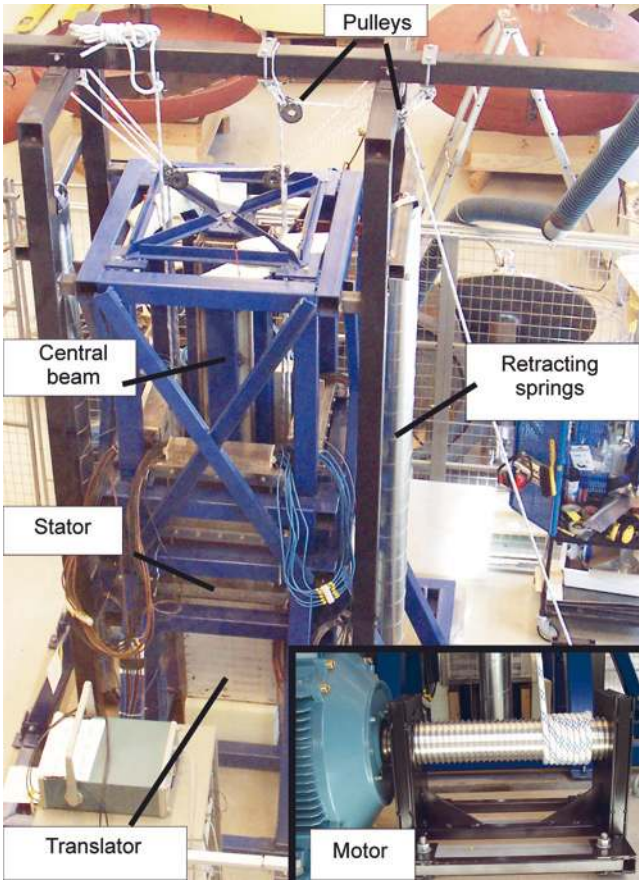

Figure 4.1: The laboratory LG experimental set-up with motor and pulleys.

4.1 Linear generator

One of the first steps in the experimental work was to implement a test rig for a laboratory experimental linear generator, see Figure 4.1. The intention of building the LG experimental set-up was to validate the FEM design tool, which was used to design the LG, and to gain practical experience in constructing and assembling a PM linear generator, one of the difficulties being the large attractive forces between the stator and the translator. Another presumed difficulty was to assemble the translator with its powerful and relatively large Nd-Fe-B magnets. The novel feature of the generator was, above all, its winding, which is made of PVC-insulated Cu-cables with circular cross-section.

The laboratory LG is a permanent magnet synchronous generator (PMSG) with surface-mounted Nd-Fe-B magnets. The stator winding conductor area is 16 mm^2. The generator was originally designed for 10 kW, but the built generator was rated at half that power [116]. The generator design rating parameters are listed in Table 4.1.

In the constructed prototype machine, an air-gap of 3 mm could never be realized since the mechanical structure was too flexible to withstand the attractive forces between the translator and the stator. The stator of the constructed machine was also made about 50 mm longer (in the vertical direction) than set in the FEM design tool. Hence, the stator of the prototype is 750 mm long which, with a pole width of 50 mm, adds up to 15 poles instead of 14 poles. Because the translator was built with half the number of poles, while the stator

Table 4.1: *The rating parameters and main features of the laboratory linear generator (design values).*

Power	5 kW
Voltage (line-to-line)	100 V
Current	28.9 A
Speed	0.67 m/s
Conductor area (Cu)	16 mm^2
Slots per pole and phase	6/5
Pole width	50 mm
Air-gap	3 mm
Stator length	700 mm (14 poles)
Translator length	650 mm (13 poles)
No. of stator sides	4
Width of stator side	400 mm
Active gen. area	1.04 m^2

was built slightly larger, the resistive Cu-losses in the constructed machine are probably slightly larger than the 10 % specified in [116]. These differences were implemented in the FEM model for comparison with experimental results.

The laboratory generator was dismantled in October 2009 to make space for assembling underwater substation no. two, see Chapter 7.

4.2 Sea cable at the Lysekil research site

In preparation of the deployment of L1, a sea cable was installed at the Lysekil research site in February 2006. Some pictures from the deployment are shown in Figure 4.2. The length of the cable is approximately 2.9 km of which about $200 - 250$ m is on shore between the shoreline and the measuring station on Härmanö, see further Section 4.3. The cable is an armored PVC-insulated cable with four Cu conductors of 95 mm^2. On land, where possible, the cable was hidden in clefts and shrubberies to keep the visual impact at a minimum. Offshore, near the site, the cable has some slack. This is partly due to that it was uncertain with what precision L1 could be submerged at its predestined position. It is also partly due to the fact that some slack is needed when the cable is lifted to the surface to make joints, which e.g. was done at the deployment of the underwater substation. Figure 4.3 shows L1 with the electrical system used in the respective experiments with L1.

4.3 On-shore measuring station

The land connection of the wave energy converter array is made to the island Härmanö, which is located approximately 2 km from the Lysekil research site in an easterly direction. Härmanö is a nature preservation area, and only a small 10 m^2 cabin was allowed to be erected. Here, a PC is installed for DAQ and for storage of data. There is also a diode rectifier and a set of voltage-smoothing ultra capacitors along with current sensors and circuit breakers allowing for control of the AC- and DC resistive loads placed on the outside wall of the measuring station.

4.4 Wave energy converter

The first prototype wave energy converter, L1, was deployed in March, 2006. It was then connected to the sea cable, see Section 4.2, and a cylindrical 3 m-diameter buoy was attached to it. In the first run it was operated for about two and a half months.

Figure 4.2: Some pictures from the installation of the sea cable which today connects the substation to the measuring station on island Härmanö.

The electromagnetic design of L1 was mainly based on the design of the laboratory generator, see Section 4.1, with minor changes. The ratings of L1 are listed in Table 4.2.

A stiff steel structure supports the linear generator and maintains the LG air-gap of 3 mm separating the translator from the stator. The structure holds the rails of a bearing system, the wheels of which are mounted on the translator. L1 is encapsulated in a 5 m tall steel casing. On top of this is a line guidance system, see further Section 4.4.1. The capsule is bolted onto a 50 tonne concrete foundation to hold it in place on the seabed. More detailed mechanical measures of L1 can be found e.g. in [117].

4.4.1 Buoy line guidance system

The piston sealing in the upper lid of the WEC capsule is very sensitive to horizontal stress. A *line guidance system* was therefore implemented in the WEC. This is seen in Figure 4.4 (a). The system consists of a mechanical steel structure welded to the top lid of the WEC capsule. The buoy line, which is connected to the top of the piston rod, runs through the structure and horizontal forces induced by the surging motion of the buoy are thus absorbed by

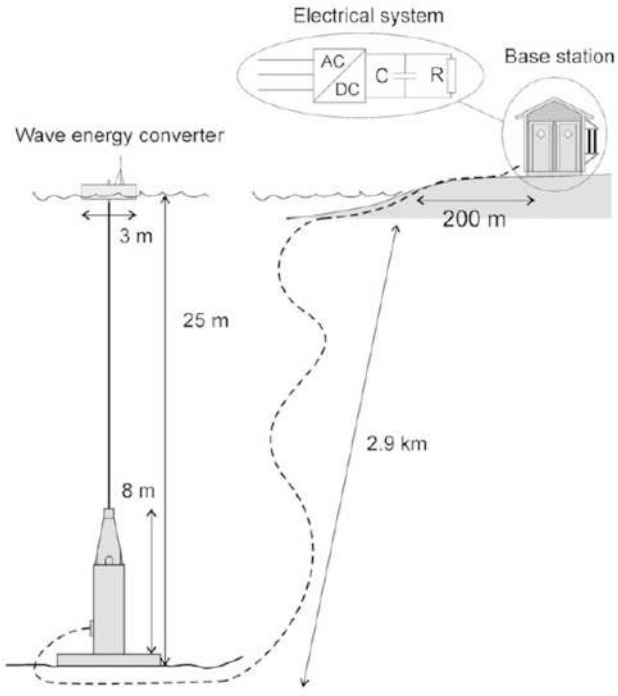

Figure 4.3: WEC L1 with its connection to shore and the electrical system in the on-shore measuring station. From Paper VI.

Table 4.2: *The rating parameters and main features of the L1 LG.*

Power	10 kW
Voltage (line-to-line)	200 V
Current	28.9 A
Speed	0.67 m/s
Conductor area (Cu)	16 mm^2
Slots per pole and phase	6/5
Pole width	50 mm
Air-gap	3 mm
Stator length	1264 mm (25 poles)
Translator length	1867 mm (37 poles)
No. of stator sides	4
Width of stator side	400 mm
Active gen. area	2.0 m^2

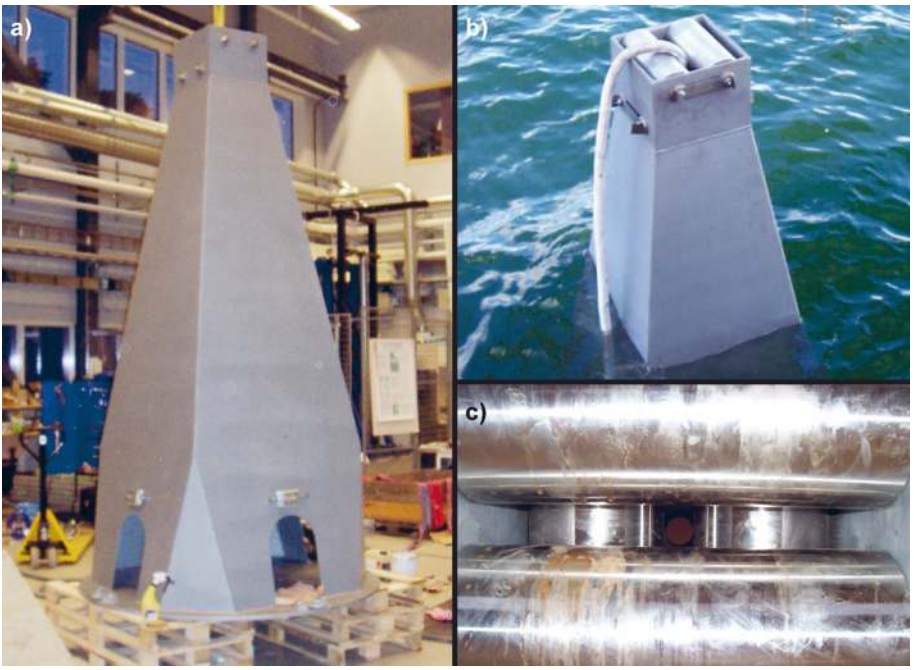

Figure 4.4: (a) The structure of the line guidance system welded to the top lid of L1. (b) The two levels of cylinders for guidance of the buoy line in the top of L1. (c) The line guidance cylinders seen from below.

the structure instead of by the sealing. The resulting stress in the mechanical structure is transmitted via the capsule to the concrete foundation.

In the top of the line guidance system, two different mechanisms for force transmission have been tested in offshore operation. The first mechanism consisted of two levels of horizontally oriented stainless steel cylinders, see Figure 4.4 (b) and (c). The axis of rotation of the two cylinders at the lower level is perpendicular to the axis of rotation of the two cylinders in the upper level. The levels of cylinders were separated by a distance preventing them from rubbing against each other. The mechanism would then fulfill its purpose to support the buoy line in the horizontal plane. However, it turned out that the stainless steel cylinder bearings and the rubber sealings, used to seal off the bearings from seawater, applied such a frictional torque that the cylinders did not rotate. Instead, the line slid on the surface of the cylinders. In addition, the diameter of the cylinders was rather small, which probably caused the line to break.

The second force transmission mechanism was a stainless steel funnel, which was fitted to the top of the line guidance structure where the cylinders had been mounted. The funnel was meant to provide an axisymmetric low-friction sliding surface for the buoy line, see Figure 4.5. This system is also implemented in WECs L2, L3 and L9.

Figure 4.5: Vectran-cored buoy line with a *Dyneema* cover running through the stainless steel funnel in the top of WEC L1. The funnel supports the line in the horizontal plane to protect the piston rod sealing in the top lid of the capsule from this stress.

4.4.2 Electrical connection

Each WEC is connected to the substation by an individual power cable. L1 is connected to the substation by the same type of cable as the sea cable between the substation and shore (an armored PVC-insulated cable with four Cu-conductors of cross section 95 mm^2). L2, L3 and L9 are connected by means of rubber-insulated cables with four Cu-conductors of cross section 16 mm^2.

The WEC power cable is connected to the WEC in an external junction box outside of the WEC capsule. The generator stator winding conductors are lead through the capsule by means of cable glands and are joined with the conductors of the WEC power cable. The junction box is filled with polyurethane resin and sealed with a steel plate. On L1, L2 and L3, the WEC power cable is strain-relieved by fastening it to the WEC capsule below the junction box, and on L1, which has a larger cable, also to the concrete foundation.

4.5 Offshore underwater collector substation

As many WEC concepts are based on relatively large machines interconnected at a voltage level of 10 kV or more, each unit is likely to deliver power at a stabilized 50 Hz electrical frequency prior to being interconnected with other machines in an offshore collector substation, see e.g. Section 2.6 and the technology review in [4]. Due to great similarities in the electrical layout with offshore wind farms, these projects or devices could benefit to a large extent from the offshore wind industry utilizing the experience from mono piled offshore

Figure 4.6: The underwater collector substation standing on the seabed.

collector substations built up to date in offshore wind farms, see e.g. [118]. However this solution might, from an economical point of view, be unrealistic for more pronounced array devices such as point absorbers which in most cases are rated at much lower power at an individual scale. The collector substation will then also be rated at relatively low power, a few MW rather than ten's or even hundred's of MW, and an elevated platform could be too expensive. For these devices an offshore underwater collector substation[1] of the type researched in this thesis could be a feasible solution.

Figure 4.6 shows an underwater image of the collector substation on the seabed. Beneath the vessel, some WEC power cables and signal cables are connected to the lower dished end.

4.5.1 Mechanical design

The substation is based on a 3 m^3 pressure vessel of 3 bars, which is moored by a concrete foundation keeping it stationary on the seabed. The cylindrical

[1] In this thesis, the word *underwater*, oftentimes preceded by *offshore*, replaces *marine* when a reference is made to the collector substation. This was chosen despite the use of the term *marine* in several of the papers, e.g. in Paper XI, VI and XII. However, in Paper XIII and XIV, *offshore underwater substation* is used. The reason for using this slightly different name is to highlight the novel features of the substation. In the author's opinion, a *marine* substation could be placed on a platform and that platform could be placed anywhere on or just outside the coastline. However, the name *offshore underwater* substation highlights both the global and local placement.

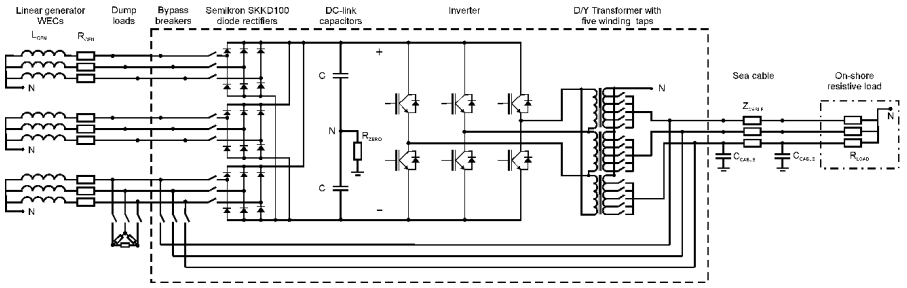

Figure 4.7: The connection diagram of the substation main circuit. The dashed rectangle indicates the components included in the substation. The dash-dotted rectangle is an indication of the components in the on-shore measuring station.

part of the shell has a diameter of 1250 mm and the material thickness is 6 mm. A dished end is welded to the top of the cylindrical shell. The lower dished end of the vessel is removable and is fastened by means of a bolt flange. Mechanical reinforcements were added to cope with possible external pressures on the construction due to its location on the seabed. A vertical orientation of the hull was chosen to prevent possible leakage in the bolt flange O-ring sealing, or dished end cable lead-throughs, from damaging any of the electrical equipment. All electrical equipment has been mounted directly onto steel plates welded to the inside of the hull some distance above the position of the bolt flange sealing. The pressure vessel is approved for operation at 3 bar according to the European standard for unfired pressure vessels [119].

4.5.2 Main circuit

The main circuit of the substation is shown in Figure 4.7 and consists of a dump load with a circuit breaker, an input circuit breaker, a rectifier, DC-bus capacitors, an inverter, a transformer and output circuit breakers. Each WEC can be by-passed through the substation in order to be operated with the resistive loads and/or rectifier available in the on-shore measuring station. The nominal ratings of the substation and its components can be found in Table 4.3

Table 4.3: *The nominal ratings (continuous) of the substation.*

Substation power	96 kVA
Substation output voltage	1 kV
Max. DC voltage	500 V
DC-link capacitance	0.24 F
Transformer winding ratios	$1000/250, 180, 125, 100, 80$

Figure 4.8: (a) A dump load during construction. (b) The dump load of L3 being prepared for deployment.

and below follows a step-by-step description, from left to right in Figure 4.7, of the main circuit components.

4.5.2.1 Dump load

Each WEC has a dump load. The dump load is a set of immersion heaters with sealed circuit breakers placed on the seabed outside the substation, see Figure 4.8. The dump loads are attached to each of the WEC power cables. For L1-L3, the resistance in delta is 12 Ω. The dump load is activated as soon as a WEC is disconnected electrically or physically from the substation. A 24 V DC signal is then disabled which closes the circuit breaker thus connecting the dump load. In this way, the WEC buoy motion is always damped should the ability of the substation to transmit power to shore cease. Upon faults, e.g. if the substation over-voltage protection would be activated, the WEC in question is disconnected from the substation and the dump load is activated.

4.5.2.2 Circuit breakers

In the main circuit, there are a number of circuit breakers. Since the voltage of the WEC LGs is rather low, 600 V-contactors are used except on the high-voltage side of the transformer where contactors for 1 kV is used. The transformer high-voltage side contactors are also used for switching between

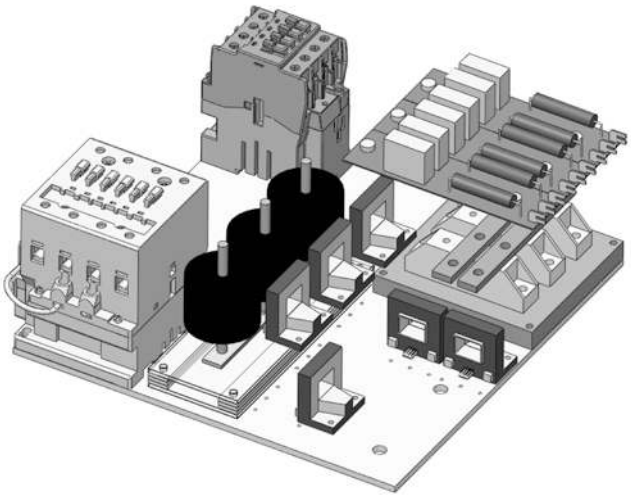

Figure 4.9: Steel plate with individual WEC circuit breaker, by-passing circuit breaker, varistors, current sensors and rectifier with its snubber circuits on top.

the winding taps of the transformer. A computer rendering of a *circuit breaker plate*, carrying circuit breakers, over-voltage protection (varistors), *LEM* current sensors, neutral-to-ground resistor, rectifier and DC-current sensors, is shown in Figure 4.9.

4.5.2.3 Rectifier

The rectifiers are passive six-pulse diode rectifiers with 100 A-diodes from *Semikron*. The diodes are mounted on an Al heat sink. The heat sink is mounted onto the *circuit breaker plate* which in turn is mounted to one of the welded plates on the inner wall of the vessel.

4.5.2.4 DC-bus capacitors

For the DC-bus, Aluminium electrolytic capacitors were chosen due to their compactness and their ability to cope with the internal pressure in the substation vessel. Two sets, of 24 parallel-connected capacitors in each set, are connected in series to achieve the necessary capacitance and voltage rating, see Figure 4.10. The capacitance achieved is 0.24 F between the positive and negative DC-busbar.

4.5.2.5 Inverter

The collector substation has a purposely built power inverter. It is based on six standard IGBTs and the switching signals are sent via one of the Programmable Automation Controllers (PACs) of the control system, see further Section 4.5.3. The IGBT driver circuits are powered from the battery system (described in Section 4.5.3.1), which enables the inverter to handle voltages

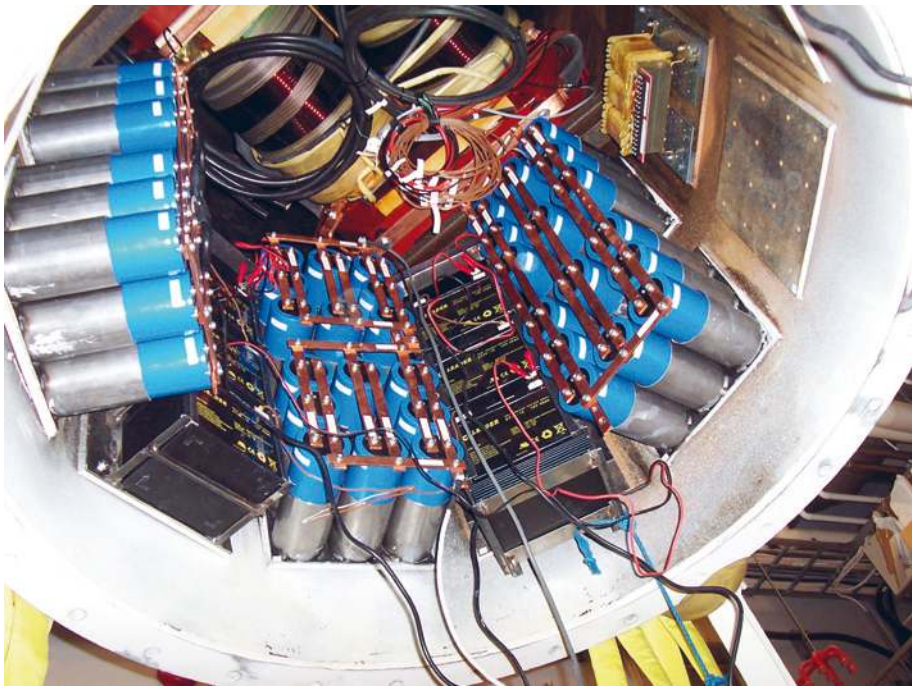

Figure 4.10: Aluminium electrolytic capacitor sets mounted in the substation.

down to 0 V DC. Since directly driven LGs are used, a range of different DC-bus voltages are needed in order to optimize the absorbed power of the WEC. Grid inverters intended to operate at a fixed DC-voltage could therefore not be used without using a DC/DC converter. The output voltage of the inverter can be changed by altering the modulation index of the inverter.

4.5.2.6 Transformer with winding taps

The transformer is a prototype transformer with five winding taps, see Figure 4.11. The taps are accessed on the high-voltage side of the transformer. In grid connection, the high-voltage side will be 1 kV. The five taps have the winding ratios 4, 5.56, 8, 10, and 12.5, thus corresponding to the voltages 250 V, 180 V, 125 V, 100 V, and 80 V on the low-voltage side. Varying the modulation index of the inverter, a range of DC-bus voltages are available.

Since the substation is not yet grid-connected, the voltage on the high-voltage side is allowed to vary in order to control the power in the resistive load located on the measuring station on Island Härmanö, see Section 4.3.

Figure 4.11: (a) The main circuit transformer being lifted down into the substation hull. (b) The main circuit transformer with its winding tap circuit breakers and high-voltage side AC busbars.

4.5.3 Auxiliary systems

The auxiliary system of the substation includes all systems that are not included in the main circuit. Hence, here, the battery system, the communication, the safety system, control and DAQ is included.

4.5.3.1 Batteries and chargers

The substation has a 24 V battery system consisting of six 40 Ah *absorbed glass-mat* (AGM) lead-acid batteries. They feed the DAQ and control PACs, the inverter driver, the communication modem, and all the various sensors. Recharging of the batteries is made by feeding power from the high-voltage side of the main circuit transformer. A three-phase step-down transformer of 1 kVA, with a winding ratio of 2.5, feeds six individual battery chargers. This enables feeding power from shore at times when the waves are too small. For reasons of redundancy, the battery system is divided into three 24 V battery groups. To make sure that the most essential PAC, the PAC dedicated to the safety system and relay control, always can be powered, all three battery groups are allowed to feed power to this PAC. Thanks to the separation into

groups, all batteries will not be discharged due to e.g. a short circuit in one of the measurement electronic's circuits.

4.5.3.2 Communication, control and DAQ

Four twisted pairs of a ten-pair signal cable is used for communication between the substation and the on-shore measuring station. Two point-to-point (PTP) modems, one in the substation and one in the on-shore measuring station, are used to transmit data.

For control of the inverter and circuit breakers, the substation is equipped with three National Instrument's FPGA-based PACs, *CompactRIO*. *PAC 1* is dedicated to control of the circuit breakers and other equipment that need to be turned on and off. Over-voltage protection is implemented in this PAC. In *PAC 2*, the control of the inverter is implemented. *PAC 3* is entirely dedicated to DAQ.

In PAC 2, which handles the control of the inverter, voltages and currents in the DC-bus are measured together with the inverter output and the voltages and currents on the high-voltage side of the transformer. These values can be used as feedback in the inverter control algorithms. PAC 2 also transmits, via the PTP modem, the collected data to the on-shore PC for storage. Two control modes are implemented:

1. manual control of the PWM index
2. an algorithm for constant DC-voltage operation.

PAC 3 samples data from sensors within the substation and in L2 and L3. It uses five 16-channel differential analogue input modules to measure WEC LG voltages and currents, translator positions, magnetic fluxes, stator temperatures and water levels in case of leakage. PAC 3 also logs strain gauges on the mechanical structure of L2 and temperatures, pressure, humidity and water level in the substation.

4.5.4 Cables and connectors

All the connectors used are from *Subconn/MacArtney*. The contact used to connect the land sea cable to the substation is a *Power 4 contact*, the inline male and flange-mounted female of which is shown in Figure 4.12 (a) and (b) respectively. The WEC power cables are joined to *High Power 4 contacts*, which are shown in Figure 4.12 (c). The connectors are strain-relieved by plastic (Delrin) locking sleeves. The different signal cable connectors used are shown in Figure 4.12 (d), (e) and (f).

4.5.5 Maintenance

The substation has been retrieved two times since the deployment in the spring of 2009. On both retrievals, the substation was taken to Lysekil harbour for service. On the retrievals, the pressure vessel was hoisted to the surface by

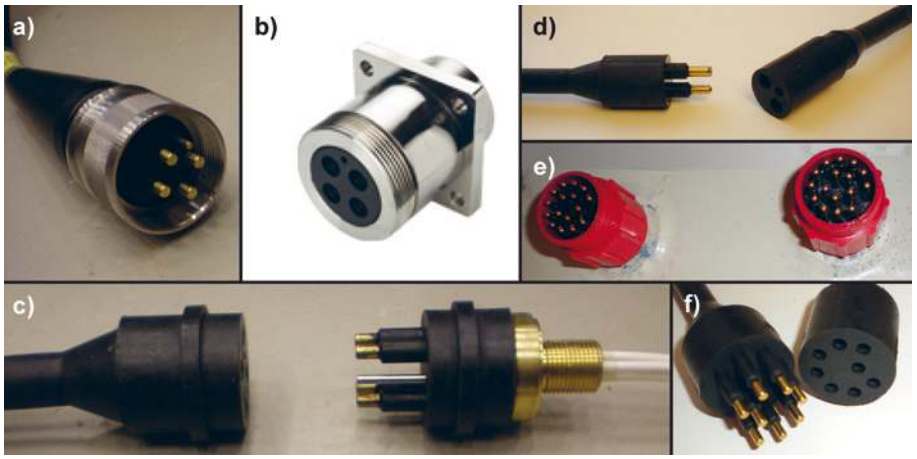

Figure 4.12: (a) and (b), *Power 4 contacts* for connection of the substation to the transmission sea cable. (c) *High power 4 contact* for connection of WECs to the substation. (d) *Micro 2 contact* for connection of dump load circuit breaker. (e) and (f), *Micro 16 contact* and *circular 8 contact* for signal transmission and supplementary battery charging respectively.

means of a pulley fastened in the foundation after the bolts, keeping the vessel in place, had been removed. The floating substation vessel was then towed behind the boat to the Lysekil harbour where it was lifted on-shore by means of a crane, see Figure 4.13. When reinstalling the substation, it was lowered into place using the pulley on the foundation and inflatable bags to pull it down-

Figure 4.13: The substation being towed behind the divers' boat to Lysekil harbour for service.

wards. The bolts keeping the vessel in place were reattached to the concrete foundation by divers.

4.6 Measurement inaccuracy

4.6.1 Voltage and current measurements

The generator AC voltages and currents, the individual DC-currents of the WECs, the temperatures in the substation and in WEC L2, and pressure and humidity in the substation etc. are sampled with a frequency of 256 Hz. The DC-link voltage and current, and all measurements that are made on the output side of the inverter, are sampled with a frequency of 500 Hz, which was chosen as a suitable frequency to capture the 50 Hz signals. To better capture the harmonics in the various voltages and currents measured, the sampling frequency would have to be raised. However, already at the present level, the need for data storage of the acquired data is quite substantial, which is the reason for choosing 500 Hz at most.

The voltages of the generators are measured with an estimated inaccuracy of $\pm 1.2\%$. The currents are measured with *LEM* current transducers[2], which have a slight non-linearity resulting in an inaccuracy in the current measurements of $\pm 1.7\%$. The measurement system was calibrated at an ambient temperature of $19°C$. After calibration, the total inaccuracy of the measurement system is estimated to approximately $\pm 4.4\%$ in the range of $19 \pm 25°C$.

4.6.2 Temperature sensors

The temperatures in L2 and in the substation are measured with sensors of the LM35 type[3], which have an operating temperature range of $-55°C - 150°C$ and an inaccuracy of $\pm 0.5°C$. The temperature sensor voltage is amplified before it is sampled with the CompactRIO DAQ system. This amplifier has an inaccuracy of $\pm 3\%$, which mainly originates in the tolerances of the resistors in the amplifier circuit.

[2]Datasheet, http://www.lem.com, accessed Dec. 21, 2009.
[3]Datasheet, http://www.national.com, accessed Dec. 21, 2009.

5. Summary of results and discussion

5.1 Linear damping in single WEC operation

A PMLG prototype was built and tested. Much practical experience was gained and the feasible solutions could be implemented in the design of L1. The magnetic circuit of the first prototype was only changed slightly for L1 apart from that the generator was made almost twice the size of the first prototype. Perhaps the most valuable results from Paper I were practical, namely how to assemble the translator and how to cope with the attractive forces between the translator and stator. This facilitated the construction of L1 to a great extent.

Figure 5.1 shows a power curve of the WEC in sea states up to slightly above 20 kW/m. This was recorded during the first operational period with

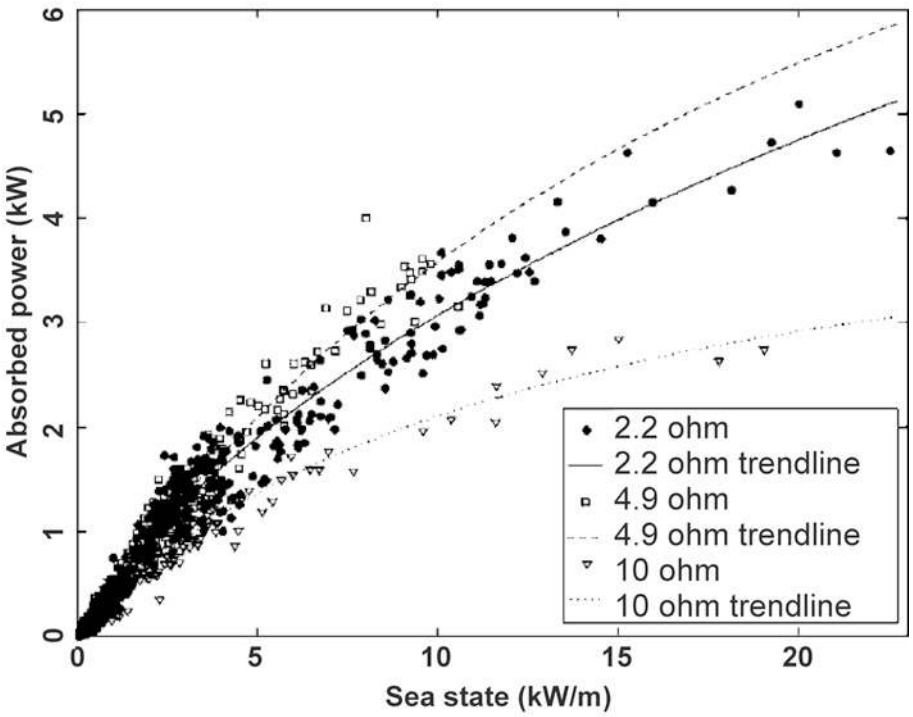

Figure 5.1: Early results of absorbed power in various sea states. From Paper II.

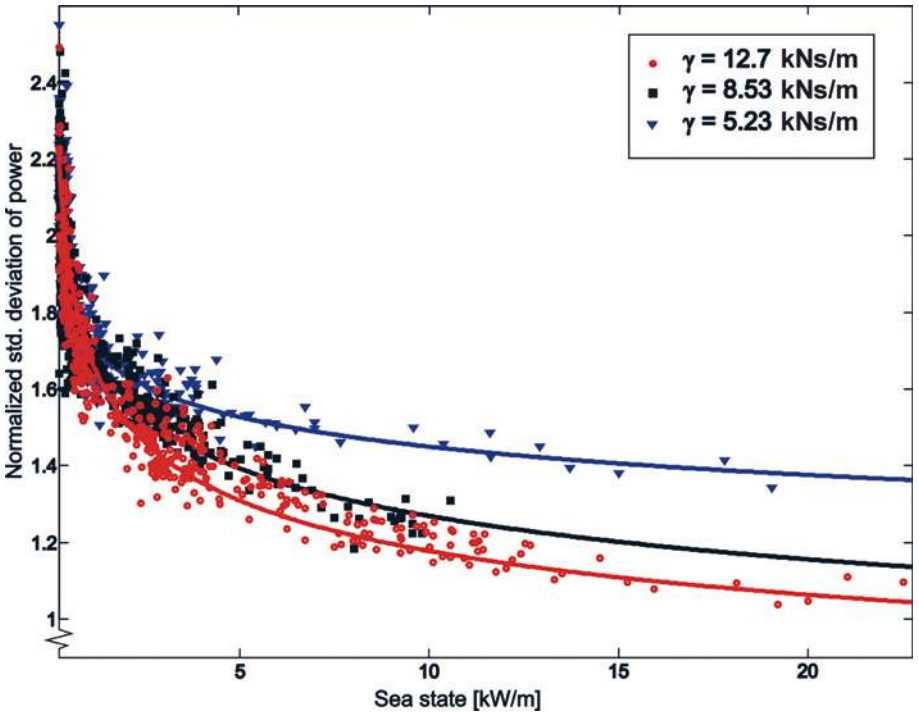

Figure 5.2: The influence of damping on the variation in absorbed power in different sea states. From Paper III.

L1, which started on March 13, 2006, and ended on May 24, 2006. The absorbed power increases in more energetic sea states. The data points are relatively scarce in the region of higher sea states compared to in modest waves, but it is rather evident that it is the same damping factor, which is realized by the 4.9 Ω resistive load, that gives the highest production in all of the sea states during the experiment. However, it should be noted that no more than three resistive loads were tested during the first period. Hence, it is not concluded that the 4.9 Ω load is an optimal load, rather that it was the most optimal among the three tested.

The measured relation between absorbed power and the significant wave height was published in Paper V. In the lower range of wave heights, the absorbed power increases quadratically with increasing wave height. However, above about 1 m significant wave height, the dependence is almost linear. This is most likely due to the frequency response of the system which for the 3 m buoy is highest at low wave heights and relatively short wave periods.

The variation in output power and its dependence on damping has been investigated, see Figure 5.2. The study is based on data collected during three months operation from March to May 2006. The three resistive loads 2.2 Ω, 4.9 Ω, and 10 Ω were used in the experiment. Keeping in mind that the 4.9 Ω

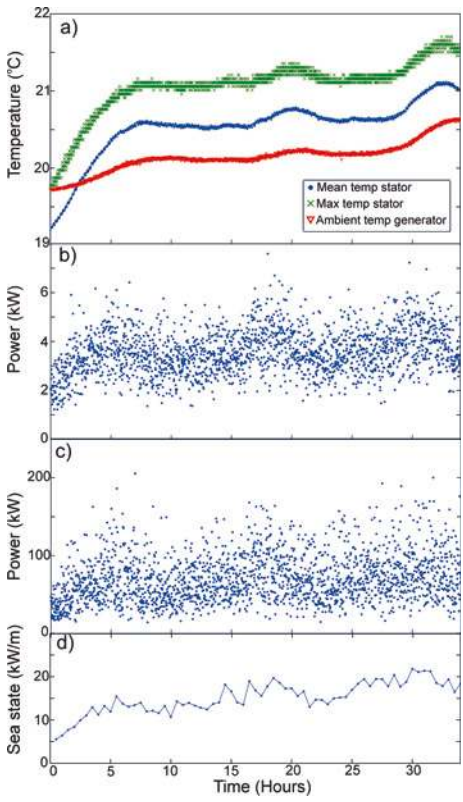

Figure 5.3: (a) Stator temperature and ambient temperature of L2. (b) Mean power in the dump load of L2. (c) Maximum power in the dump load of L2. (d) Sea state. From Paper X.

load (8.53 kNs/m damping factor) was the most optimal from the point of view of energy absorption, the damping factor resulting in the smallest standard deviation of output power was the largest one. Damping the buoy motion harder will thus reduce the fluctuations in the absorbed power seen over a time span of 30 min.. Choosing a higher damping factor, but a suboptimal one, obviously reduces the absorbed power. This would hence be interesting primarily in sea states where the nominal power of the WEC on average has already been reached. If the variation in output power from single units is less significant for the operation of a plant including several or many WECs, the most optimal load can be chosen to maximize the production.

The temperatures of the stator of WEC L2 and of a few substation components were investigated in linear damping in a sea state of about 15 kW/m. During the experiment, the ambient temperature was about $20 - 20.5$ °C. On the stator, eight temperature sensors are placed. These are sampled serially for approximately one second at a time. Thus, each sensor is sampled every

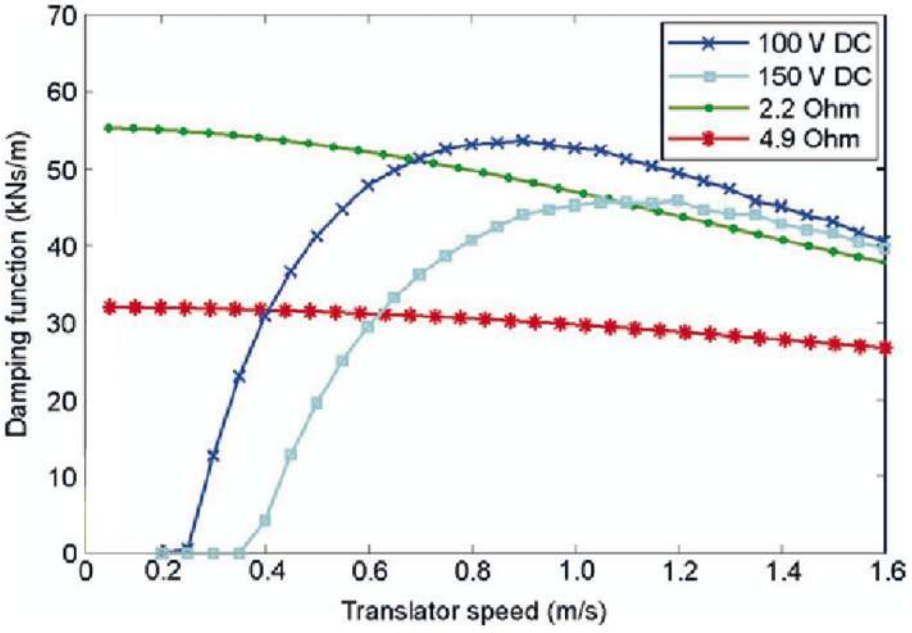

Figure 5.4: Simulation of damping resulting from different resistive loads and DC-voltages. From Paper XV.

eighth second and the presented values of temperature are one-minute mean values from these eight sensors.

Figure 5.3 shows the stator temperature of L2 along with the sea state and the one-minute mean and maximum electrical power in the L2 dump load. The mean and maximum temperatures follow the sea state rather well. The stator temperature increased only with about 0.5 °C. However, the difference between the mean and the maximum stator temperature seems to be constant and equal to about 0.5 °C. This might be due to that the one-minute maximum temperature rather is the temperature of the one sensor being placed in such a way that it experiences the largest heat load among the eight sensors.

5.2 Non-linear damping in single WEC operation

Figure 5.4 shows different damping functions, see Section 3.6, i.e. the difference between linear damping and non-linear damping of the WEC LG. The curves reflect the simulated damping force assuming a linear relation between no-load voltage and translator speed, that the stator is always covered by the translator (the translator never even partly slips out of the stator), zero LG iron losses and zero mechanical losses.

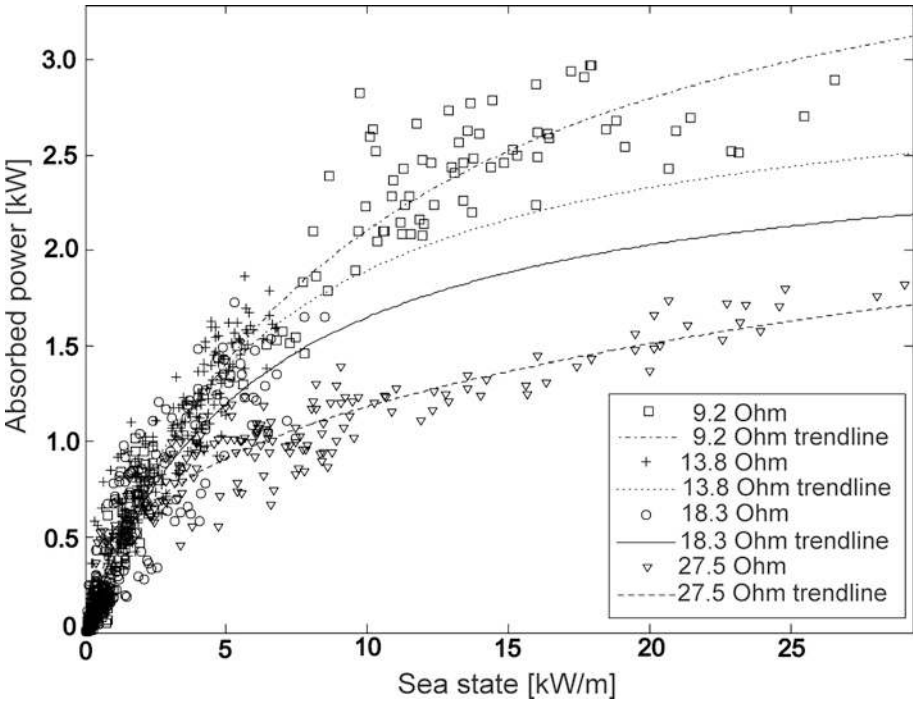

Figure 5.5: Experiments on WEC L1 with rectifier and voltage smoothing capacitors during 713.5 hours. From Paper VII.

In linear damping (with a resistive load) the damping begins immediately upon buoy movement. The damping is high from the start, slowly decreasing due to the internal voltage drop of the generator as the translator speed and hence the current is increased.

In non-linear damping, a voltage source is used as load in the model. The damping of the buoy motion does not start until a sufficiently high voltage has been reached in the generator. When twice the generator voltage amplitude plus the rectifier voltage drop (two diodes) exceeds the DC-voltage, the damping of the translator motion begins. The damping then increases with increasing translator speed. Since the load voltage of the generator will be limited by the DC-voltage, the current will instead increase resulting in higher damping, the larger the speed of the translator.

WEC L1 has been operated, and its performance evaluated, in non-linear damping, i.e when it was connected to the on-shore measuring station and the output was rectified by diode rectifiers, see Figure 4.3. It has been shown that the fluctuating output voltage can be smoothened by ultra capacitors to produce a steady DC-voltage over several wave periods. Another study with WEC L1 during 713.5 hours (about 29 days) in non-linear damping was also done. In Figure 5.5, the absorbed power in different sea states is shown as function of sea state for different load resistances in parallel with the DC-link

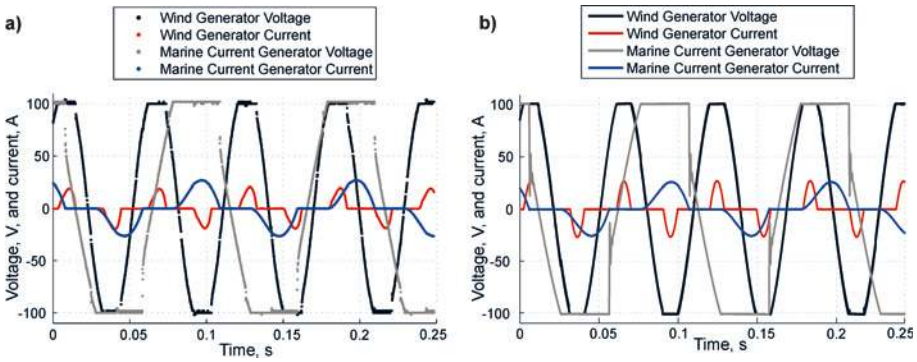

Figure 5.6: (a) Measurements and (b) simulations of voltage and current of two PMSGs connected to the substation DC-bus. From Paper XIII.

capacitors. The results differ somewhat from those in linear damping mode. With non-linear damping, among the resistive loads tested, the one resulting in the largest damping factor proved most efficient in terms of increasing the absorption. Certainly an even higher damping factor could increase the absorption further.

5.3 Laboratory experiments with two PMSGs

The design of the underwater collector substation has been described and discussed. Laboratory measurements of voltage and current wave forms in the interconnection of two rotating PMSGs on the DC-bus of the substation has been compared with Simulink simulations, see Figure 5.6. Due to that the rated speeds of the generators are different, the individual generator speeds, and thereby the electrical frequencies and voltages, are altered such that both deliver power to the DC-bus. Power is passively extracted on the DC-side by means of a resistive load. Results show that the main circuit of the substation works as expected. Due to the passive power extraction, the DC-voltage is increased if the speed of the PMSGs are increased.

5.4 Non-linear damping in array operation with two WECs

In Figure 5.7 a sample of results from offshore farm operation shows the PMLGs of WECs L2 and L3 simultaneously delivering power to the substation DC-bus. It is demonstrated that the translator speed must reach sufficient magnitude for each WEC to contribute to the total power output of the substation. The smoothing DC-link capacitors maintain the DC-voltage between

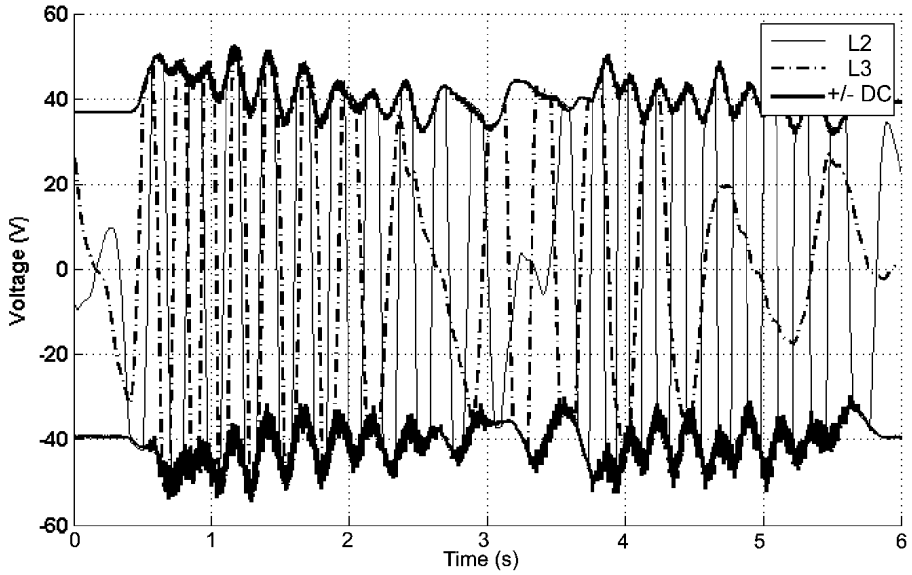

Figure 5.7: Phase voltages of two LG WECs delivering power to the common DC-bus of the underwater substation in offshore operation. From Paper XIII.

individual power bursts from the two LGs. The DC-voltage is regulated by means of a three-phase inverter. A constant DC-voltage of 80 V was set in the control system. This has the effect that as the translator of one the WECs increases its speed above the threshold speed corresponding to diode conduction to the DC-bus, the inverter increases the power transmission to the on-shore resistive load. To facilitate this, the AC-voltage on the high-voltage side must be allowed to vary, which is possible as long as the system is not grid-connected.

An investigation of the smoothing effect from interconnection of WECs in offshore array operation has been done. In the first experiment, two of the WECs, L2 and L3, were connected to the common substation DC-bus and the power contributions were measured during 15 minutes. The mean sea state was 4.5 kW/m, the significant wave height $H_{m_0} = 1.3$ m and the energy period $T_E = 5.7$ s. Keeping in mind that different buoy sizes and geometries are used for L2 and L3, results show that the ratio of maximum to mean power in array operation is 48 % lower, as a mean for the two WECs, than the ratios calculated from the individual WEC power contributions. The standard deviation of electrical power was calculated correspondingly and is shown in Figure 5.8. Here, array operation resulted in a reduction in the standard deviation of power of 27 % compared to single unit operation. This result corresponds precisely to simulations on the so-called *SEAREV* wave energy converter made in [50].

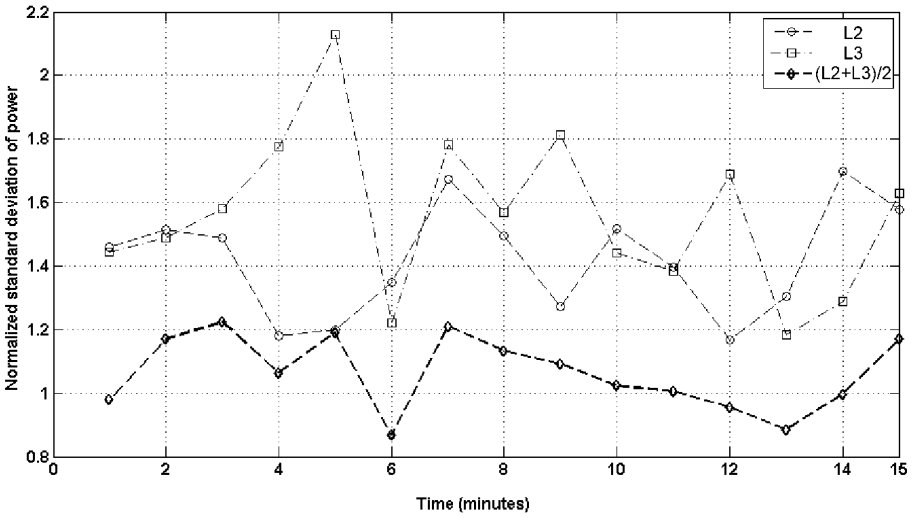

Figure 5.8: Standard deviation of electrical power with two WECs connected to the substation DC-bus (non-linear damping). Each data point corresponds to the mean of one minute of raw data. From Paper XIV.

5.5 Linear damping in array operation with three WECs

In the second experiment, all three WECs (L1, L2 and L3) were disconnected from the substation and instead connected to their individual dump loads. The WECs were thus operated in linear damping. The mean sea state during this record was 3.2 kW/m. The corresponding line-to-line voltages and the power extracted in the individual delta-connected dump loads were calculated as one-minute mean values. In Figure 5.9, for 24 hours (1440 min.) of data, the ratio of maximum power per minute to the one-minute mean power is shown along with the combined values of the array. Results show that by array operation, a reduction of 47 % is achieved compared to single unit operation. In calculating the standard deviation of electrical power for single units and for the combined array power in the second experiment, it was found that on average the reduction was 42 %. Figure 5.10 shows the 24-hour record in the second experiment with three WECs.

In Figures 5.9- 5.10, the values are somewhat biased by the wrongfully connected WECs L2 and L3, which had one phase turned the wrong way. Based on these two figures, no conclusions should therefore be drawn regarding whether the ring-shaped buoy of L1 is better or worse in lowering the ratio of maximum to mean power or the standard deviation of power than the cylindrically shaped buoys of L2 and L3. This is due to that the wrongful generator connection of L2 and L3 resulted in a significantly reduced damping for L2

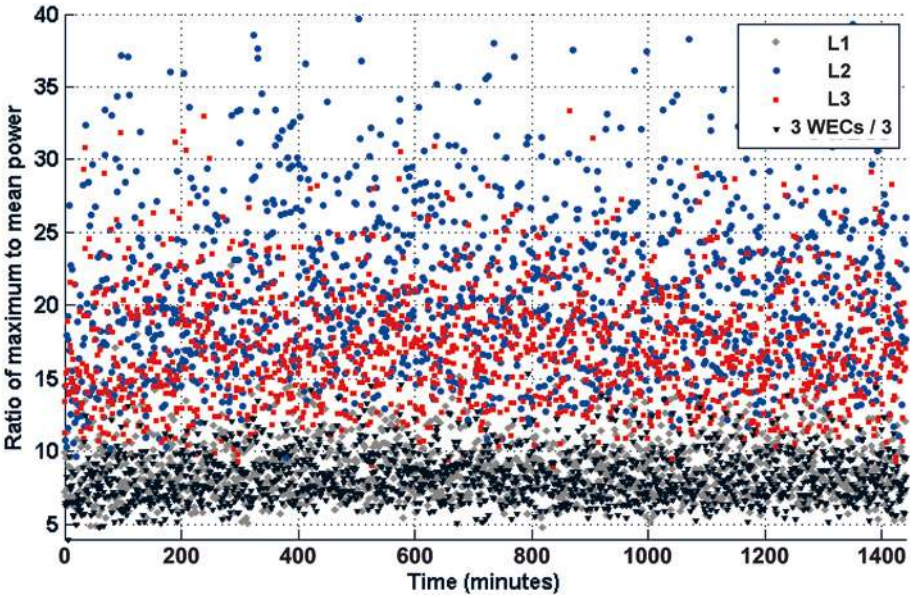

Figure 5.9: Ratio of maximum to mean power when three WECs are operated with individual dump loads (linear damping). Each data point corresponds to the mean of one minute of raw data. From Paper XIV.

and L3. The absorption and the standard deviation have been shown to depend heavily on the level of damping.

The strong correlation between power absorption and damping, between standard deviation and damping, and the fact that the power fluctuations in an array depend heavily on the number of WECs interconnected, one can expect certain control rules for a WEC array to be valid. A parallel can be drawn to the operation of a wind power plant. Increasing the breaking torque in a variable speed wind power plant in steady wind conditions operating in optimum tip-speed-ratio, the rotational speed will decrease resulting in a lower-than-optimum tip-speed-ratio and hence a reduced (lower than optimal) coefficient of power. The same principle is likely apply to WEC operation. If the WEC absorption curve relative to sea state has an optimum, and if the WEC is operating with optimum damping at nominal power in an increasing sea state, the damping can be increased to maintain nominal output power at the same time as the standard deviation of power is decreased. Since the translator speed, due to the increased level of damping, then is also lowered, decreased mechanical loads on the WEC structure and in the buoy line can be expected.

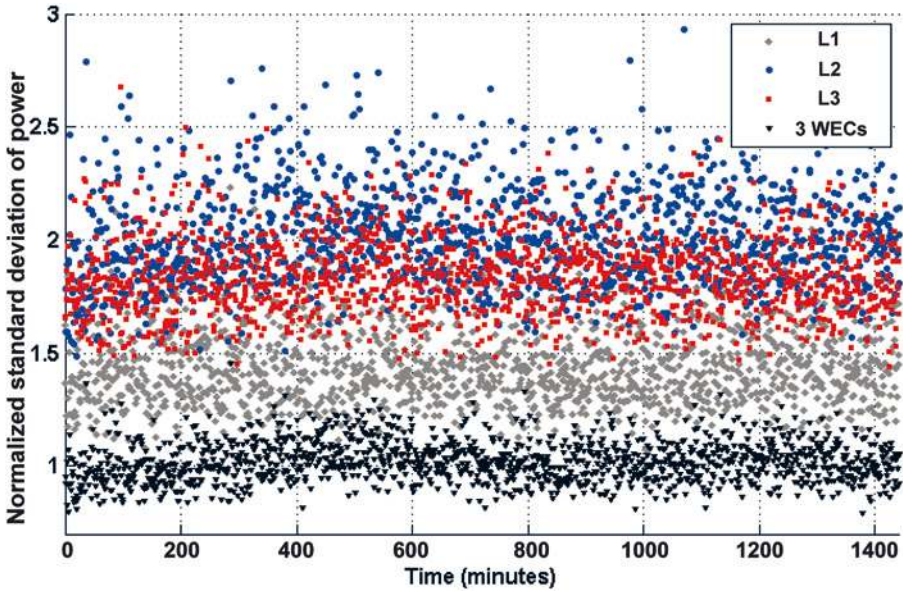

Figure 5.10: Normalized standard deviation of electrical power when three WECs are operated with individual resistive dump loads (linear damping). Each data point corresponds to the mean of one minute of raw data. From Paper XIV.

5.6 Substation design

The implementation of the substation has as a general result been successful. The substation has been installed, taken into operation and it has also been successfully retrieved for service on two occasions. The lack of lifting eyes on the hull caused some problems during the assembly in the laboratory and during transportation in Lysekil harbour. Lifting eyes could not be added after the manufacturing of the vessel since that would have required a second control according to the Pressure Vessel Standard EN13445 [119]. There was not enough time to make this modification and control prior to installation at the Lysekil research site.

The substation has fulfilled its purpose of interconnecting directly driven WECs of the PMLG type and transmitting the power to shore via a sea cable. The control has worked satisfactorily. Dump loads have been disconnected and connected properly upon the connection and disconnection of WECs. This is a very important part of the safety system of the wave farm electrical system.

The CompactRIO platform on which the control system was built was well suited for the application at hand and provides great flexibility in the design. It is modular and can handle the inverter control, safety functions and all DAQ of the substation and of external sensors. The various input/output modules facilitate the control of both fast switched semiconductor devices and circuit breakers, the latter via external relays.

6. Conclusions

From the research reported on in this thesis, some conclusions can be made:

- The WEC concept researched is feasible in the sense that it has been shown that the WEC can convert wave energy to electric energy. The electric energy has been converted to useful form and transmitted to shore for further use.
- By altering the damping of the WEC, the absorption can be enhanced. Increasing the damping will increase the absorption to a certain level where the absorption again will start to drop off.
- By altering the damping of the WEC, the standard deviation of the electrical power can be reduced. An increased damping lowers the standard deviation of electrical power.
- The thermal design of the WEC LG provides sufficient cooling of the heat generated from the resistive losses in the machine. The measured L2 stator temperature indicates that the cooling of the stator is unlikely to be an issue even in considerably more energetic sea states.
- It is possible to use an underwater collector substation to connect offshore energy converters on the seabed for further transmission of electricity to shore.
- By combining the electrical power from several WECs, an expected smoothening effect is achieved. With two WECs, a reduction in standard deviation of electrical power of 27 %, compared to single unit operation, has been shown. With three WECs, the reduction was 42 %. Larger reductions will occur with an increased number of WECs in the array and an even larger reduction can be achieved if the applied damping of the individual units is increased.
- By combining the electrical power from several WECs, the ratio of maximum instantaneous power to the one-minute mean power can be reduced.

7. Ongoing activities

7.1 Design of a second underwater substation

A new collector substation, called S2, is under construction and will, according to plan, be deployed at the Lysekil research site during 2010. This substation will transmit the total power from all of the ten WECs to be installed at the Lysekil research site. The first substation (S1), which connects WECs L1-L3, will still be operated in the park. However, S1 will be connected to S2 and S2 will be connected to the transmission sea cable to shore. The seven remaining WECs, L4-L10, will be connected to S2.

A number of details have been altered in the design of S2 compared to S1. The hull has a new design in order to simplify the construction. All contacts will be connected differently to better handle mechanical strain. The main circuit has been redesigned to handle the power from the seven new WECs and the 50 Hz, 1 kV input from S1. At the time of writing, the control system is updated and expanded.

7.1.1 Main circuit

The main circuit of S2 is based on the design of S1, but S2 is rated at higher power. The one-line diagram of the main circuit of S2 is seen in Figure 7.1. The same component types are utilized as before, the voltage and current rating of some components being altered due to the increased generator ratings of a few of the future WECs L4-L10. S2 therefore has two separate DC-buses, one for each set of generator voltage and power levels. This also requires the use of dual inverter systems and dual transformers, one set for each DC-bus. The transformers have a slightly different design than in S1. Seen from the low-voltage side, they are connected Y/delta to facilitate placing the winding taps on the low-voltage side. The switching between winding taps will be made by using two individual three-phase inverters and contactors on each DC-bus, hence S2 has a total of four inverters. The driver circuit has been redesigned to increase the robustness and efficiency of the inverters [120]. AC filters have been designed. These will be placed on the high voltage side of the transformers. The tap-change switching is implemented in the new control system algorithms which are prepared for grid connection. A comparison between a solution for tap changes based on thyristors and the chosen solution with two three-phase IGBT-inverters is made in [121].

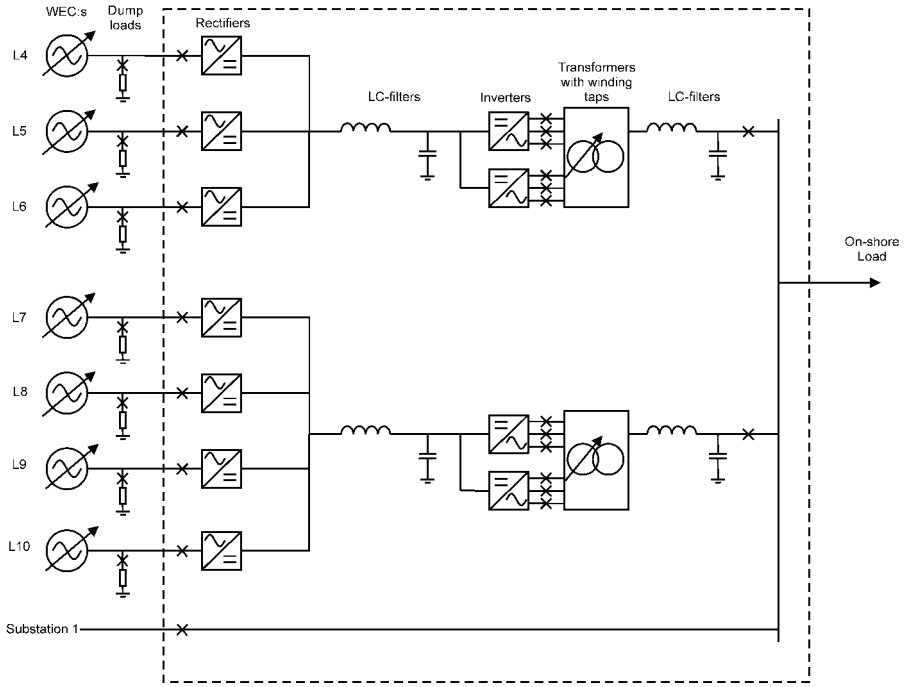

Figure 7.1: The one-line diagram of the new substation.

7.1.2 Hull

A new, larger, hull has been designed to house the components of the new main circuit, see Figure 7.2. The following has been changed:

- The hull of S2 is larger, 5 m^3 instead of 3 m^3, to fit all the components of the new main circuit.
- The hull is based on a commercial pressure vessel for compressed air of 11 bar. The pressure vessel is modified with a removable lower lid.
- Cable glands are used instead of flange-mounted connectors to lead the cables through the hull.
- Two flat steel plates, mounted on the outside of the hull, are used to fit the electrical connectors.
- The lower lid is a flat plate instead of a dished end.
- The vessel is bolted directly onto its foundation instead of having legs elevating it from the foundation. This is possible since the cable glands are mounted on the periphery of the hull instead of in the lower lid.
- The vessel is still designed according to [119], but it will be pressurized during, instead of prior to, deployment.
- The rectifiers, capacitors and the inverters are mounted on curved Aluminium plates which are pressed against the walls of the vessel in order to decrease the thermal resistance between components and the hull.

Figure 7.2: Construction: external reinforcements being welded to the hull of the new substation.

- Components are fastened to the hull according to their individual needs rather than in a standardized way for all components as in the first substation.
- Lifting eyes have been added to the exterior of the vessel to make it easier to handle during the assembly and upon transportation, deployment and retrieval.

7.1.3 Electrical connectors

Some new versions of the *Subconn/MacArtney* electrical connectors will be evaluated with S2. The power connector used on S1 for the transmission sea cable to shore is not large enough to handle the rated power of S2. This has therefore been changed to four individual *Power 1 series contacts* rated at 250 A, see Figure 7.3 (a). The *Micro series* connectors have been changed to the *Low-profile series* of connectors, see Figure 7.3 (b). The latter are believed to be slightly easier for divers to connect.

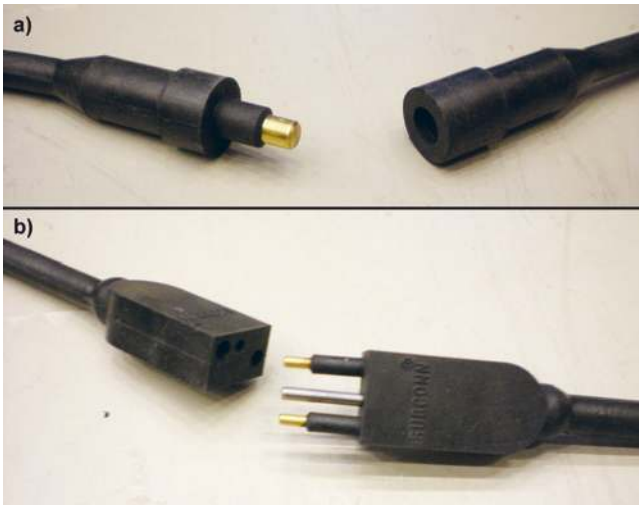

Figure 7.3: (a) One of four 250 A connectors to be used for connection of the sea cable to the new substation, here seen in the inline version. (b) The *Low-profile 2 series* of connectors that will be used to connect the WEC dump load circuit breakers in the new substation.

8. Future work

Future work will include the continuation of the ongoing work as described in Chapter 7. Future grid-connection of the substation will present several interesting possibilities. The work on power smoothing should be continued. With ten WECs in the array, considerable work could be carried out in this area. If the substation is updated with a controlled rectifier, individual WEC control can be implemented. This will have an influence on the AW of the devices and can possibly also enhance the power smoothing capability of the substation. Again considering power smoothing, an interesting approach to further even out power fluctuations would be to install an energy storage unit, e.g. a flywheel. This could be installed in one of the substatons, but a more convenient location would be in the on-shore measuring station.

Loss reduction is an important field of study. Utilizing the equipment already built and installed to its full potential, or at least to a greater extent, could be a good way to achieve cost reductions. It should be carried out in parallel with the study on how to increase the power absorption of the device. For the latter purpose, the studies on optimal control should be continued. The optimal load, or DC-level, for the WECs in array operation should be researched to maximize the power absorption. The implementation of an MPPT algorithm in the control system could exclude the need for information on present sea state, which would be needed if the control was to be based on a look-up table algorithm.

The underwater wet-mateable connectors used so far have been connected by divers. A field of future study is connection by underwater *remotely operated vehicles* (ROVs). Such connectors and ROVs exist and are available for purchase on the market. They are used within the oil- and gas industry, and are utilized for large ocean depths. However, they are unnecessarily advanced and very expensive. A possibility would be to look at new solutions for wet-mateable connectors usable with ROVs for the wave energy application.

9. Summary of papers

The papers of this thesis investigate, by an experimental approach, LG WEC operation and a substation system to facilitate park operation. The method of research includes the design, construction, testing followed by operation of prototypes of various kinds. First, various aspects of the machine are investigated. Second, a prototype is built and tested where the ambient, or environment, parameters can easily be monitored. Third, either a new prototype, modified for the real conditions, is built or the machine, which was tested in the laboratory, is taken out and is installed for real offshore testing. This method has been applied both for the LG and for the substation. Accordingly, the papers also follow this route. Paper I reports on the laboratory testing of the prototype LG. The full WEC is then built, installed on-site and tested. Papers II – V, VIII, and IX report various experimental results from offshore operation in real ocean waves of varying intensity. Then some alterations are made to take the concept to the next level. Paper X is a study on component temperature in offshore operation to investigate if the thermal design of the the WECs and of the substation is sufficient to dissipate the heat from electrical and electromagnetic losses. Papers VI – VII report on results from offshore operation in the non-linear damping mode. The LG voltage is now rectified and power is extracted in a resistive load in parallel with the capacitive filter on the DC-bus. A substation is built and initial tests are made in the laboratory. Papers XI – XII show results from such tests. The substation was then installed at the site and real offshore testing took place. Paper XIII gives a description of the substation design and how it operates in its proper elements. Paper XIV report on findings from farm operation. Paper XV looks a bit into the future elaborating on the possible layout of large wave farms based on the concept at hand.

The author's contributions to each paper are given below. For all the papers, the author has also taken part in the interpretation and discussion of results together with the co-authors.

PAPER I

Full-Scale Testing of PM Linear Generator for Point Absorber WEC

The paper describes the construction and testing of the first linear generator prototype built at the Division of Electricity at Uppsala university. The

generator, which is a shorter version of the linear generator built for the first prototype point absorber WEC, had surface-mounted Nd-Fe-B magnets and a stator winding with PVC-insulated cables instead of a conventional generator winding. The measured no-load voltage is compared with FEM simulations.

This paper was presented by the author at the 6th European Wave and Tidal Energy Conference, 28th of August to 3rd of September in Glasgow, Scotland, UK 2005.

The author took a central part in the writing of the paper and he conducted the experiment. He also participated in the design and implementation of the laboratory generator experimental set-up.

PAPER II

Experimental results from sea trials of an offshore wave energy system

The first results from offshore operation of the WEC prototype is presented here. The paper elaborates on the features of the WEC and the conditions in which it is deployed. The power absorbed in three different resistive loads are shown in various sea states. It is shown that the damping of the WEC LG significantly affects the absorption of wave energy and that the ability of the LG to withstand the large electrical power peak values occurring in more energetic sea states is vital for the survivability of the WEC. Furthermore, it was shown that optimal load does not vary with sea state.

This paper is published in Vol. 90 of *Applied Physics Letters*, 2007.

The author designed the line guidance mechanism of the WEC and took a leading part in the electrical connection of the WEC and the sea cable deployment procedures. The author also contributed to a minor extent in the writing of the paper.

PAPER III

Influence of Generator Damping on Peak Power and Variance of Power for a Direct Drive Wave Energy Converter

The paper investigates what effect an altered generator damping has on the standard deviation of power. It also studied momentary electrical peak values of electrical power and maximum instantaneous translator speed resulting from the different damping levels. It is concluded that a higher damping level reduces the standard deviation of power and the maximum translator speed that occurs. However, the effect on maximum instantaneous electrical power is less obvious.

This paper is published in Vol. 130, issue 3 of *Journal of Ocean Mechanics and Arctic Engineering*, 2008.

The author took a leading role in the writing of the paper and contributed to the design and implementation of the WEC and the electrical connection to the on-shore measuring station.

PAPER IV

Energy absorption in response to wave frequency and amplitude -offshore experiments on a wave energy converter

In this paper, results from offshore operation of the first prototype WEC are shown. The absorption in watts and in percent of incoming wave energy is shown as scatter diagrams. As a maximum, a conversion ratio (excluding mechanical losses and generator iron losses) of 25 % is achieved in around 1 m high waves of energy period 4.5 s.

This paper was submitted to *AIP Journal of Renewable and Sustainable Energy* on January 20, 2010.

The author contributed to the design and implementation of the WEC and the electrical connection to the on-shore measuring station. The author also participated to a minor extent in the writing of the paper.

PAPER V

Offshore experiments on a direct-driven Wave Energy Converter

This paper presents the sea state as measured by a Waverider buoy during the early offshore sea trials of the first prototype WEC. The influence of the wave height on the absorption of wave energy is shown.

This paper was presented by Jens Engström at the 6th European Wave and Tidal Energy Conference, 11-13 September, 2007.

The author contributed to the design and implementation of the WEC and the electrical connection to the on-shore measuring station. The author also contributed to a minor extent in the writing of the paper and attended the conference at which it was presented.

PAPER VI

Experimental results of rectification and filtration from an offshore wave energy system

The first results from sea trials in the non-linear damping mode is presented. After rectification of the amplitude and frequency modulated voltage from the LG, a capacitive filter with ultra capacitors is used to smoothen the output power from WEC L1. Results show that the power extracted in a resistive load

in parallel with the capacitive filter can be almost entirely smoothened over the time period of about one- to two wave periods. Results from a 30-hour record in a changing sea state is presented and it is concluded from the simulations and experiments that a smooth DC-voltage (and power) is achieved with less than 5% voltage ripple during 10 s.

This paper is published in Vol 34 of *Renewable Energy*, 2009.

The author contributed to the design and implementation of the WEC, the electrical connection to the on-shore measuring station and to the design of the experimental set-up in the measuring station. He contributed to a minor extent to the writing of the paper.

PAPER VII

Study of a Wave Energy Converter Connected to a Nonlinear Load

The performance of the prototype WEC L1 is evaluated in non-linear damping mode. Four different resistive loads were connected in parallel with the capacitive filter in the measuring station, and the captured power was calculated as half-hour averages. The study is based on about three months of offshore operation. The resistive load giving the largest damping factor resulted in the highest production of electricity. The results thus indicate that increasing the damping could increase the electricity production even further.

This paper is published in Vol. 34, No. 2 of *IEEE Journal of Oceanic Engineering*, 2009.

The author contributed to the design and implementation of the WEC and the electrical connection to the on-shore measuring station. The author also contributed to a minor extent in the writing of the paper.

PAPER VIII

Wave energy from the North Sea: Experiences from the Lysekil Research Site

A sample of project achievements to date are presented in this paper. Results from measurements of buoy line force are also presented along with the speed of the buoy, the LG voltage and the absorbed power excluding mechanical- and generator iron losses. An absorption curve is presented based on previously published results in linear damping mode with the 4.9 Ω resistive load in sea states of up to about 10 kW/m.

This paper is published in Vol. 29, No. 3 of *Surveys in Geophysics*, 2008. The paper was invited by the journal.

The author contributed significantly to the writing of the paper and prepared Figure 2. The author contributed to the design and implementation of the WEC and to the electrical connection to the on-shore measuring station on Island

Härmanö. He also contributed to the design of the experimental used when running the WEC in the non-linear damping mode.

PAPER IX

Catch the wave to electricity

In this paper, some basic considerations behind the concept of using a point absorber with a directly driven linear generator on the seabed are explained. Simulation results of electricity production are compared with offshore measurements for WEC L1 and some future development steps are highlighted.

This paper is published in Vol 7, No. 1 of *IEEE Power and Energy Magazine*, 2009.

The author contributed to the writing of the paper. The author also contributed to the design and implementation of the WEC and to the electrical connection to the on-shore measuring station on Island Härmanö.

PAPER X

Temperature measurements in a linear generator and marine substation for wave power

The paper presents temperature measurements made on the stator of WEC L2 and on various components in the substation. The study investigates the effect of mean and maximum instantaneous electrical power on the mean and maximum temperatures. Experiments were carried out in linear and in non-linear damping mode, i.e. when L2 was connected to its dump-load and when it delivered power to the substation. First results indicate that the thermal design of the WECs and of the substation provides sufficient cooling of the stator of L2 and of the substation components. Large temperature increases are unlikely to occur even in considerably more energetic sea states.

This paper was submitted (December 21, 2009) to the 29th International Conference on Ocean, Offshore and Arctic Engineering, OMAE2010, Shanghai, China, June 6-11, 2010. The conference is peer-reviewed. The paper will be presented by Cecilia Boström.

The author made a significant contribution to the writing of the paper. He wrote the Abstract, Results, and most of the Discussion and Conclusions. The author also contributed to the processing of measurement data. He took a leading role in the design and implementation of the substation and the electrical connection to the on-shore measuring station.

PAPER XI

Laboratory experimental verification of a marine substation

In this paper, the initial testing of the interconnection of several PMSGs on a common DC-bus is made by means of an offshore underwater substation. The paper presents laboratory measurements from the interconnection and the results are compared with simulations in MATLAB Simulink. The electrical system of the substation in explained and the way the interconnection will work in offshore operation is discussed. It is emphasized that the DC-bus voltage level will determine at which LG translator speed the buoy motion of the WEC will start to be damped.

This paper was presented by the author at the 8th European wave and tidal energy conference, EWTEC, 7-10 September, 2009. The conference is peer-reviewed.

The author took a leading role in conducting the laboratory experiment, in writing the paper and he also took a leading role in the design and implementation of the substation.

PAPER XII

Description of the control and measurement system used in the Low Voltage Marine Substation at the Lysekil research site

The control and measurement system of the offshore underwater substation is based on the *CompactRIO* PAC from *National Instruments*. Here, the main circuit power flow is controlled and the safety and relay system is managed. All data acquisition, both in WEC L2 and L3 and in the substation is made by one of the PACs. Measured voltages and currents on the low-voltage side and the high-voltage side of the transformer and the voltage on the DC-bus upon testing of the system in a laboratory environment under the inverter control algorithm *constant modulation index* are shown.

This paper was presented by Olle Svensson at the 8th European wave and tidal energy conference, EWTEC, 7-10 September, 2009. The conference is peer-reviewed.

The author contributed to some extent to the development and implementation of the control and measurement system. He also made a minor contribution to the writing of the paper and attended the conference at which it was presented.

PAPER XIII

Offshore underwater substation for wave energy converter arrays

The paper takes an engineering approach and gives as such a description of most of the important aspects on the design, implementation, deployment, recovery and maintenance of the substation. It elaborates on various design considerations and explains the various systems in the substation in detail. Results from initial laboratory measurements using two PMSG are compared with simulations. Results from interconnection of two WEC LGs in offshore operation in the Lysekil wave energy research site are shown and the difference between these and the laboratory measurements are discussed.

This paper was submitted to *IET Renewable Power Generation* on November 20, 2009, to be included in the EWTEC 2009 special issue.

The author took a leading role in conducting the laboratory experiment and in writing the paper, in which he made all the illustrations. He also took a leading role in the design and implementation of the substation, the electrical connection to the on-shore measuring station and in the external electrical connections of the prototypes L2 and L3. He designed and implemented the line guidance system and electrical connections of the first prototype, WEC L1.

PAPER XIV

Power smoothing in an offshore wave energy converter array

The smoothing effect from interconnection of several WECs in a farm is investigated. A 15-minute and a 24-hour run with two- and three WECs respectively are evaluated regarding converted electrical power, the ratio of maximum to mean power and the standard deviation of power. It is concluded that adding the individual power contributions lowers the standard deviation of power. The power smoothing effect is stronger with three WECs than with two and the results agree very well with previously published results.

This paper was submitted to the *AIP Journal of Renewable and Sustainable Energy* on November 3, 2009.

The author took a leading role in writing the paper and made all the calculations and illustrations. He also took a leading role in the design and implementation of the substation, the electrical connection to the on-shore measuring station and in the external electrical connections of the prototypes L2 and L3. He designed and implemented the line guidance system and electrical connections of the first prototype WEC, L1.

PAPER XV

Design proposal of electrical system for linear generator wave power plants

The paper presents an electrical system of a larger wave farm with two levels of substations, both low-voltage marine substations and medium voltage marine substations. Several low-voltage substations are connected to one medium-voltage substation to form array interconnection and successive voltage elevation before power is transmitted to shore in a single sea cable. Simulation results of how linear and non-linear damping factors are related to the LG translator speed are presented. Measured power absorption during three months in 2007 of WEC L1 is shown along with the parameters of the corresponding sea state.

This paper was presented by Cecilia Boström at the 35th annual conference of the IEEE Industrial Electronics Society, IECON, Porto, Portugal, November 3-5, 2009. The conference is peer-reviewed.

The author took part in the design of the electrical system. He took a leading role in the design and implementation of the university substation and the electrical connection to the on-shore measuring station. He designed and implemented the line guidance system and electrical connections of the first prototype WEC, L1. The author made a minor contribution to the text.

10. Svensk sammanfattning

Tillgången på förnybar energi på jorden är otroligt stor. Med endast de s.k. flödande energikällorna, såsom strömmande vatten i älvar och hav, vind och sol, i åtanke finns långt mer att tillgå än vad vi använder i världen idag. Den samlade elproduktionen i världen har prognostiserats till 20600 TWh år 2010, motsvarande en medeleffekt av $2,35$ TW. Med svårtillgänglig areal, bergsområden o.s.v., och de områden med sämst energitäthet borträknade, är potentialen hos enbart sol och vind tillsammans fortfarande $620-665$ TW motsvarande $5,4-5,8$ miljoner TWh årligen. Potentialen för vågkraft har beräknats till $1-10$ TW, vilket även med det lägre värdet skulle innebära att lite mer än 40% av världens elproduktion skulle kunna täckas av vågkraft i framtiden. Den totala årliga användningen av all slags energi i världen motsvarar medeleffekten $12,5$ TW[1]. Att fullständigt fasa ut användningen av fossila bränslen i världen är alltså inte ett resursproblem, vilket är en vanlig uppfattning. Detta resonemang utelämnar dock problemet med energikällornas variation i relation till när energin behövs samt vilken energiform som efterfrågas.

Vid avdelningen för elektricitetslära, institutionen för teknikvetenskaper på Uppsala universitet bedrivs forskning på vågkraft. Detta görs dels inom Lysekilsprojektet och dels inom Centrum för förnybar elenergiomvandling (CFE). Lysekilsprojektet hanterar uppbyggnaden av en forskningsanläggning utanför Lysekil, på västkusten. Inom CFE, där det finns full tillgång till data från forskningsanläggningen, görs studier inom en rad områden från hydrodynamik till generatorteknologi och elektriska system.

Vågkraftforskningen inom CFE syftar till att ta fram en gångbar vågkraftteknik och att studera frågor relevanta för dess drift och utveckling. Författarens fokusområde är sammankoppling av vågkraftverk till havs. Arbetet har innefattat både den fysiska sammankopplingen och utformningen av det elektriska systemet i syfte att möjliggöra en sammankoppling. Arbetet har också innefattat hur de elektriska komponenter, som behövs i sammankopplingen, ska skyddas mot havsvattnet. För dessa ändamål har ett så kallat *undervattensställverk* konstruerats, byggts och driftsatts i forskningsanläggningen för vågkraft utanför Lysekil. Undervattensställverk för elproduktionsanläggningar är helt nytt. Runt om i Europa finns, eller planeras, dock ett antal testområden för prototyper av vågkraftverk. Flera av anläggningarna är fortfarande i planeringsstadiet medan några har fått

[1]The U.S. Energy Information Administration, http://www.eia.doe.gov 2009-12-08

tillstånd och har börjat byggas. Några få är i drift. Av de åtta anläggningar (utöver forskningsanläggningen utanför Lysekil) som listas i denna avhandling kommer bara en att ha ett undervattensställverk, *WaveHub*, som byggs utanför Englands sydvästra kust. De andra byggs som en förlängning av det landbaserade elnätet, med utdragna inkopplingspunkter på havsbotten.

Det koncept för omvandling av havsvågor till el som studeras här är en så kallad *punktabsorbator*. Med en punktabsorbator avses en på något sätt svängande (oscillerande) kropp vars mått är betydligt mycket mindre än avståndet mellan två vågtoppar, d.v.s. våglängden. En av fördelarna med en punktabsorbator är dess förmåga att under vissa omständigheter absorbera energi från en bredare del av den infallande vågen än kroppens bredd. En liknelse kan göras med antennen i en radio som drar nytta av samma s.k. resonanseffekt. En annan fördel med punktabsorbatorer är att konstruktionen kan göras relativt okomplicerad, speciellt om man använder en s.k. direktdriven generator vilket är fallet här, se nedan. Detta tros inte bara minska behovet av underhåll utan också öka vågkraftverkets förmåga att överleva stormar.

Vågkraftverket består av en boj som via en lina är kopplad till en s.k. linjärgenerator som hålls på plats på havsbotten av ett betongfundament. En linjärgenerator rör sig upp och ned istället för att rotera, som vanliga generatorer gör. Linjärgeneratorn är inkapslad i ett hölje av stålplåt för att skydda generatorn mot det korrosiva havsvattnet. I kapselns övre lock finns en kolvstång och en tätning som ser till att vatten inte tränger in i kapseln trots bojens, och därmed kolvstångens, rörelse upp och ned. På generatorns rörliga del, translatorn, sitter starka magneter. När bojen lyfts av vågorna rör sig translatorn uppåt och spänning induceras i generatorns lindningar. Eftersom generatorn är direkt kopplad till bojen kommer den inducerade spänningen att pulsera på ett sätt som gör att det inte går att koppla vågkraftverket direkt till elnätet. I undervattensställverket sker den nödvändiga utjämningen och omformningen av spänningen. Här sker också sammanlagring av effekten från flera vågkraftverk så att endast en kabel behövs för överföring av effekten till land.

Författarens arbete har förutom arbetet med ställverket också omfattat test av första prototypen av en linjärgenerator som legat till grund för konstruktionen av generatorn i första prototypen av vågkraftverket, kallad L1. Till L1 konstruerades en mekanisk struktur som sitter på toppen av vågkraftverket, en lininstyrning som ser till att dragkraften i linan från bojen dels inte sidobelastar den kolvtätning som förhindrar vatten att tränga in i kapseln, och dels inte leder till horisontell kraftpåverkan på generatorns translator.

Med L1 har ett antal experiment till havs genomförts. Generatorn har kopplats till olika resistiva laster placerade i en mätstuga på Härmanö, Orust. Generatorn har också belastats med en spänningslast åstadkommen genom likriktning av spänningen och, med hjälp av ultrakondensatorer, kraftig utjämning av densamma. Efter att ställverket och ytterligare två prototyper av vågkraftverket, *L2* och *L3*, installerats har experiment i parkdrift genomförts.

Från de studier som presenteras i avhandlingen kan några slutsatser dras. Dessa presenteras nedan i punktform.

- Vågkraftkonceptet är gångbart så tillvida att det går att använda för att omvandla energin i havsvågor till el och göra den tillgänglig på land.
- Genom att ändra bojens dämpning kan man påverka hur mycket vågenergi som absorberas. I enklaste fallet ändras dämpningen genom att ansluta en annan last (resistans) till generatorn. En optimal dämpnivå kan hittas. Genom de experiment som hittills genomförts har bara en "bästanivå" hittats bland flera testade. Huruvida denna är den optimala återstår att ta reda på.
- Genom omvandling av den genererade växelspänningen till likspänning och kraftig utjämningen av likspänningen kan den pulserande generatoreffekten över en vågperiod jämnas ut helt. Detta gör nätanslutning enklare eftersom effektvariationer leder till spänningsvariationer. Enligt de bestämmelser och riktlinjer som finns för nätanslutning måste spänningsvariationer begränsas.
- Genom att öka generatorns dämpning kan man minska standardavvikelsen av elektriska effekten.
- Utformningen av vågkraftverkens generatorer har visat sig ge tillräcklig kyleffekt för att undvika temperaturökningar som kan vara skadliga för den PVC-baserade isoleringen runt ledarna i generatorlindningen. Eventuell upphettning sker framför allt p.g.a. de resistiva förlusterna. Med tanke på den mycket begränsade uppvärmningen av statorn vid så pass kraftig sjöhävning som 15 kW/m är det rimligt att anta att man inte heller kommer att kunna notera några stora temperaturhöjningar vid betydligt högre nivåer av vågenergitransport än så.
- Ett resultat av parkdrift av vågkraftverk är att elektriska effekten från parken blir jämnare än vågkraftverkens individuella bidrag. Detta är ett förväntat resultat. Med två vågkraftverk minskade standardavvikelsen av elektriska effekten med 27% jämfört med vågkraftverkens individuella bidrag. Med tre vågkraftverk blev minskningen 42%. En ännu större reduktion kommer att ske med fler vågkraftverk och med högre dämpning av aggregaten. Jämförelserna har gjorts på enminutsbasis.
- Ett annat mått på utjämningseffekten från parkdrift av vågkraftverk är kvoten mellan maximal elektrisk effekt per minut och genomsnittlig elektrisk effekt per minut. Studien i denna avhandling påvisar en ungefär lika stor minskning av denna med tre vågkraftverk som med två vågkraftverk i parken jämfört med de individuella aggregatens bidrag.

I det pågående arbetet konstrueras och byggs ett nytt, större, undervattensställverk. Ställverket kommer att installeras på forskningsområdet utanför Lysekil. Det nya ställverket ska ansluta det gamla ställverket samt de sju nya vågkraftverken L4-L10. Den befintliga sjökabeln för kraftöverföring till mätstugan på Härmanö skarvas om till havs och ansluts till nya ställverket istället för till det första.

I det framtida arbetet är fortsatta studier av utjämningen av elektriska effekten vid parkdrift av intresse. Speciellt intressant är det att studera utjämningseffekten från fler aggregat än tre. Hur absorptionen av vågenergi i ett vågkraftverk påverkar absorptionen hos omkringliggande bojar är ett annat viktigt forskningsområde för implementeringen av vågkraftparker. Här behövs fler studier och verifiering av beräkningsmodeller med experiment till havs. Avslutningsvis kan nämnas att undersökning och utvärdering av olika metoder för att minska elektriska och elektromagnetiska förlusterna i hela systemet från generator till elnät är centrala.

11. Acknowledgments

Jag vill tacka min handledare Mats Leijon för möjligheten att doktorera på den här avdelningen där det ständigt händer massor av spännande saker. Tack för ditt förtroende, för den stora frihet under stort ansvar som jag kontinuerligt fått av dig. Jag har lärt mig otroligt mycket och är säker på att jag kommer att fortsätta lära mig hela livet. Tack för de möjligheter du hittills gett mig och de dörrar du öppnar lite här och var. Tack också för ditt slit med att ordna finansiering för den forskarassistenttjänst jag kommer att tillträda.

Hans Bernhoff, min biträdande handledare. Tack för ditt engagemang i allmänhet och i synnerhet i det arbete med vindkraft som vi delade för ett par år sen. Testerna på Hovgården var otroligt spännande och riktigt kul.

Alla våra finansiärer förtjänar ett stort tack. Min lön har under doktorandtiden betalats via CFE som finansieras av Energimyndigheten och Vinnova. Därtill följer en rad finansiärer som bidragit till uppbyggnaden av testanläggningen utanför Lysekil. Ett särskilt tack vill jag rikta till Sveriges Ingenjörers Miljöfond och Stiftelsen J. Gust. Richert från vilka jag mottagit ekonomiskt stöd för arbetet med ställverket.

Monika, min nära kära. Tack för ditt enorma stöd och all uppmuntran du gett mig, och ditt tålamod då jag behövt jobba kvällar och helger. Du är den bästa co-drivern. Tack också för den fina framsidan och övrig grafisk support.

Rafael. Min fina vän och vågkraftkollega. Du var min första kontakt på Energisystemprogrammet för i skrivande stund ganska precis nio år sedan. Du har varit ett stabilt bollplank för alla upptänkliga sociala och tekniska frågeställningar både gällande jobb och privatliv. Det är skönt att veta att du finns där.

Min egen och Monikas familj, ni har varit ett stort stöd med det intresse ni kontinuerligt visat.

Johan och Daniel, mina fina vänner. Tack bland annat för luncherna på Grindstugan med givande diskussioner om parkerade bilar som tippar upp på högkant efter sex timmar. Tack för att ni finns, och förresten, jag tror banne mig att det står “Johans tur å peja” på en, vid det här laget, skitskrynklig gammal lapp i min väska. Men det kan ju förstås vara förbrukad och bara kvarglömd...

Ställverksgruppen, Cecilia och Olle. Vi lyckades tillsammans, med mycket slit och under bildandet av många gråa hår, från grunden bygga världens första undervattensställverk för vågkraft. Det var riktigt, riktigt bra gjort. Nästa ställverk ska vi, med god hjälp av Boel och Rickard, se till att det blir ännu bättre.

Våggruppen. Tack för samarbetet så här långt. Vi jobbar med ett viktigt område och vi kan försöka se till att det blir ännu viktigare. I år, 2010, kommer det hända mycket i Lysekil och vi ska förhoppningsvis bidra till att visa att svensk vågkraftteknik är att räkna med när Härmanöborna så småningom kanske får lite vågskvalp i vägguttagen.

Rafael och Simon, mina polare i det fabulösa *Electric Acoustics*. Bandet som uppstått och kanske lever vidare, om än något intermittent. Det har blivit några härliga spelningar och det blir förhoppningsvis några till. Och tack också alla ni andra som förgyllt disputations- och julfester med sång och musik.

Simon, Mårten, Katarina, Venu, Sandra, Rafael, Cecilia, Olle, Jens, Monika, Urban, Micke och Jan I har läst olika delar av min avhandling och gett mycket värdefulla synpunkter som jag inte hade kunnat vara utan. Tack vare er får nu erratan förhoppningsvis acceptabel storlek.

Senad och Henrik. Ni var De stabila två i mitt alldeles egna lilla sidoprojekt som fortfarande väntar på min uppmärksamhet. Henrik, dig vill jag önska lycka till på ABB medan jag får nöjet att fortsätta språka med Senad på avdelningen.

Anneli Andersson Snygg, tack för fotot som nu pryder framsidan på min första bok.

När nån frågar säger jag alltid att jag trivs väldigt bra på mitt jobb. Det har jag delvis er, alla kollegor på avdelningen för ellära, att tacka för. I höst fortsätter jag gärna att diskutera senaste Ny Teknik-floskeln med er.

Slutligen vill jag tacka Gunnel, Christina, Thomas och Ingrid för er hjälp med olika administrativa uppgifter, samt Ulf för tillverkningsteknisk support.

References

[1] M.Z. Jacobson and M.A. Delucchi. A path to sustainable energy by 2030. *Scientific American*, 2009(November):58 – 65, 2009.

[2] R. Boud. *Status and Research and Development Priorities, Wave and Marine Accessed Energy, DTI Report FES-R-132, AEAT Report, AEAT/ENV/1054*. UK Dept. of Trade and Industry (DTI), UK, 2003.

[3] B. Drew, A.R. Plummer, and M.N. Sahinkaya. A review of wave energy converter technology. *Journal of Power and Energy*, 223(8):887 – 902, 2009.

[4] A.F. de O. Falcao. Wave energy utilization: A review of the technologies, article in press, accessed dec. 8, 2009. *Renewable and Sustainable Energy Reviews*, 2009.

[5] Girard père et fils. *Pour divers moyens d'employer les vagues de la mer, comme moteurs*. Brevet D'invention De Quinze Ans, Paris, France, 1799.

[6] F. Neumann, A. Brito-Melo, E. Didier, and A. Sarmento. Pico OWC Recovery Project: Recent Activities and Performance Data. In *Proc. of the 7th European Wave and Tidal Energy Conference, EWTEC*, Porto, Portugal, September 2009.

[7] J.P. Kofoed, P. Frigaard, E. Friis-Madsen, and H.C. Sørensen. Prototype testing of the wave energy converter Wave Dragon. *Renewable Energy*, 31(2):181 – 189, 2006.

[8] J. Falnes. Research and development in ocean-wave energy in Norway. In *Proc. of International Symposium on Ocean Energy Development*, pages 27 – 39, Muroran, Hokkaido, Japan, 1993. August.

[9] R. Henderson. Design, simulation, and testing of a novel hydraulic power take-off system for the Pelamis wave energy converter. *Renewable Energy*, 31(2):271–283, 2006.

[10] H. Polinder, M.E.C. Damen, and F. Gardner. Design, modelling and test results of the AWS PM linear generator. *European Transactions on Electrical Power*, 15(3):245–256, 2005.

[11] I.A. Ivanova, O. Ågren, H. Bernhoff, and M. Leijon. Simulation of a 100 kW permanent magnet octagonal linear generator for ocean wave conversion. In *Proc. of the 5th European Wave Energy Conference, EWEC'03*, Cork, Ireland, 2003.

[12] I.A. Ivanova, O. Ågren, H. Bernhoff, and M. Leijon. Simulation of a 100 kW permanent magnet octagonal linear generator for ocean wave energy conversion and utilization. *Scientific Technical Review Journal*, 1:239 – 244, 2004.

[13] I.A. Ivanova, O. Ågren, H. Bernhoff, and M. Leijon. Simulation of cogging in a 100 kW permanent magnet octagonal linear generator for ocean wave conversion. In *Proc. of the International Symposium on underwater technology*, Taipei, Taiwan, 2004.

[14] I.A. Ivanova, O. Ågren, H. Bernhoff, and M. Leijon. Simulation of wave-energy converter with octagonal linear generator. *IEEE Journal of Oceanic Engineering*, 30(3):619 – 629, 2005.

[15] O. Langhamer. *Wave energy conversion and the marine environment*. Doctoral thesis, Uppsala University, Sweden, 2009.

[16] R. Waters, J. Engström, J. Isberg, and M. Leijon. Wave climate off the Swedish west coast. *Renewable Energy*, 34(6):1600 — 1606, 2009.

[17] K. Budal and J. Falnes. A resonant point absorber of ocean waves. *Nature*, 256:478 – 479, 1975.

[18] D.V. Evans. A theory for wave-power absorption by oscillating bodies. *Journal of Fluid Mechanics*, 77:1 – 25, 1976.

[19] J.N. Newman. The interaction of stationary vessels with regular waves. In *Proc. of the 11th Symposium on Naval Hydrodynamics, Mechanical Engineering*, London, UK, 1976.

[20] C.C. Mei. Power extraction from water waves. *Journal of Ship Research*, 20:63, 1976.

[21] N. Ambli, K. Budal, J. Falnes, and A. Sorenssen. Wave power conversion by a row of optimally operated buoys. In *Proc. of the 10th World Energy Conference*, pages 1 – 17, Istanbul, Turkey, 1977. Sept. 19-23.

[22] K. Budal, J. Falnes, A. Kyllingstad, and G. Oltedal. Experiments with point absorbers. In *Proc. of the first Symposium on Wave Energy Utilization*, pages 252 – 282, Göteborg, Sweden, 1979.

[23] K. Budal and J. Falnes. *Interacting point absorbers with controlled motion*. In B. Count, editor, Power from sea waves, Academic Press, ISBN 0-12-193550-7, London, UK, 1980.

[24] K. Budal and J. Falnes. Wave power conversion by point absorbers: A Norwegian project. *Int. Journal of Ambient Energy*, 3(2):21 – 28, 1982.

[25] D.V. Evans. Maximum wave-power absorption under motion constraints. *Applied Ocean Research*, 3(4):200 – 2003, 1981.

[26] L.C. Iversen. Numerical method for computing the power absorbed by a phase-controlled point absorber. *Applied Ocean Research*, 4(3):173 – 180, 1982.

[27] D.J. Pizer. Maximum wave-power absorption of point absorbers under motion constraints. *Applied Ocean Research*, 15:227 – 234, 1993.

[28] M. Vantorre, R. Banasiak, and R. Verhoeven. Modelling of hydraulic performance and wave energy extraction by a point absorber in heave. *Applied Ocean Research*, 26:61 – 72, 2004.

[29] P. McIver. Some hydrodynamic aspects of arrays of wave-energy devices. *Applied Ocean Research*, 16:61 – 69, 1994.

[30] S.A. Mavrakos and P. McIver. Comparison of methods for computing hydrodynamical characteristics of arrays of wave power devices. *Applied Ocean Research*, 19:283 – 291, 1998.

[31] B.F.M. Child and V. Venugopal. Interaction of waves with an array of floating wave energy devices. In *Proc. of the 7th European Wave and Tidal Energy Conference, EWTEC*, Porto, Portugal, September 2007.

[32] C. Fitzgerald an G. Thomas. A preliminary study on the optimal formation of an array of wave power devices. In *Proc. of the 7th European Wave and Tidal Energy Conference, EWTEC*, Porto, Portugal, September 2007.

[33] G. De Backer, M. Vantorre, C. Beels, J. De Rouck, and P. Frigaard. Performance of closely spaced point absorbers with constrained floater motion. In *Proc. of the 7th European Wave and Tidal Energy Conference, EWTEC*, Porto, Portugal, September 2007.

[34] P. Ricci, J.B. Saulniera, and A.F. de O. Falcão. Point-absorber arrays: a configuration study off the Portuguese West-Coast. In *Proc. of the 7th European wave and tidal energy conference, EWTEC*, Porto, Portugal, September 2007.

[35] A. Babarit and A.H. Clément. Optimal latching control of a wave energy device in regular and irregular waves. *Applied Ocean Research*, 28:77 – 91, 2006.

[36] A. Babarit, B. Borgarino, P. Ferrand, and A.H. Assessment of the influence of the distance between two wave energy converters on the energy production. In *Proc. of the 8th European Wave and Tidal Energy Conference, EWTEC*, Uppsala, Sweden, 2009.

[37] M. Eriksson, R. Waters, O. Svensson, J. Isberg, and M. Leijon. Wave power absorption: Experiments in open sea and simulation. *Journal of Applied Physics*, 102:084910, 2007.

[38] M. Eriksson. *Modelling and Experimental Verification of Direct Drive Wave Energy Conversion. Buoy-Generator Dynamics*. Doctoral thesis, Uppsala University, Sweden, 2007.

[39] M. Eriksson, J. Isberg, and M. Leijon. Hydrodynamic modelling of a direct drive wave energy converter. *International Journal of Engineering Science*, 43(17-18):1377 – 1387, 2005.

[40] J. Engström, M. Eriksson, J. Isberg, and M. Leijon. Wave energy converter with enhanced amplitude response at frequencies coinciding with Swedish west coast sea states by use of a supplementary submerged body. *Journal of Applied Physics*, 106:064512, 2009.

[41] S.H. Salter. World progress in wave energy - 1988. *International Journal of Ambient Energy*, 10(1):3 – 24, 1989.

[42] L. Wang, D.J. Lee, W.J. Lee, and Z. Chen. Analysis of a novel autonomous marine hybrid power generation/energy storage system with a high – voltage direct current link. *Journal of Power Sources*, 185(2):1284 – 1292, 2008.

[43] D.B. Murray, G. Egan, J.G. Hayes, and D.L. O'Sullivan. Applications of Supercapacitor Energy Storage for a Wave Energy Converter System. In *Proc. of the 8th European Wave and Tidal Energy Conference, EWTEC*, pages 786–795, Uppsala, Sweden, September 2009.

[44] A. E. Kiprakis and A. R. Wallace. Power control and conditioning for wave energy converters. In *Proc. of the 7th European Wave and Tidal Energy Conference, EWTEC*, Glasgow, UK, September 2005.

[45] P.R.M. Brooking and M.A. Mueller. Power conditioning of the output from a linear vernier hybrid permanent magnet generator for use in direct drive wave energy converters. *IEE Proc. of Generation, Transmission and Distribution*, 152(5):673–681, 2005.

[46] A. Naikodi and G.R. Sridhara. A new controller for efficient wave power generation. In *Proc. of the IEEE/IAS International Conference on Industrial Automation and Control, (Cat. No.95TH8005)*, pages 357–363, 1995. Jan 5-7.

[47] M. Molinas, O. Skjervheim, P. Andreasen, T. Undeland, J. Hals, T. Moan, and B. Sorby. Power electronics as grid interface for actively controlled wave energy converters. In *Proc. of the International Conference on Clean Electrical Power, ICCEP*, 2007. 21-23 May, pp. 188-195.

[48] J. Robinson and G. Joos. VSC HVDC transmission and offshore grid design for a linear generator based wave farm. In *Proc. of the Canadian Conference on Electrical and Computer Engineering, CCECE '09*, pages 54 – 58, 2009.

[49] M. Molinas, O. Skjervheim, B. Sorby, P. Andreasen, S. Lundberg, and T. Undeland. Power Smoothing by Aggregation of Wave Energy Converters for Minimizing Electrical Energy Storage Requirements. In *Proc. of the 7th European Wave and Tidal Energy Conference, EWTEC*, Porto, Portugal, September 2007.

[50] J. Tissandier, A. Babarit, and A. H. Clément. Study of the smoothing effect on the power production in an array of SEAREV wave energy converters. In *Proc. of the 18th annual conference of the International Society of Offshore and Polar Engineers, ISOPE*, pages 374–381, Vancouver, Canada, 2008.

[51] D. Ramsay, I. Elders, G. Ault, and J. McDonald. Scenario-based analysis of the impact of marine energy development on Scotland's electricity network. In *Proc. of the 6th European Wave and Tidal Energy Conference, EWTEC*, Glasgow, UK, August 29 – September 2 2005.

[52] J.K.H. Shek, D.E. Macpherson, M.A. Mueller, and J. Xiang. Reaction force control of a linear electrical generator for direct drive wave energy conversion. *IET Renewable Power Generation*, 1(1):17 – 24, 2007.

[53] J.K.H. Shek, D.E Macpherson, and M.A. Mueller. Phase and amplitude control of a linear generator for wave energy conversion. In *Proc. of 4th IET Conference on Power Electronics, Machines and Drives, PEMD 2008*, pages 66 – 70, 2008.

[54] L. Ran, P.J. Tavner, M.A. Mueller, N.J. Baker, and S. McDonald. Power Conversion and Control for a Low Speed, Permanent Magnet, Direct-Drive, Wave Energy Converter. In *Proc. of the 3rd IET International Conference on Power Electronics, Machines and Drives*, pages 17 – 21, 2006.

[55] N.J. Baker, M.A. Mueller, and E. Spooner. Permanent magnet air-cored tubular linear generator for marine energy converters. In *Proc. of the 2nd International Conference on (Conf. Publ. No. 498) Power Electronics, Machines and Drives,PEMD.*, pages 862 – 867, 2004. 31 March-2 April.

[56] J. Xiang, P.R.M. Brooking, and M.A. Mueller. Control requirements of direct drive wave energy converters. In *Proc. of IEEE Region 10 Conference on Computers, Communications, Control and Power Engineering, TENCON'02*, pages 2053 – 2056, 2002.

[57] M.A. Mueller. Electrical generators for direct drive wave energy converters. *IEE Proc. of Generation, Transmission and Distribution*, 149(4):446–456, 2002.

[58] M.A. Mueller and M.J. Baker. A low speed reciprocating permanent magnet generator for direct drive wave energy converters. In *Proc. of International Conference on (Conf. Publ. No. 487) Power Electronics, Machines and Drives*, pages 468 – 473, 2002.

[59] H. Polinder, M.A. Mueller, M. Scuotto, and M. Goden de Sousa Prado. Linear generator systems for wave energy conversion. In *Proc. of the 7th European wave and tidal energy conference, EWTEC*, Porto, Portugal, September 2007.

[60] H. Polinder, B.C. Mecrow, A.G. Jack, P.G. Dickinson, and M.A. Mueller. Conventional and TFPM linear generators for direct-drive wave energy conversion. *IEEE Transaction on Energy Conversion*, 20(2):260–267, 2005.

[61] H. Polinder, M.E.C. Damen, and F. Gardner. Linear PM generator system for wave energy conversion in the AWS. *IEEE Trans. on Energy Conversion*, 19(3):583 – 589, 2004.

[62] K. Rhinefrank, E.B. Agamloh, A. von Jouanne, A.K. Wallace, J. Prudell, K. Kimble, J. Aills, E. Schmidt, P. Chan, B. Sweeny, and A. Schacher. Novel ocean energy permanent magnet linear generator buoy. *Renewable Energy*, 31(9):1279 – 1298, 2006.

[63] J. Prudell, M. Stoddard, T.K.A. Brekken, and A. von Jouanne. A novel permanent magnet tubular linear generator for ocean wave energy. In *Proc. of the IEEE Energy Conversion Congress and Exposition, ECCE*, pages 3641 – 3646, 2009. 20-24 Sept.

[64] D. Elwood, A. Schacher, K. Rhinefrank, J. Prudell, S. Yim, E. Amon, T. Brekken, and A. von Jouanne. Numerical modeling and ocean testing of a direct-drive wave energy device utilizing a permanent magnet linear generator for power take-off. In *Proc. of the ASME 2009 28th international conference on Ocean, Offshore and Arctic Engineering, OMAE2009*, Honolulu, Hawaii, USA, 2009. May 31-June 5.

[65] D. Elwood, S.C. Yim, J. Prudell, C. Stillinger, A. von Jouanne, T.K.A. Brekken, A. Brown, and R. Paasch. Design, construction, and ocean testing of a taut-moored dual-body wave energy converter with a linear generator power take-off. *Renewable Energy*, 35(2):348 – 354, 2010.

[66] T.K.A. Brekken, A. von Jouanne, and H.Y. Han. Ocean wave energy overview and research at oregon state university. In *Proc. of IEEE Power Electronics and Machines in Wind Applications, PEMWA*, pages 1 – 7, 2009. June 24-26.

[67] M. Trapanese. Optimization of a sea wave energy harvesting electromagnetic device. *IEEE Transactions on Magnetics*, 44(11):4365 – 4368, 2008.

[68] V. Cecconi and M. Trapanese. An optimum design of the magnetic circuit of a PM linear electrical generator for the exploitation of sea waves. In *International Symposium on Power Electronics, Electrical Drives, Automation and Motion, SPEEDAM*, pages 116 – 119, 2006.

[69] R. Miceli and M. Trapanese. Evaluation of the power quality from a seawave power farm for different interconnection schemes. In *Proc. of OCEANS 2007 - Europe*, June 2007.

[70] H. Luan, O.C. Onar, and A. Khaligh. Dynamic Modeling and Optimum Load Control of a PM Linear Generator for Ocean Wave Energy Harvesting Application. In *Proc. of the 24th Annual IEEE Applied Power Electronics Conference and Exposition, APEC.*, pages 739 – 743, 2009. 15-19 Feb.

[71] N.M. Kimoulakis, A.G. Kladas, and J.A. Tegopoulos. Power Generation Optimization From Sea Waves by Using a Permanent Magnet Linear Generator Drive. *IEEE Transactions on Magnetics*, 44(6):1530 – 1533, 2008.

[72] T.K.A. Brekken, H. Hapke, and J. Prudell. Drives comparison for reciprocating and renewable energy applications. In *Proc. of the 24th annual IEEE Applied Power Electronics Conference and Exposition, APEC*, pages 732 – 738, 2009. Feb. 15-19.

[73] M.A. Mueller, M.J. Baker, L. Ran, N.G. Chong abd W. Hong, P.J.Tavner, and P. McKeever. Experimental tests of an air-cored PM tubular generator for direct drive wave energy converters. In *Proc. of 4th IET Conference on Power Electronics, Machines and Drives, PEMD 2008.*, pages 747 – 751, 2008.

[74] R. Crozier and M.A. Mueller. Modelling and first order optimisation of the air-cored tubular PM machine using polynomial approximation. In *Proc. of the 18th International Conference on Electrical Machines, ICEM*, pages 1 – 6, 2008. 6-9 Sept.

[75] W.C. Beattie. IEE colloquium on wave power: An engineering and commercial perspective (digest no: 1997/098). In *Proc. of the 6th European Wave and Tidal Energy Conference, EWTEC*, 1997. March 13.

[76] D. O'Sullivan and G. Dalton. Challenges in the grid connection of wave energy devices. In *Proc. of the 8th European Wave and Tidal Energy Conference, EWTEC*, Uppsala, Sweden, 2009.

[77] J. Bard, J. Schmid, P. Caselitz, and J. Giebhardt. Electrical engineering aspects of ocean energy converters. In *Proc. of the 6th European Wave and Tidal Energy Conference, EWTEC*, Glasgow, UK, 2005. Aug 29-Sept 2.

[78] B. Czech, P. Bauer, H. Polinder, Y. Zhou, and P. Korondi. Comparing the electrical transmission systems for Archimedes Wave Swing parks. In *Proc. of the 8th European Wave and Tidal Energy Conference, EWTEC*, Uppsala, Sweden, 2009.

[79] H.C. Soerensen, R. Hansen, E. Friis-Madsen, W. Panhauser, G. Mackie, H.H. Hansen, P. Frigaard, T. Hald, W. Knapp, J. Keller, E. Holmén, B. Holmes, G. Thomas, P. Rasmussen, and J. Krogsgaard. The Wave Dragon—now ready for test in real sea. In *Proc. of the 4th European Wave Energy Conference*, Aalborg, Denmark, 2000.

[80] C.K. Gordon. Wave driven power generation system. *US Pat. 4.781.023*, 1988.

[81] W.W. Hirsch. Wave energy conversion system. *US Pat. 7.199.481*, 2007.

[82] M. Leijon and K. Thorburn. A system for generating electric energy. Int. patent WO/2007/111546, 2007.

[83] B. Das and B.C. Pal. Voltage control performance of AWS connected for grid operation. *IEEE Transactions on Energy Conversion*, 21(2):353–361, 2006.

[84] E.A. Amon, A.A. Schacher, and T.K.A. Brekken. A novel maximum power point tracking algorithm for ocean wave energy devices. In *Proc of the IEEE Energy Conversion Congress and Exposition, ECCE.*, pages 2635 – 2641, 2009. Sept. 20-24.

[85] K. Thorburn, H. Bernhoff, and M. Leijon. Wave energy transmission system concepts for linear generator arrays. *Ocean Engineering*, 31(11-12):1339–1349, 2004.

[86] U. Henfridsson, V. Neimane, K. Strand, R. Kapper, H. Bernhoff, O. Danielsson, M. Leijon, J. Sundberg, K. Thorburn, E. Ericsson, and K. Bergman. Wave energy potential in the Baltic Sea and the Danish part of the North Sea, with reflections on the Skagerrak. *Renewable Energy*, 32(12):2069 – 2084, 2007.

[87] I. Martinez de Alegria, J.L. Martin, I. Kortabarria, J. Andreu, and P.I. Ereño. Transmission alternatives for offshore electrical power. *Renewable and Sustainable Energy Reviews*, 13(5):1027 – 1038, 2009.

[88] H. Lendenmann, K-C. Strømsem, M. Dai Pre, W. Arshad, A. Leirbukt, G. Tjensvoll, and T. Gulli. Direct generation wave energy converters for optimized electrical power production. In *Proc. of the 7th European Wave and Tidal Energy Conference, EWTEC*, Porto, Portugal, 2007.

[89] P. Frigaard, J.P. Kofoed, and M.R. Rasmussen. Overtopping measurements on the Wave Dragon Nissum Bredning prototype. In *Proc. of the 14th Annual International Offshore and Polar Engineering Conference, ISOPE*, Toulon, France, 2004.

[90] E. Callaway. To catch a wave. *Nature*, 450(8), 2007.

[91] C. Huertas-Olivares, F. Neumann, and A. Sarmento. Environmental management recommendations for the wave energy Portuguese pilot zone. In *Proc. of the 7th European Wave and Tidal Energy Conference, EWTEC*, Porto, Portugal, September 2007.

[92] H. Mouslim, A. Babarit, A. Clément, and B. Borgarino. Development of the French Wave Energy Test Site SEM-REV. In *Proc. of the 8th European Wave and Tidal Energy Conference, EWTEC*, pages 31 – 35, Uppsala, Sweden, 2009.

[93] J.V. Norris and E. Droniou. Update on EMEC activities, resource description, and characterisation of wave-induced velocities in a tidal flow. In *Proc. of EWTEC, the 7th European Wave and Tidal Energy Conference*, Porto, Portugal, 2007. Sept 11-13.

[94] D.M. Greaves, G.H. Smith, and J. Wolfram. Development of Marine Renewable Energy in the South West of England: The Wave Hub and PRIMaRE. In *Proc. of the 8th European Wave and Tidal Energy Conference, EWTEC*, Uppsala, Sweden, 2009. 7-10 September.

[95] UK wave project given go ahead. *Renewable Energy Focus*, 8(6):16, 2007.

[96] A. Westwood. Marine and offshore wind and marine project update. *Renewable Energy Focus*, 8(6):29, 2007.

[97] K. Gillanders, N. Harrington, and A. Taylor. Development of the South West Wave Hub. In *Proc. of the 6th European Wave and Tidal Energy Conference, EWTEC*, Glasgow, UK, 2005.

[98] The Institute of Electrical and Electronics Engineers. IEEE 1547-2003, IEEE Standard for Interconnecting Distributed Resources with Electric Power Systems, 2003.

[99] *Affärsverket svenska kraftnäts föreskrifter och allmänna råd om driftsäkerhetsteknisk utformning av produktionsanläggningar (SvKFS 2005:2)*. Affärsverket svenska kraftnät, Vällingby, Sweden, 2005.

[100] H. Polinder and M. Scuotto. Wave energy converters and their impact on power systems. In *Proc. of the International Conference on Future Power Systems*, 2005.

[101] K. Rothenhagen, M. Jasinski, and M.P. Kazmierkowski. Grid connection of multi-megawatt clean wave energy power plant under weak grid condition. In *Proc. of EPE-PEMC, the 13th International Power Electronics and Motion Control Conference*, pages 1904 – 1910, 2008.

[102] E. Amon, T.K.A. Brekken, and A. von Jouanne. A Power Analysis and Data Acquisition System for Ocean Wave Energy Device Testing. In *Proc. of the 24th annual IEEE Applied Power Electronics Conference and Exposition*, pages 750 – 754, 2009. Feb. 15-19.

[103] A. von Jouanne, S. Dai, and H. Zhang. A Multilevel Inverter Approach Providing DC-Link Balancing, Ride-Through Enhancement, and Common-Mode Voltage Elimination. *IEEE Transactions on Industrial Electronics*, 49(4):739 – 745, 2002.

[104] J. Falnes. *Ocean waves and oscillating systems*. The press syndicate of the University of Cambridge, Cambridge, United Kingdom, 1 edition, 2002.

[105] D. Jiles. *Magnetism and magnetic materials*. Chapman & Hall/CRC, Boca Raton, Florida, USA, 2 edition, 1998.

[106] Timothy L. Skvarenina. *The power electronics handbook*. CRC Press LLC, Boca Raton, Florida, USA, 2002.

[107] Robert T. Hudspeth. *Waves and wave forces on coastal and ocean structures*, volume 21. World Scientific Publishing Co. Pte. Ltd., Singapore, 2006.

[108] João Cruz. *Ocean Wave Energy, Current Status and Future Perspectives*. Springer-Verlag, Berlin Heidelberg, Germany, 2008.

[109] J.N. Newman. The exciting forces on fixed bodies in waves. *Journal of Ship Research*, 6:10 – 17, 1962.

[110] Chandur Sadarangani. *Electrical Machines - Design and Analysis of Induction and Permanent Magnet Motors*. KTH, Royal Institute of Technology, Division for Electrical Machines and Power Electronics, ISBN 91-7170-627-5, Stockholm, Sweden, 2006.

[111] Gordon R. Slemon. *Electrical Machines and Drives*, volume ISBN 0-201-57885-9. Addison-Wesley Publishing Company, Inc., Toronto, US, 1992.

[112] J. Selvaraj and N.A. Rahim. A novel pulse width modulation for grid-connected multilevel inverter. *Journal of Renewable and Sustainable Energy*, 1(5):053102, 2009.

[113] P. Panagis, F. Stergiopoulos, P. Marabeas, and S. Manias. Comparison of state of the art multilevel inverters. In *Proc. of the IEEE Power Electronics Specialists Conference, PESC*, pages 4296 – 4301, 2008. 15-19 June.

[114] I.-D. Kim, E.-C. Nho, H.-G. Kim, and J.S. Ko. A Generalized Undeland Snubber for flying capacitor multilevel inverter and converter. *IEEE Transactions on Industrial Electronics*, 51(6):129 – 1296, 2004.

[115] K. Fujii, R.W. De Doncker, and S. Konishi. A novel DC-link voltage control of PWM-switched cascade cell multi-level inverter applied to STATCOM. In *Proc. of the 40th IAS Industry Applications Conference Annual Meeting*, pages 961 – 967, 2005. October 2-6.

[116] O. Danielsson. *Wave Energy Conversion, Linear Synchronous Permanent Magnet Generator*. Doctoral thesis, Uppsala University, Sweden, 2006.

[117] R. Waters. *Energy from Ocean Waves – Full Scale Experimental Verification of a Wave Energy Converter*. Doctoral thesis, Uppsala University, Sweden, 2008.

[118] M. Bazargan. Renewables offshore wind—offshore substation. *Power Engineer*, 21(3):26–27, 2007.

[119] EN 13445, the European standard for unfired pressure vessels.

[120] R. Ekström. *Inverter system design and control for a wave power substation*, volume UPTEC ES 09024. Masters thesis, Uppsala University, Sweden, 2009.

[121] B. Ekergård. *Control and synchronization of a marine substation*, volume UPTEC ES 09026. Masters thesis, Uppsala University, Sweden, 2009.

Acta Universitatis Upsaliensis

Digital Comprehensive Summaries of Uppsala Dissertations from the Faculty of Science and Technology 711

Editor: The Dean of the Faculty of Science and Technology

A doctoral dissertation from the Faculty of Science and Technology, Uppsala University, is usually a summary of a number of papers. A few copies of the complete dissertation are kept at major Swedish research libraries, while the summary alone is distributed internationally through the series Digital Comprehensive Summaries of Uppsala Dissertations from the Faculty of Science and Technology. (Prior to January, 2005, the series was published under the title "Comprehensive Summaries of Uppsala Dissertations from the Faculty of Science and Technology".)

Distribution: publications.uu.se
urn:nbn:se:uu:diva-112915

ACTA
UNIVERSITATIS
UPSALIENSIS
UPPSALA
2010